UNIVERSITÉ DE MONTRÉAL

# CARBON NANOTUBE NETWORKS FOR THIN FILM ELECTRONIC APPLICATIONS

CARLA MARIA AGUIRRE-CARMONA

DÉPARTEMENT DE GÉNIE PHYSIQUE

ÉCOLE POLYTECHNIQUE DE MONTRÉAL

THÈSE PRÉSENTÉE EN VUE DE L'OBTENTION

DU DIPLÔME DE PHILOSOPHIÆ DOCTOR

(GÉNIE PHYSIQUE)

DÉCEMBRE 2007

**Canada**

UNIVERSITÉ DE MONTRÉAL

ÉCOLE POLYTECHNIQUE DE MONTRÉAL

Cette thèse intitulée:

CARBON NANOTUBE NETWORKS FOR THIN FILM ELECTRONIC
APPLICATIONS

présentée par : AGUIRRE-CARMONA Carla María

en vue de l'obtention du diplôme de : Philosophiæ Doctor

a été dûment acceptée par le jury d'examen constitué de :

M. ROCHEFORT Alain, Ph.D., président

M. DESJARDINS Patrick, Ph.D., membre et directeur de recherche

M. MARTEL Richard, Ph.D., membre et codirecteur de recherche

M. MASUT Remo A., Ph.D., membre

M. HERSAM Mark C., Ph.D., membre

# ACKNOWLEDGEMENTS

My research group has been part of the reason the past four years have been so gratifying. I have had the luck to work with a superb team of aspiring scientists that I can now call my friends. Maxime Trudel and Stephane Auvray, we were the original three. Before you two, I did not believe buying beakers, syringes and pipettes could be so exciting. Benoit Cardin, Elyse Adam, Janie Cabana, Éric Anglaret and Laetitia Marty, I am happy to have collaborated with you on different research projects. I am grateful for your patience and your enthusiasm. Matthieu Paillet and Céline Ternon, you played a major part in helping me finish this thesis. I hope this will not be the last of our projects. Jean-Nicolas Beaudry, you know you have been instrumental to my success in most of my scholarship applications. Thank you for so generously providing me with your assistance and friendship. François Lapointe, Pierre Lévesque, François Meunier, Fabienne Dragin and Delphine Bouilly, it has been a pleasure working with you. I also want to acknowledge Annie Lévesque, Simon Gaudet, Cédrik Coia, Stéphane Turcotte and Caroline Dion, members of the brat pack at the Desjardins Group. Finally, because a group is not complete without the technical team that keeps everything working, I want to thank Joël Bouchard, Olivier Grenier, Marie-Hélène Bernier and Phillipe Vasseur.

I have belatedly come to realize the importance of family and friends to the successful completion of a project of this magnitude. I want to particularly thank Marie-France Pépin who offered me her friendship and mentorship, as well as many sleepless hours, during the writing of this thesis. I hope we will continue being friends so I may someday repay you in-kind. Katrie Dupont-Chalaoui and Beatrice Cormier, thank you for being there when I stubbornly refused to acknowledge I needed your help. A special thanks to my Mom and Dad, whose trust in me never seems to falter. I love you and hope I will continue making you proud. Finally, to Geneviève Gauthier and Le Thi Nguyen, *amies pour la vie,* to you, I dedicate this thesis because sometimes family and friends are one of the same.

# RÉSUMÉ

Après des décennies de progression soutenue axée sur la miniaturisation, le domaine des matériaux et dispositifs électroniques subit en ce moment des bouleversements importants. De nouveaux matériaux tels les semi-conducteurs organiques et les nanotubes de carbone font compétition aux semi-conducteurs conventionnels pour une large gamme d'applications allant des circuits électroniques et des cellules photovoltaïques, aux senseurs et aux dispositifs d'affichage. En particulier, les nanotubes de carbone ont souvent été proposés pour la fabrication de dispositifs innovateurs de haute performance alors que l'utilisation à large échelle des semi-conducteurs organiques est envisagée pour les biens de consommation à plus faible valeur ajoutée.

Les travaux rapportés dans cette thèse contribuent à rapprocher ces deux domaines de recherche traditionnellement distincts en exploitant les propriétés uniques des nanotubes de carbone pour aborder certains des défis liés notamment à l'électronique organique. Nous nous sommes concentrés sur la mise en œuvre des techniques nécessaires à l'ingénierie des propriétés de réseaux de nanotubes de carbones requises pour permettre leur exploitation à grande échelle.

Dans la première partie de la thèse, nous présentons les résultats de l'étude des propriétés électroniques de réseaux de nanotubes de carbone préparés par un procédé de filtration sous vide. Puisque les mélanges non-traités de nanotubes de carbone monoparoi contiennent une distribution statistique d'un tiers de tubes métalliques pour deux tiers de tubes semi-conducteurs, il est possible de fabriquer les réseaux ayant des faibles densités (nombre de nanotubes par unité de surface) pour lesquels les seuls chemins de percolation entre deux électrodes ont un comportement semi-conducteur. Nous avons d'abord déterminé la densité surfacique à laquelle les propriétés électriques des réseaux passent d'isolant à semi-conducteur et de semi-conducteur à métallique. Les

dispositifs à transistors en couches minces (thin film transistors, TFTs) fabriqués à partir de réseaux semi-conducteurs ont montré des transconductances (valeurs proportionnelles à la mobilité effective des dispositifs) de plus de 0,015 S/m et des courants d'opération d'environ 20 μA pour des ratios de courants dans l'état On et l'état Off ($I_{on}/I_{off}$) de plus de $10^5$, une valeur suffisamment élevée pour les utiliser, par exemple, dans la fabrication d'écrans plats. Lorsque la densité des réseaux augmente, on observe une augmentation de la transconductance. Cependant, l'apparition de parcours métalliques (chemins de percolation) entre les électrodes provoque une augmentation considérable du courant dans l'état Off, réduisant ainsi les valeurs $I_{On}/I_{Off}$. Nous avons identifié l'étroite plage de densités surfaciques de nanotubes qui permet d'obtenir le meilleur compromis entre ces deux propriétés ($I_{On}/I_{Off}$ et transconductance) pour la fabrication de transistors en couche mince performants. Nous avons par ailleurs démontré que le claquage électrique et la fonctionnalisation sélective des nanotubes métalliques, deux stratégies fréquemment proposées pour éliminer les parcours métalliques et augmenter la transconductance, ne sont pas des solutions efficaces. En contrepartie, dans le cadre de l'utilisation de réseaux denses comme électrodes métalliques conductrices, semi-transparentes et flexibles, nous avons identifié le complexe 2,3-dichloro-5,6-dicyano-1,4-benzoquinone comme étant le dopant le plus efficace pour convertir la vaste majorité des nanotubes semi-conducteurs en des semi-conducteurs dégénérés ayant un comportement métallique. Une augmentation de la conductance du réseau d'un facteur sept découle de ce traitement. Des couches minces de nanotubes de carbone dopés ayant une transparence (80%) et une résistance de feuille (58 Ω/carré) ont été fabriquées. Ces caractéristiques, obtenues pour des matériaux flexibles pouvant être mis en forme à la température de la pièce via des procédés en solution, sont comparables à celles des meilleurs oxydes inorganiques déposés sous vide à haute température.

Le transport électronique dans les réseaux de nanotubes de carbone est gouverné par la conduction par sauts. Peu de choses étant comprises sur les lois d'échelle applicables dans les dispositifs à base de réseaux de nanotubes de carbone qui opèrent dans un

régime de transport par percolation, nous avons étudié le transport électronique en fonction de la longueur du canal pour des réseaux comprenant différentes configurations de nanotubes. Pour ce faire, nous avons développé une méthode de fabrication chimique par voie liquide qui a permis d'obtenir des réseaux de nanotubes de carbone aléatoires ou alignés latéralement uniformes. Le substrat est d'abord fonctionnalisé par une monocouche auto-assemblée de molécules d'aminosilane connue pour son affinité importante pour les nanotubes de carbone. Des réseaux aléatoires peuvent alors être fabriqués en exposant la surface fonctionnalisée à une solution contenant les nanotubes de carbone. Des réseaux alignés peuvent être produits en déposant la solution lorsque le substrat est en rotation à 8000 rpm. L'uniformité de réseaux obtenus a permis la réalisation de la première étude systématique des lois d'échelle régissant les dispositifs TFT ayant diverses configurations (densité et alignement). La caractérisation détaillée des propriétés électriques de ces dispositifs TFT dont les longueurs de canaux avaient typiquement 1 à 100 μm a permis d'extraire les caractéristiques de variabilité d'échelle de ce nouveau matériau. Pour des dispositifs TFT ayant des densités de nanotubes de carbone bien en deçà du seuil de percolation métallique, il est possible de fabriquer des dispositifs ayant des ratios élevés de courants ouvert/fermé ($I_{on}/I_{off}$) pour une longueur de canal aussi faible que 6 μm. Finalement, nous avons démontré qu'il est possible de contrôler les propriétés des réseaux de nanotubes en ajustant les arrangements de nanotubes sur le substrat, les réseaux alignés de différentes densités ayant des propriétés différentes des réseaux aléatoirement orientés.

Bien que les nanotubes de carbone soient en principe de bons conducteurs d'électrons et de trous, il est bien connu que les transistors à base de ce matériaux sont normalement caractérisés par une comportement de type-p (porteurs de charge positifs), le comportement ambipolaire n'était possible que lors de mesures des caractéristiques électriques sous vide après recuit thermique. Ce comportement impose des limites sévères à l'utilisation de ce matériau dans les nombreux circuits microélectroniques pour lesquels les deux types de transistors (type-p et type-n) sont requis. Afin d'expliquer

l'origine de ce comportement et aussi pour trouver une solution à ce problème technique majeur, nous avons étudié des dispositifs préparés sur des substrats possédant des fonctionnalités chimiques spécifiques : le répandu oxyde thermique de silicium et le parylene-C, un polymère isolant hydrophobique et exempt d'oxygène. Une étude détaillée des caractéristiques électriques des dispositifs fabriqués sur ces différents substrats et sujets à différents traitements a permis d'une part, de fabriquer des dispositifs montrant de caractère bipolaire dans l'air et, d'autre part, de clairement mettre en évidence que l'adsorption de molécules provenant du milieu ambiant est à l'origine de ce comportement. En nous basant sur les caractéristiques connues des substrats étudiées et des températures requises pour l'obtention de caractéristiques ambipolaires après recuit sous vide, nous proposons que la vapeur d'eau contenue dans l'air est fort probablement l'espèce chimique responsable de ce comportement. Cette étude, réalisée aussi bien pour des dispositifs à base de nanotubes individuels et de réseaux de nanotubes, est d'intérêt direct pour la communauté de l'électronique organique qui fait actuellement face à ce même problème d'envergure.

Nous avons poursuivi avec une ddémonstration du potentiel des réseaux denses de nanotubes de carbone comme électrode transparente à performance élevée pour les dispositifs électroluminescents organiques comme alternative aux fragiles couches d'alliages d'oxydes d'étain et d'indium (ITO, indium tin oxide). Nous avons effectué une étude systématique de la conductivité et de la transparence des membranes de nanotubes en fonction de leur épaisseur. Pour la première fois, des diodes électroluminescentes organiques à performance élevée ont été fabriquées sur des membranes transparentes et conductrices de nanotubes de carbone monoparoi. En utilisant des membranes de 130 nm d'épaisseur ayant une résistance de feuille de 60 $\Omega$/carré nous avons atteint une luminance maximale de 2 800 cd/m$^2$ avec une efficacité de 1,4 cd/A. L'efficacité de nos diodes électroluminescentes organiques est comparable à celles de dispositifs optimisés utilisant une électrode d'ITO, 1,9 cd/A, mesurée dans les mêmes conditions expérimentales. Une mince couche tampon de parylène intercalée

entre l'anode de nanotubes et la couche transformatrice des trous est requise pour atteindre les performances citées.

Afin d'étudier plus en détail l'origine de la bonne efficacité d'injection de charges électriques observée dans les dispositifs organiques électroluminescents mentionnés ci haut, nous avons conçu et mis au point des méthodes de fabrication permettant de réaliser des dispositifs dans lesquels des îlots semi-conducteurs organiques de pentacène établissent le contact entre deux électrodes de nanotube de carbone individuels. Nous avons démontré que ces électrodes d'un diamètre moyen de 2,7 nm peuvent injecter des courants importants (~10 µA) dans les îlots de pentacène. Cette approche a aussi été implémentée dans des rangées d'électrodes de nanotubes de carbone pour l'injection de charge dans des TFT organique réalistes ayant des largeurs de canal de 200 µm. Dans les deux cas, l'injection était efficace et supérieure à celle obtenue à l'aide d'électrodes traditionnelles constituées de métaux nobles.

Globalement, cette thèse contribue de plusieurs manières à l'avancement de la science et de la technologie des réseaux de nanotubes de carbone pour des applications en électronique et en optoélectronique. Premièrement, nous avons montré qu'une stratégie efficace pour contourner le fait que les propriétés des nanomatériaux varient considérablement avec la taille consiste à exploiter les propriétés nouvelles d'ensembles de nanotubes de carbone dans des applications innovatrices. En second lieu, nous avons insisté pour développer des techniques de fabrication en solution qui sont compatibles avec des procédés à grande échelle et à faible température. Finalement, nous avons clairement mis en évidence que le substrat influence de manière déterminante les caractéristiques électriques des dispositifs fabriqués à partir de nanomatériaux, un fait qui avait été négligé dans le passé.

# ABSTRACT

The field of electronic materials and devices, characterized by decades of steady but incremental progress, is now undergoing fundamental transformations. New materials such as organic semiconductors and carbon nanotubes are pushing to replace conventional semiconductors in a wide array of applications including microelectronic circuits, photovoltaic cells, sensors, and displays. In particular, carbon nanotubes have generally been proposed for the fabrication of high performance and novel devices, whereas the use of organic semiconductors is typically envisioned for low-cost consumer products.

This thesis contributes to bringing these two traditionally distinct research fields together by exploiting the unique properties of carbon nanotubes to address major challenges faced by organic electronics. We have focused on the development of materials processing and device fabrication techniques required to engineering the necessary morphologies in order to permit the exploitation of their unique properties, especially for large-scale applications.

In the first part of the thesis, we present the results of an investigation of the electronic properties of carbon nanotube networks made from a vacuum filtration method. Considering the fact that as-prepared single-walled carbon nanotube mixtures consist of a statistical distribution of 1/3 metallic and 2/3 semiconducting species, it is possible to fabricate low-density networks (number of nanotubes per unit area) in which percolation paths between two electrodes have semiconducting behavior. We have first determined the carbon nanotube densities for which the transitions from insulating to semiconducting and semiconducting to metallic behaviors are observed. Thin film transistor (TFT) devices fabricated from semiconducting networks displayed transconductances (values proportional to the effective mobility of the devices) over 0.015 S/m at current outputs of ~ 20 µA for ratios of On state/Off state currents ($I_{On}/I_{Off}$)

over $\sim 10^5$. This last value is sufficiently large for the use of these TFTs in, for example, active displays. The transconductance increases with the carbon nanotube density in the networks. Unfortunately, the appearance of metallic percolation paths between the device electrodes results in a considerable increase of the Off state current thus decreasing $I_{On}/I_{Off}$ values. We have identified the narrow range of carbon nanotube densities which offers the best compromise between these two properties ($I_{On}/I_{Off}$ and transconductance) for the fabrication of high performance TFT devices. Furthermore, we have demonstrated that electrical breakdown and the selective functionalization of metallic nanotubes, two often-cited strategies for removing the metallic conduction paths and thus to increase transconductance values, are not efficient solutions. Also, in the context of the use of dense metallic networks as conducting, flexible and transparent electrodes, we have identified that 2,3-dichloro-5,6-dicyano-1,4-benzoquinone is a most effective dopant, allowing us to convert the vast majority of semiconducting nanotubes into degenerately doped semiconductors exhibiting metallic behavior. This treatment resulted in a 7-fold increase in the network conductance. Doped carbon nanotube sheets with optical transparencies (80%) and sheet resistances (58 $\Omega$/square) have been fabricated. These characteristics, obtained for flexible materials prepared at room temperature using a solution-based process, are comparable to those of state-of-the-art inorganic oxides deposited under vacuum at high temperature.

Transport in carbon nanotube networks is governed by hopping conduction. Little being known about the scaling properties of carbon nanotube TFT devices that operate in a percolation transport regime, we have conducted a study of electronic transport as a function of channel length for networks having different nanotube configurations. We first developed a wet chemical fabrication method which allows us to fabricate laterally uniform networks of random and aligned carbon nanotubes. The surface is first functionalized using an aminosilane self-assembled monolayer that is known to have a strong affinity to carbon nanotubes. Random networks can be made by exposing the functionalized surface to a solution of carbon nanotubes whereas aligned networks are

fabricated by releasing drops of the nanotube solution on a rapidly rotating (8000 rpm) substrate. The lateral uniformity of these networks allowed us to systematically investigate for the first time the scaling laws of TFT devices in the percolation regime for various configurations (density and alignment). The detailed electrical characterization of TFT devices having channel lengths ranging from 1 to 100 μm allowed us to extract the scaling characteristics of this new thin film material. For random network TFT devices having carbon nanotube densities well below the metallic percolation threshold, scaling leads to devices having large $I_{On}/I_{Off}$ ratios for channel lengths as small as 6 μm. Finally, we showed that it is possible to control the scaling properties of nanotube networks by adjusting the arrangements of carbon nanotubes on the substrate. Aligned networks having different densities resulted in scaling properties that are distinct from those of random networks.

Despite the fact that carbon nanotubes can in principle transport both electrons and holes, it is well known that transistors based on this material are typically characterized by a type-p behavior (positive charge carriers), the ambipolar behavior being observed only when the electrical measurements are carried out under vacuum after annealing. This behavior imposes severe limitations to the use of carbon nanotubes in several microelectronic circuits necessitating both types of transistors (type-p and type-n). In order to understand the origin of this behavior and to find a solution to this major technological problem, we have studied devices made on substrates having distinct chemical functionalities: the usual thermal oxide on silicon and a layer of parylene-C, an oxygen-free insulating hydrophobic polymer. A detailed study of the electrical characteristics of the devices fabricated on these substrates and subjected to different treatments has, on one side, enabled us to fabricate devices that exhibit ambipolar devices in air and, on the other side, to clearly show that adsorption of molecules from ambient causes this behavior. Based on the known properties of the selected substrates and the temperatures required for obtaining ambipolar behavior after vacuum annealing, we propose that water vapor in air is the most probable species responsible for the loss

of the n-branch in carbon nanotube field effect devices. This investigation, carried out for both individual and network carbon nanotube devices, is of direct and immediate interest for the organic electronics community that is currently facing the same problem.

We have then demonstrated the potential of dense conducting carbon nanotube networks as high performance transparent electrodes in organic-light emitting devices as a replacement of brittle indium tin oxide layers. We have carried out a systematic investigation of the conductivity and transparency of carbon nanotube membranes as a function of thickness. High performance organic light emitting diodes (OLEDs) were implemented for the first time on transparent and conductive single wall carbon nanotube sheets. Using a 130 nm thick carbon nanotube membrane having a sheet resistance of 60 $\Omega$/square, we achieved a maximum brightness of 2 800 cd/m$^2$. The corresponding luminance efficiency of our carbon nanotube-based OLED of 1.4 cd/A is comparable to the 1.9 cd/A measured for an optimized indium tin oxide (ITO) anode device made under the same experimental conditions. A thin parylene buffer layer between the carbon nanotube anode and the hole transport layer is required in order to readily achieve the measured performance.

In order to further investigate the origin of the high charge injection efficiency of the carbon nanotube electrode observed in OLED devices, we have devised fabrication protocols which enabled us to fabricate devices where a single organic semiconductor island of pentacene is contacted by individual carbon nanotube electrodes. We demonstrated that these electrodes, although only 2,7 nm in diameter, can inject large currents (~10 µA) into pentacene islands. This approach was extended to carbon nanotubes array electrodes to inject charge in realistic organic TFT having channel widths of 200 µm. In both cases the injection efficiency was found to be superior to traditional noble metal electrodes.

Overall, this thesis contributes to the science and to the engineering of carbon nanotube networks for electronic and optoelectronic applications in several ways. First, we have clearly shown that an efficient strategy to circumvent the issue of the strong variability of nanomaterials properties with size is to use their novel 'bulk-like' ensemble properties for innovative applications. Second, we have insisted in developing solution-based techniques that are directly amenable to large-scale processes and low processing temperatures. Finally, we have clearly highlighted the importance of the substrate in controlling the electrical characteristics of devices made from nanomaterials, a fact that had been largely overlooked in the past.

# CONDENSÉ EN FRANÇAIS

Les matériaux organiques conducteurs et semi-conducteurs suscitent un intérêt grandissant dans le domaine de l'électronique. Contrairement aux matériaux inorganiques traditionnels, ils peuvent être mis en forme sur des substrats rigides ou souples en utilisant des techniques de fabrication à basse température et peu coûteuses. Ces matériaux sont particulièrement prometteurs pour les applications dites « macroélectroniques » pour lesquelles il est nécessaire de fabriquer des circuits électroniques sur de très grandes surfaces, souvent bien supérieures à une dizaine voire une centaine ou même un millier de centimètres carrés. Les matrices actives pour écrans plats, les imageurs médicaux à rayons-x numériques et les panneaux solaires sont tous des exemples d'applications macroélectroniques. La dégradation prématurée des matériaux organiques, notamment en raison de leur sensibilité à la chaleur, à l'humidité et aux solvants, constitue l'enjeu principal pour leur adoption dans ces applications à forts volumes. Dans ce contexte, l'objectif de plusieurs laboratoires industriels et académiques est de trouver de nouveaux matériaux électriquement actifs, robustes et durables pouvant être mis en forme sur des substrats souples de très grande taille, le tout à un coût très modique.

Les réseaux en nanotubes de carbone représentent un candidat idéal parmi les matériaux alternatifs pour les applications macroélectroniques mentionnées ci haut. En effet, un réseau composé d'un mélange de nanotubes comptant en moyenne deux nanotubes semi-conducteurs pour chaque nanotube métallique présente des caractéristiques électriques bien définies qu'on peut exploiter pour la fabrication de dispositifs électroniques. Par exemple, les seuls chemins de percolation électrique entre deux électrodes dans un réseau de nanotubes de faible densité (nombre de nanotubes par unité de surface) ont un comportement semi-conducteur. Par ailleurs, en raison de la très grande mobilité effective de chaque nanotube semi-conducteur ($10\,000\ cm^2/V.s$), la mobilité d'un tel réseau peut dépasser, comme nous le démontrons dans cette thèse, celle du silicium

amorphe (1 cm$^2$/V.s), la référence dans ce domaine. D'autre part, la percolation des nanotubes métalliques domine lorsque le réseau est suffisamment dense; le matériau se comporte alors comme un conducteur. Tel que nous le détaillons ci-dessous, nous avons réalisé des réseaux dont la conductivité dépasse d'un ordre de grandeur celle des matériaux organiques conducteurs tels le polyaniline et le Poly(3,4-ethylenedioxythiophene) (PEDOT). De minces couches de ces réseaux peuvent être déposées sur de grandes surfaces en utilisant des procédés par voie liquide simples et peu coûteux. En plus de posséder une très grande stabilité chimique et thermique, ces couches – semblables à des feuilles de papier dont les fibres sont des nanotubes de carbone – sont flexibles et transparentes.

L'objectif général de cette thèse était de contribuer à l'avancement de la science et de la technologie des réseaux de nanotubes de carbone dans le contexte d'applications en électronique et en optoélectronique, plus particulièrement dans le secteur de la macroélectronique tel qu'énoncé plus haut. Pour l'ensemble de nos travaux, nous avons préconisé des procédés de nanofabrication des réseaux de nanotubes par voie liquide – où les étapes se déroulent en solution et généralement à la température de la pièce, ces procédés offrant l'avantage d'être compatibles avec une grande gamme de substrats en plus de pouvoir être facilement mis à l'échelle pour la fabrication sur de grandes surfaces. Nos objectifs spécifiques furent de :

(1) Perfectionner les méthodes de fabrication de réseaux en nanotubes de carbone par voie liquide de manière à contrôler précisément la densité de nanotubes sur des substrats rigides et flexibles;

(2) Étudier le comportement électrique des réseaux en fonction de leur densité, du procédé de fabrication et de la source de nanotubes;

(3) Optimiser les propriétés semi-conductrices des réseaux de nanotubes en contrôlant leur densité et leur degré d'alignement sur le substrat afin de les incorporer à des transistors en couches minces (thin film transistors, TFTs);

(4) Étudier le transport électronique et les lois d'échelle applicables dans des dispositifs à base de nanotubes de carbone qui opèrent dans un régime de transport par percolation;

(5) Évaluer l'impact du substrat et du milieu ambiant sur les caractéristiques électriques des transistors à effet de champ à base de réseaux semi-conducteurs de nanotubes de carbone;

(6) Optimiser les propriétés des réseaux métalliques de nanotubes afin d'obtenir un maximum de transparence et de conductivité pour leur utilisation comme électrode flexible et transparente dans une diode électroluminescente organique (organic light-emitting diode, OLED);

(7) Déterminer si les nanotubes de carbone peuvent constituer des électrodes efficaces dans les TFT organiques.

Nous avons dans un premier temps établi des méthodes chimiques de purification de nanotubes de carbone permettant d'éliminer les résidus de carbone amorphe et graphitique présents dans la source brute sans toutefois endommager ou raccourcir les nanotubes. Cette étape préliminaire s'est avérée essentielle pour la mise au point et l'optimisation d'un protocole de fabrication des réseaux de nanotubes par filtration. Dans ce procédé, une solution aqueuse de nanotubes dispersés dans un surfactant est premièrement filtrée sous vide. Lors la filtration, les faisceaux de nanotubes se posent horizontalement à la surface du filtre formant ainsi un réseau de percolation bidimensionnel. La mince couche de nanotubes formée par le filtrat peut ensuite être transférée sur un substrat en dissolvant le filtre. Le contrôle de la densité du réseau se fait en variant le volume de la solution de nanotubes filtrée. Il est intéressant de noter que l'étape de filtration agit en fait comme un processus d'autorégulation assurant l'homogénéité de la couche mince de nanotubes. En effet, au fur et à mesure que les nanotubes s'accumulent sur la surface du filtre, le débit de la solution à travers le filtre diminue. Ainsi, si la couche de nanotubes devient plus épaisse dans une région donnée, le dépôt de nanotubes sera favorisé dans une autre partie du filtre ayant accumulé moins

de nanotubes. Les réseaux de très faible densité ($< 3$ nanotubes/cm$^2$) présentent cependant une certaine inhomogénéité due à l'agrégation de nanotubes sous forme d'amas. Ces amas sont typiques de nanotubes dispersés dans des solutions aqueuses de surfactants.

Un deuxième protocole de fabrication par auto-assemblage a par conséquent été développé de manière à obtenir des réseaux épars très homogènes. Pour ce faire, la surface du substrat est d'abord fonctionnalisée avec une monocouche de molécules d'aminosilane (3-aminopropyltriéthoxysilane) par un procédé de dépôt en phase vapeur. Ces surfaces fonctionnalisées ont une grande affinité pour les nanotubes de carbone dispersés dans un solvant aminé qui offre l'avantage de bien disperser les nanotubes individuels contrairement aux solutions aqueuses dans lesquelles des amas sont formés. Le dépôt sur la surface se fait alors simplement en immergeant les surfaces fonctionnalisées dans la solution de nanotubes. Il a par ailleurs été possible de promouvoir l'alignement des nanotubes selon une direction préférentielle durant le dépôt en exploitant les forces centrifuges et de séchage auxquelles sont soumis les nanotubes lorsqu'une goutte de solution est déposée sur un substrat tournant rapidement (8000 rpm). Le dépôt de gouttes additionnelles permet d'augmenter progressivement la densité du réseau de façon contrôlée.

Les propriétés électriques des réseaux fabriqués par les méthodes détaillées ci haut ont été caractérisées en utilisant une géométrie TFT. Cette configuration permet d'évaluer indépendamment les propriétés conductrices et semi-conductrices des réseaux. Lorsque la grille n'est pas polarisée (champ nul), les parcours métalliques sont les seuls responsables de la conduction dans le réseau. À partir de cette mesure la conductivité électrique des réseaux a pu être évaluée. À l'opposé, les nanotubes semi-conducteurs et métalliques participent tous deux à la conduction lorsque la grille est polarisée. La conductance du réseau en fonction du champ électrique appliqué par la grille permet d'extraire la transconductance et la mobilité effective des réseaux.

Cette approche a été utilisée pour caractériser les propriétés électriques des réseaux préparés par filtration dont les densités ($\rho$) variaient entre 2 et 300 nanotubes/$\mu m^2$. La conductivité à champ nul augmente de ~5 ordres de grandeur, de $5 \times 10^{-4}$ à 8 S/m, lorsque la densité de nanotubes passe de 4 à 7 nanotubes/$cm^2$. Au delà d'une densité de 30 nanotubes/$cm^2$, la conductivité demeure constante à 250 S/m. Ce comportement s'explique bien en considérant le réseau de nanotubes comme un système de percolation bidimensionnel composé de cylindres conducteurs. Selon les modèles développés pour les systèmes de percolations dans lesquels les cylindres sont orientés de manière aléatoire, la conductivité ($\sigma$) suit la loi de puissance donnée par $\sigma \propto (\rho - \rho_c)^{\alpha}$ où $\rho_c$ correspond à la densité critique (aussi appelé seuil de percolation) et $\alpha$ est un exposant qui dépend de la dimensionnalité du système. L'ajustement de nos données expérimentales avec ce modèle permet d'extraire une valeur de $\alpha = 1.4$, en bon accord avec la valeur prévue de 1.3 pour un réseau bidimensionnel idéal. On trouve également que la densité critique pour la percolation est de 3,7 nanotubes/$cm^2$.

Tel que nous l'avons souligné précédemment, les réseaux denses de nanotubes de carbone s'avèrent être conducteurs, flexibles et partiellement transparents. Ils sont donc particulièrement appropriés pour, par exemple, servir d'électrode transparente dans les dispositifs organiques électroluminescents (organique light-emitting diode, OLED) et les cellules photovoltaïques. Nous avons donc procédé au dopage des nanotubes semi-conducteurs par transfert de charge afin de diminuer la résistance de feuille des réseaux sans réduire leur transparence. Nous avons évalué l'efficacité de deux accepteurs d'électrons pour le dopage type-p des nanotubes de carbone : le complexe 2,3-dichloro-5,6-dicyano-1,4-benzoquinone (DDQ) et la molécule $FeCl_3$. Dans les deux cas la conductivité a été améliorée d'un facteur 7. La stabilité environnementale du dopage par DDQ rend ce complexe le plus intéressant pour les applications électroniques. Des réseaux épais de nanotubes de carbone (~ 80 nm) ayant des résistances de feuilles de 58 $\Omega$/carré pour des transmittances de 80% à une longueur d'onde de 520 nm ont ainsi

été fabriqués. Ce résultat est parmi les meilleurs rapportés dans la littérature. De plus, ces caractéristiques, obtenues pour des matériaux flexibles pouvant être mis en forme à la température de la pièce via des procédés en solution, sont comparables à celles des meilleurs oxydes inorganiques déposés sous vide à haute température présentement utilisés dans les applications commerciales.

Les caractéristiques semi-conductrices des réseaux ont également été évaluées pour toute la gamme de densités surfaciques. En premier lieu, la variation du courant lorsque la grille est polarisée (État ON) a été mesurée en fonction de la densité. Contrairement au régime conducteur décrit précédemment, la conductance du réseau varie de façon linéaire sur toute la gamme de densités. Ceci reflète le fait que la densité des réseaux est toujours au-dessus du seuil de percolation critique pour les réseaux semi-conducteurs considérés. La variation du courant dans l'état On ($\Delta I_{on}$) en fonction du potentiel appliqué à la grille ($V_g$) pour différentes valeurs de potentiel appliqué entre les électrodes source et drain ($V_{ds}$) a permis de déterminer la transconductance du réseau ($\Delta I_{on}/\Delta V_g$). Des valeurs de transconductance normalisées allant de 0.002 à 0.13 S/m ont été obtenues pour des réseaux dont la densité varie de 2 à 30 nanotubes/cm$^2$. Comme dans le cas du comportement conducteur, on observe une saturation de la transconductance (0.13 S/m) pour des densités supérieures à 30 nanotubes/cm$^2$. Cette densité est donc caractéristique (« bulk value ») des réseaux de nanotubes fabriqués par la méthode de filtration. Des valeurs de mobilités effectives – tenant compte de la géométrie des dispositifs et proportionnelles aux valeurs de transconductance – ont été évaluées afin de comparer les performances semi-conductrices des réseaux avec les valeurs citées dans la littérature. Nous avons obtenu une valeur de mobilité maximale de 42 cm$^2$/V.s pour les réseaux ayant des densités supérieures à 30 nanotubes/cm$^2$. Cependant, pour ces valeurs de densité, la percolation des chemins conducteurs mène à des courants substantiels même lorsque le potentiel appliqué à la grille est nul (État Off). Nous avons ainsi pu identifier l'étroite plage de densités surfaciques de nanotubes qui permet d'obtenir le meilleur compromis entre les deux caractéristiques électriques

essentielles pour les applications macroélectroniques des transistors en couches minces : un ratio de courants dans l'état On et Off élevé ($I_{On}/I_{Off} > 10^4$) et une transconductance maximale. Au voisinage de la densité critique pour la percolation métallique (4 nanotubes/cm$^2$), nous avons obtenu une valeur de mobilité de $\sim 5$ cm$^2$/V.s pour des ratios de courants dans l'état On et Off de $\sim 10^6$. Cette performance est parmi les meilleures mesurées jusqu'à présent pour les réseaux de nanotubes de carbone et dépasse largement celles de tout autre dispositif organique.

Nos résultats suggèrent que si les parcours purement métalliques pouvaient être éliminés, des dispositifs ayant des hautes valeurs $I_{on}/I_{off}$ et des mobilités effectives pouvant atteindre 42 cm$^2$/V.s seraient en principe réalisables. Nous avons démontré que le claquage électrique et la fonctionnalisation sélective des nanotubes métalliques, deux stratégies fréquemment proposées pour éliminer les parcours métalliques et augmenter la transconductance, ne sont pas des solutions efficaces. Un contrôle précis de la densité des réseaux semble être la stratégie la plus efficace pour contrôler les propriétés semi-conductrices.

Le transport électronique dans les réseaux de nanotubes de carbone est gouverné par la conduction par sauts. Peu de choses étant comprises sur les lois d'échelle applicables dans les dispositifs à base de réseaux de nanotubes de carbone qui opèrent dans un régime de transport par percolation, nous avons étudié le transport électronique en fonction de la longueur du canal pour des réseaux comprenant différentes configurations de nanotubes. L'uniformité de réseaux obtenus par filtration et par auto-assemblage a permis la réalisation de la première étude systématique des lois d'échelle régissant les dispositifs TFT ayant diverses configurations (densité et alignement). La caractérisation détaillée des propriétés électriques de ces dispositifs TFT dont les longueurs de canaux avaient typiquement 1 à 100 μm a permis d'extraire les caractéristiques de variabilité d'échelle de ce nouveau matériau. Pour des dispositifs TFT ayant des densités de nanotubes de carbone bien en deçà du seuil de percolation métallique, il est possible de

fabriquer des dispositifs ayant des ratios élevés de courants ouvert/fermé ($I_{on}/I_{off}$) pour une longueur de canal aussi faible que 6 µm. Finalement, nous avons démontré qu'il est possible de contrôler les propriétés des réseaux de nanotubes en ajustant les arrangements de nanotubes sur le substrat, les réseaux alignés de différentes densités ayant des propriétés différentes des réseaux aléatoirement orientés.

Bien que les nanotubes de carbone soient en principe de bons conducteurs d'électrons et de trous, il est bien connu que les transistors à base de ce matériaux sont normalement caractérisés par un comportement de type-p (porteurs de charge positifs), le comportement ambipolaire n'était possible que lors de mesures des caractéristiques électriques sous vide après recuit thermique. Ce comportement impose des limites sévères à l'utilisation de ce matériau dans les nombreux circuits microélectroniques pour lesquels les deux types de transistors (type-p et type-n) sont requis. Afin d'expliquer l'origine de ce comportement et aussi pour trouver une solution à ce problème technique majeur, nous avons étudié des dispositifs préparés sur des substrats possédant des fonctionnalités chimiques spécifiques : le répandu oxyde thermique de silicium et le parylene-C, un polymère isolant hydrophobique et exempt d'oxygène. Une étude détaillée des caractéristiques électriques des dispositifs fabriqués sur ces différents substrats et sujets à différents traitements a permis d'une part, de fabriquer des dispositifs montrant de caractère bipolaire dans l'air et, d'autre part, de clairement mettre en évidence que l'adsorption de molécules provenant du milieu ambiant est à l'origine de ce comportement. En nous basant sur les caractéristiques connues des substrats étudiées et des températures requises pour l'obtention de caractéristiques ambipolaires après recuit sous vide, nous proposons que la vapeur d'eau contenue dans l'air soit fort probablement l'espèce chimique responsable de ce comportement. Cette étude, réalisée aussi bien pour des dispositifs à base de nanotubes individuels et de réseaux de nanotubes, est d'intérêt direct pour la communauté de l'électronique organique qui fait actuellement face à ce même problème d'envergure.

Dans la dernière partie de cette thèse, l'applicabilité des réseaux en nanotube de carbone comme électrode dans les dispositifs organiques à été examinée. Un réseau de 130 nm d'épaisseur ayant 60 $\Omega$/carré de résistance de feuille pour une transparence de presque 50% dans les longueurs d'onde visibles a été choisi pour l'implémentation dans un dispositif OLED fabriqué à partir de couches sublimées de molécules organiques. L'empilement de couches semi-conductrices utilisé est basé sur la couche émettrice de tris(8-hydroxyquinoline) aluminium (Alq$_3$). Ce choix est idéal pour ces travaux puisque cette géométrie est la plus étudiée à ce jour et qu'elle est communément utilisée comme étalon pour évaluer la performance des électrodes. La performance de l'électrode en nanotubes a été évaluée en mesurant l'intensité de la lumière émise par le dispositif en fonction de la tension appliquée et du courant. Au maximum de sa luminance (2800 cd/m$^2$), le dispositif fabriqué sur l'électrode en nanotubes de carbone a une efficacité de 1,4 cd/A, valeur très voisine de celle obtenue pour un dispositif fabriqué sur ITO dans les mêmes conditions expérimentales (1,9 cd/A). L'utilisation d'une mince couche tampon de parylène placée entre l'anode et la couche organique transporteuse de trous s'est avérée essentielle afin d'éliminer la formation de piqûres (pin-holes) dans les couches de matériaux organiques évaporées sur les réseaux de nanotubes de carbone. Les dispositifs fabriqués sans cette couche de mouillage étaient court-circuités alors que les pertes de courant ont pu être réduites à seulement 20% avec l'ajout du parylène. Cette étude souligne l'importance des interfaces pour la fabrication de dispositifs qui utilisent des électrodes en nanotubes de carbone.

La remarquable performance de l'électrode plane décrite plus haut nous a mené à considérer la possibilité qu'un mécanisme propre aux nanotubes de carbone puisse promouvoir une injection plus efficace de charges. La possibilité que l'amplification de champ par effet de pointe soit à l'origine de la performance exceptionnelle a donc été étudiée. La géométrie de l'électrode plane, aléatoire et désordonnée excluant la possibilité d'étudier l'injection en détail, nous avons considéré un système modèle : un transistor nanoscopique constitué d'un îlot semi-conducteur en pentacène connecté par

deux nanotubes de carbone. Les caractéristiques électriques ont été mesurées pour 13 de ces dispositifs. Les résultats démontrent qu'un unique nanotube peut injecter de très grandes quantités de courant; des valeurs allant jusqu'à 10 µA ont été mesurées. La comparaison de ces performances avec celles des nanotransistors fabriqués avec des électrodes traditionnelles en Au nous permet de conclure que les électrodes en nanotubes de carbone injectent des charges 100 fois plus efficacement. Pour démontrer la généralité de cette approche, des électrodes de 200 µm de largeur sur lesquelles sont latéralement répartis de l'ordre de 1000 nanotubes de carbone ont été fabriquées et utilisées pour la réalisation de TFT à base de semi-conducteurs organiques. La variation linéaire du courant dans le canal pour des valeurs de tension source-drain faibles est typique d'une injection efficace de charge. Cette étude permet de conclure que les nanotubes de carbone facilitent l'injection de charge dans les semi-conducteurs organiques en comparaison avec les électrodes métalliques traditionnelles. L'effet d'amplification de champ dû à la géométrie des nanotubes semble être à l'origine de cette amélioration.

Globalement, cette thèse contribue de plusieurs manières à l'avancement de la science et de la technologie des réseaux de nanotubes de carbone pour des applications en électronique et en optoélectronique. Premièrement, nous avons insisté pour développer des techniques de fabrication en solution qui sont compatibles avec des procédés à grande échelle et à faible température.

Par ailleurs, nous avons montré qu'une stratégie efficace pour contourner le fait que les propriétés des nanomatériaux varient considérablement avec la taille consiste à exploiter les propriétés nouvelles d'ensembles de nanotubes de carbone dans des applications innovatrices. En effet, un message important qui ressort de ce travail est que les matériaux nanoscopiques doivent aussi être considérés pour les applications macroscopiques. Jusqu'à récemment, la grande majorité des applications envisagées pour les nanotubes étaient confinées à la fabrication de transistors ultra-petits. Comme

pour la majorité des matériaux nanométriques, les propriétés des nanotubes de carbone sont extrêmement variables. C'est lorsqu'on exploite leurs propriétés d'ensemble que les nanotubes se démarquent et deviennent une alternative valable aux matériaux étudiés jusqu'à présent.

Finalement, et il s'agit probablement de notre contribution la plus importante, nous avons clairement mis en évidence l'importance des interfaces dans les circuits organiques. Nous montrons comment le comportement électrique d'un dispositif TFT peut être fondamentalement modifié en variant la chimie de l'interface entre le diélectrique de grille et le canal semi-conducteur. Nous avons également fait ressortir, à travers la fabrication de dispositifs OLED performants sur des électrodes en nanotubes de carbone, que la morphologie et la chimie de l'interface entre un semi-conducteur organique et l'électrode est également primordiale. Finalement, bien que nous n'avons pas pu identifier clairement le mécanisme responsable de l'injection plus efficace de charges à partir de nanotubes de carbone, il semble évident que la morphologie de l'interface joue un rôle clé.

xxvii

# TABLE OF CONTENTS

# LIST OF TABLES

# LIST OF FIGURES

# CHAPTER 1: Introduction

## 1.1  Scope of the thesis

After decades of steady but incremental progress, we are starting to witness the beginning of a revolution in the field of electronic materials and devices. Carbon nanotubes, for example, have been proposed for the fabrication of high performance or novel devices, whereas the use of organic semiconductors is envisioned for a wide range of relatively inexpensive consumer products. This thesis brings aspects of these two fields together, exploiting the unique properties of carbon nanotubes to address challenges currently faced by organic electronics.

In this chapter, we first summarize the current performance, limitations, and challenges of organic electronic materials. We then highlight the unusual properties of carbon nanotubes and explain how these can in principle be exploited to improve the properties and manufacturing of organic electronic devices.

## 1.2  The advent of flexible organic macroelectronics

Since the Nobel prize winning discovery of electrical conductivity in polymers by Heeger, MacDiarmid and Shirakawa,[1; 2] researchers have sought ways to improve the electrical behavior of organic materials. Thanks in part to the development of new materials by improved synthetic methods, the electrical performance of organics is now close to the threshold that allows them to be considered a viable alternative to traditional inorganic materials for a large range of commercial applications.[3-5] In contrast with inorganic conductors (metals) and semiconductors (silicon, germanium, etc.), they can be patterned on both rigid and flexible substrates by using low-cost and low-temperature fabrication techniques. Presently, organic semiconductors have been shown to exhibit

field-effect mobilities between 0.1 and 10 cm$^2$/V.s.[6; 7] Although these mobility values do not yet permit these materials to compete with the silicon based technologies that are used in high performance integrated circuits, they are an ever more probable alternative for large area (> 10 cm$^2$) applications that do not require ultra-fast response times (<10 kHz). Organic semiconductors can be substituted for their inorganic counterparts in the fabrication of thin-film transistors (TFTs),[6; 7] photovoltaic cells,[8-10] and light-emitting diodes (LEDs). [11-13] Their flexibility could allow these devices to be fabricated on plastic substrates using inexpensive printing methods, thus paving the way for flexible *macroelectronics*. Organic light emitting diodes (OLEDs) for display applications are one of the first demonstrations of the organic electronics technology.[14] However, there remain considerable hurdles to be overcome for these prototypes go from the lab-bench onto commercial reality.

## 1.3   Current challenges

Perhaps the most significant obstacle to the widespread introduction of organic technologies is the susceptibility of organic materials to heat, humidity, oxygen, and most solvents.[15-18] Indeed, most organic semiconducting devices suffer from limited lifetimes due to a gradual deterioration of their properties during operation. Prototype OLEDs for flat panel displays have been demonstrated by companies such as Samsung, Sony and Phillips. However, the lifetimes of blue-emitting OLEDs are limited to 10 000 h which is an order of magnitude below what is necessary for their large scale commercialization.[1] As is the case with all other organic devices, organic TFTs are also prone to a modification over time of their operating characteristics. Pentacene TFTs, which are the most environmentally stable OTFTs, still suffer from a deterioration of their On and Off current characteristics and considerable shifting of their threshold voltage.[20] N-type organic semiconductors are particularly prone to irreversible changes

---

[1] Sony announced that it would launch a 11" OLED display on December 2007. At 2000 units per month, the production is not aimed at large scale commercialization.[19]

when exposed to air. Although many recent studies have revealed that electron conduction is a general property of organic semiconductors,[21] it is still an open question as to what makes these materials sensitive to the environment. Compounding these problems is the difficulty of making efficient electrical contacts to organic semiconductors. It is known that barriers to charge injection at the organic – electrode interface result in high operating voltages and heating.[22] Both effects rapidly accelerate the decay of device properties. Stable operation of both n-type and p-type devices is a vital requirement to building organic complementary logic circuits.

Processing is an important issue that must also be addressed. The fabrication of electronic circuits is in general accomplished through a number of processing steps in order to pattern the gate oxide, source, and drain contacts as well as interconnects. For example, the manufacturing process for thin film transistor backplanes, commonly employed in notebook computers, desktop monitors, and other display devices requires more than 5 lithography steps.[23] Optical lithography is in general not accessible because the solvents that are used with photoresists are not compatible with organic materials. Ink jet printing is often cited as an alternative to optical lithography for patterning organic circuits.[24; 25] However, these devices exhibit performances that are orders of magnitude below that of prototypes fabricated without patterning.

It is widely understood that the challenges faced by the emerging organic electronics industry is largely a materials science issue. Synthetic chemists are constantly engineering new molecules with improved stability, functionalities, and performances. An alternative strategy has been to incorporate both inorganic and organic nanoparticles into device architectures. Inorganic semiconducting nanoparticles, such as quantum dots, can be embedded into polymeric semiconductors to fabricate hybrid devices having high luminescence efficiencies.[26; 27] Metal nanoparticles are frequently dispersed in conducting polymers in order to enhance their catalytic activity, as well as their magnetic [28] and electrical properties.[29] The quest for new materials that are

electrically active while remaining robust and durable to be used with traditional organic semiconductors has become a pressing research subject in both academic and industrial laboratories. Because of their unique electrical, mechanical and thermal properties, carbon nanotubes lend themselves to the incorporation into hybrid electronic devices. Carbon nanotubes possess the chemical and environmental stability and exceptional electric transport properties that allows us to tackle long outstanding issues with organic materials.

## 1.4    Carbon nanotubes: powering up organics with nanotechnology

Among the wide range of nanomaterials that have in recent years captured the imagination of both the public and the scientific community, carbon nanotubes have generated particular excitement stemming from the revolutionary applications that have been envisioned for them.[30] Single graphite sheets rolled up to form carbon cylinders a few nanometers in diameter, single wall carbon nanotubes (SWNT) come in both the semiconducting and metallic variety. Carbon nanotubes, although highly conducting organic molecules, have been largely ignored by the organic electronics community. Most research has been dedicated to conjugated polymers and oligomers (e.g. polyaniline, polythiophenes, etc.) as well as molecular crystals from small conjugated molecules (e.g. pentacene, rubrene, anthracene).[6] Carbon nanotubes for their part have been mostly confined to the study of ultra-fast single-molecule transistors.

Indeed, individual metallic carbon nanotubes have been shown to be ballistic conductors able to withstand very high current densities without any degradation[31; 32] (100X what is possible with copper). Individual semiconducting nanotubes exhibit high current throughputs which translates into effective mobilities in the order of 10 000 $cm^2$/V.s,[33] which greatly exceed the mobilities of single crystalline silicon, the standard bearing inorganic semiconductor.

Because of their small size carbon nanotubes allow in principle very high scale integration, significantly exceeding that of current silicon based technologies.[34] Consequently, the vast array of microelectronic applications that have been proposed for carbon nanotubes require that an individual metallic or semiconducting nanotube be positioned at a precise location on a substrate. [35] This is a time consuming and complex nanofabrication technique which limits the commercialization of these devices. Materials composed of a random ensemble of carbon nanotubes have been attracting considerable amount of attention in recent years as they exploit the extraordinary properties of their nanoscale constituents while avoiding the processing drawbacks of individual carbon nanotube applications.[36-38] In particular, two-dimensional networks of mixtures of carbon nanotubes have been shown to display both conducting and semiconducting properties. Metallic carbon nanotube networks can be used in order to make flexible and transparent electrodes.[39-42] On the other hand, semiconducting nanotube networks can be used to make thin film transistor devices, bolometers and sensors. [43-45] In addition to their remarkable electrical transport properties, carbon nanotube networks are chemically inert and can withstand very high temperatures. The objective of this thesis is to investigate the potential of carbon nanotube networks to transform the field of thin film and organic electronics.

## 1.5 Objectives of the present work

The objective we set out to accomplish at the beginning of this doctoral thesis project was the demonstration that the unique electrical, mechanical and optical properties of carbon nanotubes could be put to use in thin film devices by adding functionality and improving their performance. In particular, we wanted to show that metallic carbon nanotube networks can be used as efficient electrodes in both OLEDs and OTFTs configurations. We also wanted to reveal the potential of semiconducting carbon nanotube networks as an alternative material for the fabrication of OTFTs. As the main advantage of organic electronics is the inexpensive fabrication of electronic devices over

large areas, the main focus of this work was to achieve these objectives by using solution-based fabrication techniques. In addition to devising fabrication protocols for the introduction of carbon nanotube networks in thin film device architectures, we wanted to explore in depth the transport properties and scaling issues for this new class of materials.

The thesis project can be summarized by the following detailed objectives:

- Perfect solution-based fabrication techniques that enable the production of carbon nanotube networks having controllable number densities on both rigid and flexible substrates.
- Study the electrical behavior of carbon nanotube networks as a function of their number density, fabrication procedure and carbon nanotube source.
- Optimize the semiconducting behavior of carbon nanotube networks for TFTs by controlling the density of nanotubes and their alignment on a substrate.
- Determine the scaling limits for carbon nanotube network TFTs
- Evaluate the impact of the environment on the electrical behavior of carbon nanotube networks.
- Optimize the performance of metallic carbon nanotube networks in order to achieve both the transparency and conductivity that enables their incorporation as a flexible anode for OLEDs
- Determine if carbon nanotubes can also be considered as electrodes for planar TFT type devices.

## 1.6 Outline of the thesis

In chapter 2 we introduce carbon nanotubes and carbon nanotube networks. An overview of recent advances in the field of carbon nanotube network fabrication and characterization is given. Transport in these percolating two-dimensional systems is

reviewed. Also, we present how carbon nanotube networks can be used for thin film applications. In chapter 3, the experimental techniques that were used during the course of this work are described in detail. This chapter provides in depth explanations to the experimental approach that we decided to pursue.

Chapters 4 through 8 contain the main body of the work and are where the experimental results will be presented. Each chapter is written to be self-contained and presents a specific topic relating to carbon nanotube networks and their applications. Each one of the objectives enumerated above can be found in these sections. Chapter 4 begins with the study of the electronic properties of carbon nanotube networks as a function of their density. The use of the filtration method allowed us to explore the limits of both the semiconducting and metallic performance of carbon nanotube networks. As we will see in Chapter 5, an alternate fabrication method can provide means to study how the alignment of carbon nanotubes can be used to improve the semiconducting transport properties. The scaling of carbon nanotube devices was also studied and our results are presented in this chapter. Chapter 6 explores the influence of the environment on the electronic properties of carbon nanotube networks. Our study has wide ranging implications for all thin film TFTs. The introduction of metallic carbon nanotubes as electrodes for organic devices begins in Chapter 7. We will show that metallic carbon nanotube networks are in fact compatible with organic semiconducting materials and can thus be incorporated as an efficient electrode in OLED devices. In Chapter 8 we present our results for carbon nanotubes electrodes in planar organic field-effect transistors. The advantages of carbon nanotubes over traditional electrode materials will be clearly demonstrated.

Finally, Chapter 9 provides a general discussion of the results that are presented in the thesis. We will discuss what implications our work will have in the future of organic electronic technology. The document will end with general conclusions and an outlook on the future directions of research for carbon nanotube networks in organic electronics.

# CHAPTER 2: Overview of carbon nanotube networks

The breadth of the literature covering carbon nanotube science and technology is very vast and we will only give a very brief introduction aimed at presenting the essential physical properties of this nanoscale material. For a comprehensive review of carbon nanotubes and their applications, we refer the reader to the numerous books that have been written on the subject.[46; 47]

The remainder of this chapter will be devoted to a review of the recent foray of carbon nanotubes into the field of thin film and organic electronics applications. For the past five years the main force driving developments in the field of thin carbon nanotube networks has been the introduction of improved nanofabrication techniques. All techniques that have been used to fabricate these networks will be described in detail. The electrical properties of these networks will also be reviewed. Finally, special attention will be given to the incorporation of carbon nanotube networks as passive (i.e. electrodes) and active (i.e. transistors) elements in thin film device applications, the main focus of this thesis work.

## 2.1 A brief introduction to carbon nanotubes

Discovered by Ijiima in 1991,[48] carbon nanotubes are part of the family of carbon fullerenes. They can be thought of as a graphene sheet rolled to form a seamless tube as pictured in Figure 2-1. The length and direction along which the tube is rolled will give rise to a distinct structure. For this reason, carbon nanotubes are identified by their chiral or roll-up vector, $C_h = na_1 + ma_2$, where $n$ and $m$ are integers $(0 < m < n)$, $a_1$ and $a_2$ are the real space unit vectors of the hexagonal lattice of a graphene sheet shown in Fig. 2-1. The nanotube is formed by joining both ends of the roll-up vector.

A

zigzag

roll-up vector

armchair

Roll-up vector
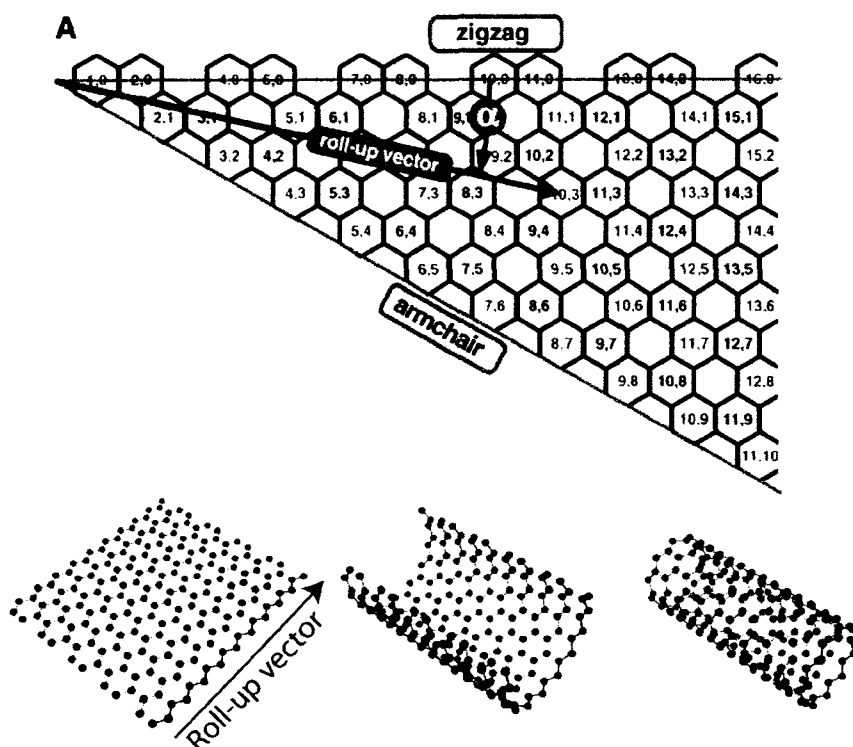
Figure 2-1. Hexagonal structure of a graphene sheet with all possible carbon nanotube chiral vectors indicated. In red and blue are the metallic and semiconducting carbon nanotubes respectively. The nanotube is formed by joining the ends of the roll-up vector as illustrated in the bottom figure for an arm-chair nanotube. (Image modified from references [49; 50])

The one-dimensional electronic band structure of carbon nanotubes can be calculated by zone folding methods of the two-dimensional band structure of graphite. First approximation tight binding calculations allow the prediction of the electronic properties of carbon nanotubes for every possible roll-up vector. From this model, it is known that $(n,m)$ nanotubes will be metallic if $(2n + m)$ is a multiple of 3 and semiconducting for the other combinations. Moreover, the one-dimensional confinement results in Van Hove singularities in the density of states. The optical properties of carbon nanotubes are dominated by the excitonic transitions associated with these Van Hove singularities. Figure 2-2 displays an example of the density of states for both semiconducting and metallic carbon nanotubes. The first and second transitions for the semiconducting

carbon nanotube having chiral indices (10,9) are indicated as $E_{11}^S$ and $E_{22}^S$, respectively. For semiconducting carbon nanotubes it has been determined that the band gap follows the inverse relationship:

$$E_{gap} \propto \frac{1}{d} \qquad (2.1)$$

where $E_{gap}$ is the band gap and d is the nanotube diameter. For the carbon nanotube having chiral indices (10,10) the density of states is non vanishing at the Fermi level resulting in a metal. The first interband metallic transition is also identified in Figure 2-2.
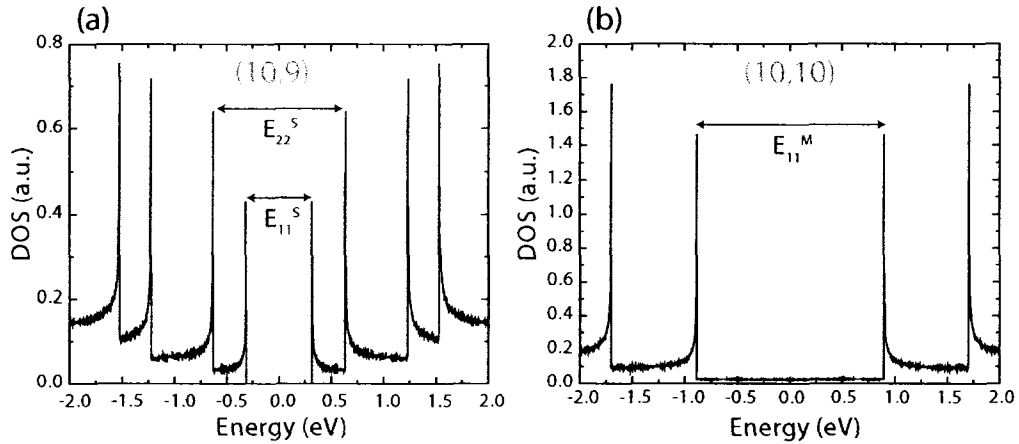


Figure 2-2. Density of states evaluated by tight-binding calculations for a semiconducting carbon nanotube having chiral indices (10,9) and a metallic carbon nanotube having chiral indices (10,10). The optical transitions associated from the van Hove singularities are indicated.

The so-called Kataura plot representing the optical transitions as a function of carbon nanotube diameters is commonly used in order to rapidly characterize a bulk sample. In particular, the diameter distribution can be estimated by the position and linewith of the associated peaks appearing in the absorption spectrum. Figure 2-3 shows the Kataura plot superimposed with the diameter distribution of 1 to 1.4 nm that is typical of laser ablation carbon nanotubes with their corresponding absorbance spectrum.
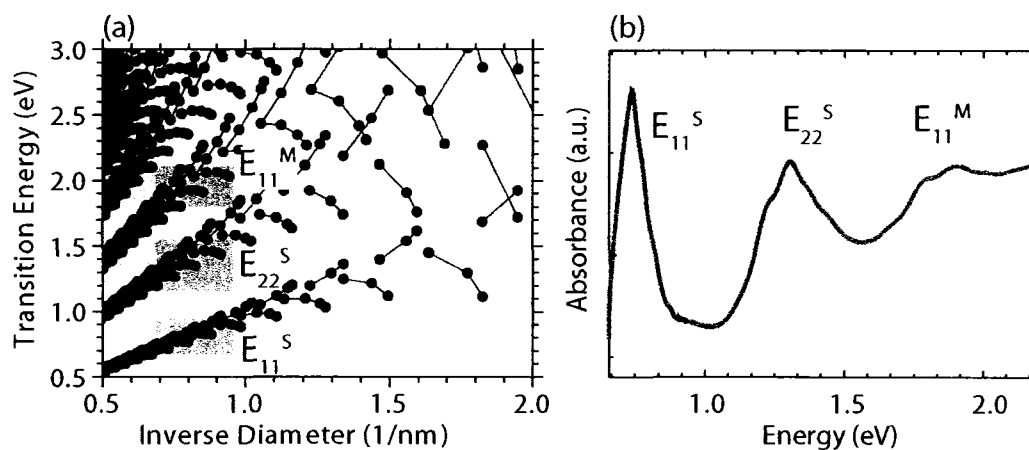
Figure 2-3. Determination of the diameter distribution for a bulk sample of laser ablation carbon nanotubes. (a) Kataura plot with the diameter distribution (1-1.4 nm) highlighted in green and (b) The corresponding optical absorption spectrum from an aqueous carbon nanotube solution

In general, all synthetic methods result in a statistical distribution of carbon nanotubes having different chiralities around a given diameter. Based on the tight-binding approximation model, there should be about two semiconducting carbon nanotubes for every metallic one. All optoelectronic properties of networks of carbon nanotubes will reflect the spread in diameters of the given bulk sample. For example, the near-infrared photoluminescence spectra from aqueous dispersions of carbon nanotubes show sharp well resolved peaks corresponding to excitonic transitions from individual carbon nanotubes. Our group has recently shown that the broad electroluminescence spectrum of these networks is a superposition of the individual peaks of the many nanotubes that compose the network.[51] The study of carbon nanotube networks relies on our ability to fabricate devices having controllable electrical and optical properties.

## 2.2    Fabrication of carbon nanotube networks

The techniques enabling the fabrication of carbon nanotube networks can be based on three different strategies: the direct growth of carbon nanotube networks onto substrates, the inclusion of nanotubes into a polymeric embedding medium, and wet-chemical and self-assembly techniques from solution.
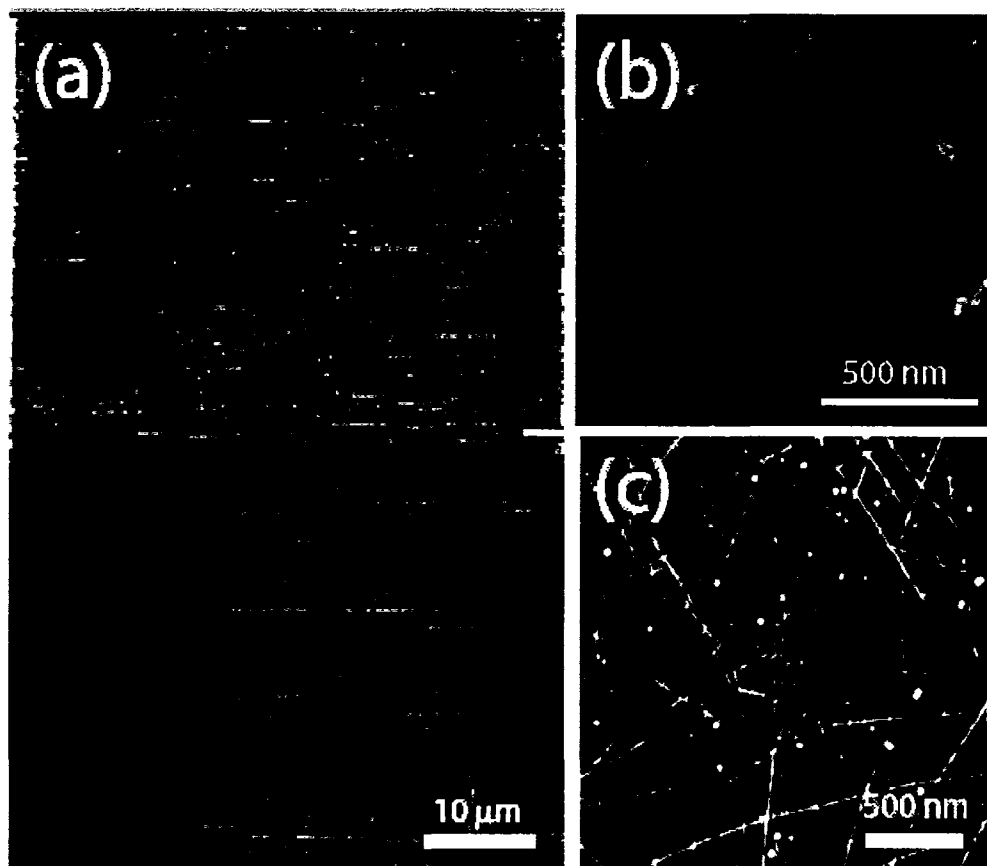


Figure 2-4. Carbon nanotube networks using different fabrication techniques (a) Carbon nanotubes fabricated by CVD on quartz substrates [52] where the control of both the density and alignment was shown possible. (b) Dense network fabricated using the vacuum filtration technique (this work). Note that with this approach nanotubes are in the form of small bundles of 2 to 5 nanotubes. (c) Networks fabricated by self-assembly on functionalized substrates (this work). Nanotubes do not agglomerate and they are mostly individualized.

The growth of carbon nanotube networks directly onto a substrate surface is generally accomplished by chemical vapor deposition methods (CVD). [53; 54] This requires metallic catalyst nanoparticles (Fe, Ni, Au, Co,etc) to be deposited on the substrate surface in order to promote nucleation and the high temperature catalytic decomposition of hydrocarbon precursors (e.g. methane, ethanol, ethylene, etc). Since the processes of nucleation and growth of carbon nanotubes takes place on the surface of the catalysts, the carbon nanotube network coverage can be controlled by varying the density of the deposited nanoparticles. Other synthesis parameters such as the temperature, pressure, humidity, carbon feedstock, and the flow rate also influence the final outcome. Control of network properties thus relies on one's ability to reproduce the growth parameters.

Most CVD methods normally produce SWNTs having diameters between 1 to 6 nm.[53] The density of the networks is limited to single monolayer coverages as the growth of carbon nanotubes depends on the availability and activity of the catalyst particles. However, one of the main advantages of this method is the possibility of producing networks in a continuous fabrication process. This method is also quite versatile. Moreover, carbon nanotubes can be aligned along a given direction by either applying an electric field during their growth [55] or growing them along the step edges of quartz or sapphire substrates (see Figure 2-2a for aligned nanotubes). [56] The main disadvantage is the large diameter distributions (0.9-3 nm). This in turn will yield networks having a large range of optoelectronic properties. Furthermore, the high temperature growth conditions required are incompatible with polymeric substrates. A solution to this was explored and consists of transfering onto flexible substrates after their growth. The necessity to transfer the nanotubes from one substrate to the other adds a nontrivial fabrication step to this protocol.[52]

The second strategy consists in dispersing carbon nanotubes into a polymeric matrix where they form a three-dimensional percolation network. The composite polymer-

nanotube material can then be deposited in thin films using traditional printing techniques, such as flexography, heliography, ink jet printing or with the help of a spin coater. The polymeric matrix may or may not be electrically active thereby giving the functionality of the material. However, the difficulty in dispersing uniformly a large fraction of carbon nanotubes into polymers is an important drawback[57-60] as carbon nanotubes tend to agglomerate together in the matrix. So far, researchers have been able to disperse up to 10% by weight of nanotube material into polymeric matrices. The conducting properties of the composites are at best 30 S/cm[61] and could be significantly increased, if loading of dispersed carbon nanotubes could be achieved.

Solution based methods for making nanotube networks on the other hand do not rely in the presence of the embedding medium; the dispersion of carbon nanotubes onto substrates involves simply the assembly directly from the solution. Solution based assembly is particularly attractive since it avoids the drawbacks of the previous two techniques. Firstly, it enables the fabrication of networks having a wide range of thicknesses, from sub-monolayer coverage to over 1 μm thick. Secondly, since carbon nanotubes are the sole constituents of the network there is no upper limit on the number of nanotubes imposed by dispersion issues. Thirdly, the possibility of working with commercially available carbon nanotube sources opens new possibilities. For example, the full range of optoelectronic properties of carbon nanotubes can be explored with carbon nanotubes having a given diameter or chirality. This in possible since they can be separated in solution prior to their deposition using the most recent experimental protocols. Finally, solution based techniques are most amendable to large scale production, given the simplicity of the equipment required. Spray coating,[62; 63] Langmuir-Blodgett, [64] vacuum filtration,[37; 41] and functionalization driven self-assembly[65-67] are examples of solution based methods. Special interest will be given during this chapter to the last two cited techniques as they are the ones that were retained for this work. The reasons that motivated our choice will be made clear when we present the bulk of our work.

Two main strategies are currently used to make solution based network: i) vacuum filtration and ii) self-assembly on a functionalized substrate. The vacuum filtration method for fabricating carbon nanotube networks was developed independently by two research groups.[41; 68] Networks having different thicknesses (e.g. optical transparencies) made from the vacuum filtration method deposited on both glass and PET substrates are shown in Figure 2-5. The networks are semitransparent thus the university logos can be seen through them.[2] The different thicknesses of the networks result in different degrees of optical transparencies as can be seen in the bottom three networks. The fabrication protocol requires that a solution of individualized carbon nanotubes be filtered using a standard vacuum filtration apparatus. In Wu *et al.*[41] version of this procedure, an aqueous suspension of nanotubes in a surfactant is filtered through acetate cellulose filters. During the filtration, the carbon nanotubes will gradually deposit on the filter surface forming a percolation network. This thin carbon nanotube film, which is in fact the filter cake, can then be transferred on a surface by dissolving the filters in an appropriate solvent. An elegant alternative strategy was recently proposed by Rogers *et al.*[68] and consists of using rigid insoluble filters. The nanotube networks are then transferred to another substrate by using an elastomeric stamp. In either case, the thickness of the network can be controlled by varying the amount of carbon nanotube solution that is filtered. Homogeneity is assured by the process of filter cake formation. Indeed, as carbon nanotubes accumulate on the filter surface, the flow resistance in these regions increases. If the carbon nanotube network becomes thicker in certain regions, the flow of solution will increase towards regions that have accumulated less carbon nanotubes and so forth. Thin sheets of carbon nanotubes that are optically homogeneous and exhibit low surface roughness (~12 nm RMS) can easily be fabricated using this method.[39; 41; 68] (See Figure 2-5)

---

[2] Note that the glass substrates are transparent and thus cannot be clearly seen in the image. For all three networks deposited on glass, microscope slides where used as the substrate.

Université
de Montréal

Figure 2-5. Carbon nanotube networks having different thicknesses fabricated using the vacuum filtration method. The networks can be deposited on both glass (bottom three networks) and flexible polyethylene terephthalate (top network).

The second strategy we have explored is the self-assembly of carbon nanotube networks on functionalized substrates. Functionalization is achieved through the deposition of a layer of amino-silane molecules.[65-67] The silane end-group covalently attaches to the oxide surface through a reaction with hydroxyl groups (-OH). Such amino functionality imparts the surface with an affinity to colloidal particles. Amino-terminated surfaces are commonly used to immobilize enzymes, DNA and metal nanoparticles.[69; 70] It is believed that the primary amine on the surface is what renders these surfaces reactive. Although the mechanism of adhesion is not well understood, it has been demonstrated that carbon nanotubes attach to these surfaces with high yield.[65; 66] This strategy had been used to anchor individual carbon nanotubes in predefined regions of a substrate. As will be demonstrated in Chapter 5, the use of this technique has enabled us to fabricate networks from individual carbon nanotubes with and without preferential alignment on a

substrate. This strategy allows us to make features that are not possible using the vacuum filtration method described above.

## 2.3 Electrical properties of carbon nanotube networks

The electrical properties of carbon nanotube networks depend on the characteristics of the nanotube source that was used to fabricate them as well as on the number density of nanotubes that compose the network. As discussed above, the different methods used to fabricate the networks lead to nanotubes having different distributions of diameters, lengths, and chiralities. Most synthetic approaches lead however to a statistical distribution of nanotubes that contains on average two semiconducting nanotubes for every metallic nanotube. Regardless of the source of nanotubes that is used, the properties of the networks will depend on their density. The network will undergo a transition from insulating to semiconducting to metallic electric transport behavior as the density of carbon nanotube increases. As explained in section 2.3.2, the intermediate semiconducting regime can only be probed using a three terminal device where the transverse electric field dependent characteristics of the network are revealed.

## 2.3.1 Metallic networks

Under no external electric field, the semiconducting carbon nanotubes are insulating and only the metallic carbon nanotubes are responsible for electric conduction.[68; 71; 72] Percolation theory can be applied to conducting carbon nanotube networks in order to explain their behavior.[73; 74] As the surface number density of metallic carbon nanotubes in the network increases from a sparse coverage to a dense continuous coverage, the system will undergo a transition from insulating to metallic. The critical density for the transition, called the percolation threshold ($\rho_c$), is a function of the length ($L_{NT}$) of the nanotubes in the network. For percolation of conducting sticks the critical density in nanotubes per unit area is given by,[52]

$$\frac{\rho_c L_{NT}^2}{3} \sim \frac{4.326^2}{\pi} , \text{[3]}$$  (2.2)

Because of the very high aspect ratio of carbon nanotubes ($L_{NT}/d > 1000$), the percolation threshold is achieved at very low carbon nanotube densities.[75] In the case of carbon nanotubes dispersed in a polymeric matrix (3D networks), this has been found to correspond to approximately 0.1 %[59] of nanotubes by weight. In the case of carbon nanotubes deposited on a surface (2D networks), the percolation density corresponds to $\sim 2.6$ nanotubes/$\mu m^2$[76] for nanotubes approximately 1.5 $\mu m$ in length.

Percolation in carbon nanotube networks can be studied by evaluating their DC conductivity in the region close to their percolation threshold. At this point, the conductivity ($\sigma$) should follow a power law dependency given by:

$$\sigma \sim (c - c_c)^\alpha ,$$  (2.3)

where $c$ is the number density of metallic nanotubes deposited on the surface and $\alpha$ is the power law exponent whose value will depend on the dimensionality of the network (2D or 3D), as well as on geometrical parameters (alignment, bunching, etc.). This value will be $\alpha = 1.3$ and $\alpha = 1.9$ for random 2D and 3D networks, respectively as determined from numerical models. Well above the percolation threshold, metallic conduction dominates and the material behaves like a bulk metal.[68; 77] The conductivity of the network is then constant and the resistance varies linearly with the effective thickness[4] of the network. The bulk value of the conductivity is a function of the conductivity of the individual metallic paths (i.e. metallic carbon nanotube conductivity) but is mostly

---

[3] The 3 in the denominator takes into account that only a third of the nanotubes in the network are metallic.

[4] The effective thickness refers to the thickness measured by atomic force microscopy for thick nanotube networks (20-200 nm). This value is inferred for thin networks (< 15 nm) from the optical density using Beer's law.

limited in carbon nanotube networks by the contact resistance at each nanotube-nanotube junction. An example of the evolution of the DC conductivity as a function of the thickness (i.e. density) is given in Figure 2-6. The conductivity follows the expected power law dependence with a critical density of 1 nanotube/$\mu m^2$ and critical exponent of 2.6.
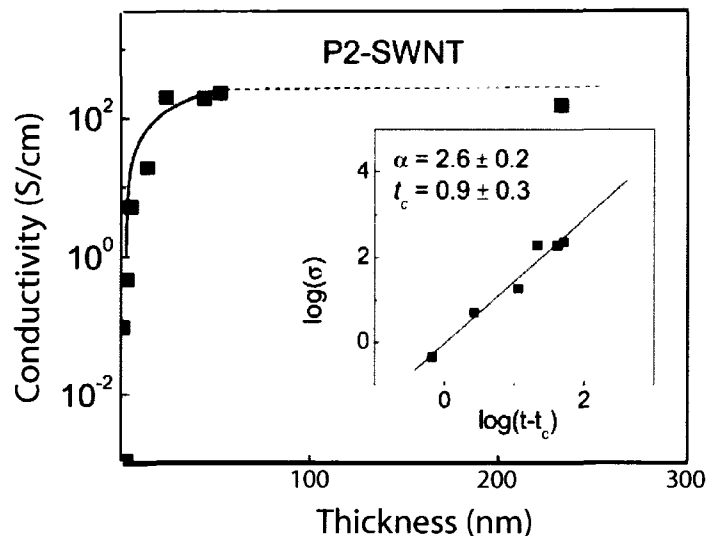


Figure 2-6. Conductivity as a function of the network thickness ($t$) for carbon nanotube synthesized using the arc discharge technique.[77] The power law dependence is typical of transport in percolation systems with a critical density given by $t_c$ and a power law exponent $\alpha$.

Many academic and industrial research groups are working towards achieving conducting carbon nanotube networks.[37] In optoelectronic applications, the challenge is to fabricate networks that are highly conducting while remaining sufficiently thin to be transparent. This imposes the least amount possible of carbon nanotube material to be used. The group at Dupont, for example, has attempted to achieve this by embedding carbon nanotube in polyaniline. With this, they have demonstrated a conducting polymer that it is possible to increase the conductivity by simply adding carbon nanotubes.[61] However, thin conducting sheets containing only carbon nanotubes exhibit higher conductivity values. Table 1 presents a summary of the electrical conductivities of transparent carbon nanotube networks fabricated through a number of different techniques, carbon nanotube sources and embedding media.

Table 2-1. Conductivity of carbon nanotube networks fabricated using different protocols and carbon nanotube sources

| Description | Year | Nanotube source | Conductivity | Reference |
|---|---|---|---|---|
| Carbon nanotube/polyaniline composite | 2003 | HiPCO | 30 S/cm | Dupont[61] |
| Affinity template driven assembly | 2004 | Raw laser ablation | 50 S/cm | UT-Dallas[78] |
| Filtration and dissolution | 2004 | Purified laser ablation | 6600 S/cm | UF-Gainesville[79] |
| Spay coating | 2005 | Purified electric arc | 400 S/cm | UC Riverside[77] |
| Filtration and transfer | 2006 | Electric arc | 2 000 S/cm | UCLA[79] |
| Filtration and dissolution | 2006 | Purified laser ablation | 1 200 S/cm | This work[39] |

## 2.3.2 Semiconducting networks

Near the metallic percolation threshold discussed in the previous section, carbon nanotube networks usually exhibit semiconducting behavior. The semiconducting carbon nanotubes in the network are responsible for the field-effect modulation of the conductivity. When a transverse electrical field is applied to the network, the semiconducting carbon nanotubes become electrostatically doped which adds new percolation paths and increases the conductance. We refer to this as field-effect induced percolation.[6; 52] In a thin film transistor where the networks compose the semiconducting channel, when the gate is not polarized (zero field), metallic percolation paths are the only ones responsible for the conduction in the network. On the other hand, both metallic and semiconducting carbon nanotubes participate to the conduction in the channel when the gate is polarized. The ratio of the current in these two regimes ($I_{on}/I_{off}$)

is a measure of the number of semiconducting versus purely metallic percolation paths. As for the case of field-effect transistors fabricated from a single carbon nanotube, carbon nanotube network TFTs (TFT-NT) exhibit p-type conduction behavior in air. As explained in section 2.5 of this chapter, an effective value for the mobility can be extracted from the transconductance for TFT-NTs. Although this value is not a true measure of the drift velocity of charge carriers, it is calculated in order to benchmark the performance of TFT-NT to other TFT devices. It has been observed that in general the mobility of carbon nanotube networks increases with the number of carbon nanotubes. Unfortunately, increasing the density of carbon nanotubes also increases the number of metallic percolation paths. The challenge in the case of semiconducting carbon nanotubes is to obtain the largest possible values of mobility (i.e. transconductance), while maintaining $I_{on}/I_{off}$ ratios that are sufficiently high for allowing these devices to be considered for electronic applications (>10 000).

## 2.4 Applications of carbon nanotube networks

### 2.4.1 Metallic carbon nanotubes networks as electrodes

The search for alternative materials that can be used as electrodes for organic devices is motivated by the poor performance of most electrodes used to date. Indeed, it is difficult to efficiently inject charges at the electrode – organic interface. Barriers to charge injection result from the band offset between the metal Fermi level and the HOMO or LUMO level of the semiconductor.[80; 81] A number of theoretical and experimental works have highlighted the importance of the electrode work function,[80; 82; 83] doping levels, [84] interfacial traps and dipoles[85] as factors determining the height of the barriers at these interfaces.[13; 84; 86] It has been found that the morphology of the interface also plays a primary role. Because of these barriers most organic devices require high voltages for their operation. The power that is consumed by the device is considerable and leads to the rapid degradation of organic materials.

Few studies have explored the use of carbon nanotubes as a potential electrode for organic electronics in spite of the numerous advantages that this material displays.[87-89] Because an individual carbon nanotube (~ 1 nm in diameter) can be several micrometers long, the length/diameter ratio is extremely large. The field at the tip of the nanotube is thus enhanced by several hundred times compared to the applied external voltage. This, in turn, narrows the effective barrier for an electron to escape the carbon nanotube through Fowler-Nordheim tunneling. This effect is exploited in carbon nanotube field-effect emitters, which emit electrons into the vacuum.[90] In principle, the same effect can also be employed in order to enhance the injection of charge from a carbon nanotube into an organic semiconductor. In Figure 2-7 the field enhancement at the tip of a metallic carbon nanotube placed in vacuum as a function of the aspect ratio is shown. The electric field is enhanced more than 350 times for a carbon nanotube 1 μm long and 1 nm in diameter. In addition to providing an alternative route to lowering injection barriers at the electrode-organic interface, carbon nanotube networks are transparent and flexible. Their work function has been calculated to be between 4.5 and 5.1 eV,[91; 92] which is comparable to the work function of ITO, the traditionally used transparent electrode for organic photovoltaic devices and OLEDs. Moreover, it is possible to tune the carbon nanotube work function through charge transfer doping to better match the HOMO and LUMO band of a given organic semiconductor, allowing in principle both the injection of electrons and holes respectively.
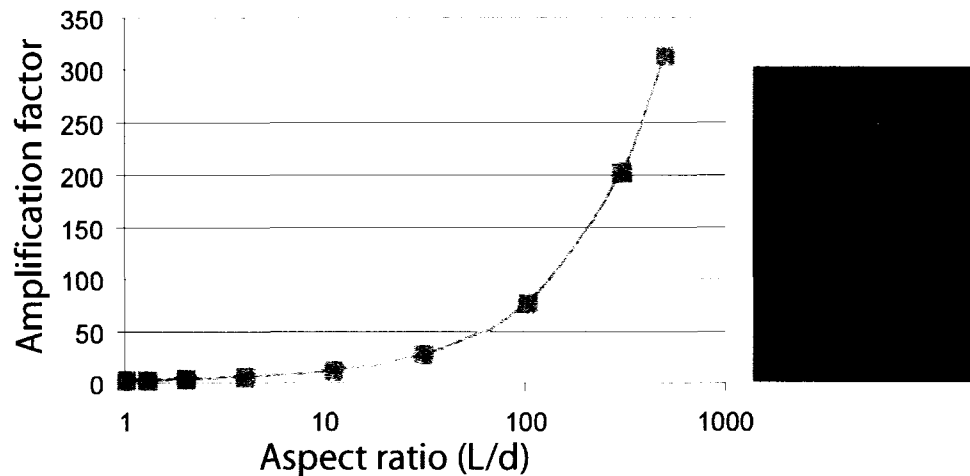
Figure 2-7. Finite element calculation of the field amplification at the tip of a carbon nanotube as a function of the aspect ratio calculated using a numerical simulation package (Comsol). The inset illustrates the amplitude of the field for a carbon nanotube 20 nm in length and 1 nm in diameter.

The use of metallic carbon nanotube networks as transparent and flexible electrodes is not a new idea. The first patent for a transparent and conducting carbon nanotube network was granted in 1998. [93] The team at the École Polytechnique Fédérale de Lausanne published in 1996 the first study of the junction between carbon nanotubes and a semiconducting polymer. They reported that the threshold voltages necessary to observe current flow at this interface were lower than with ITO. It was not until recently, more than 10 years later, that the first prototype organic devices incorporating carbon nanotube electrodes finally emerged. The principal obstacle to the incorporation of carbon nanotube networks in these devices was the unavailability of appropriate fabrication protocols for making carbon nanotube networks that were homogeneous and optically transparent, while remaining sufficiently conductive. As we have described in section 2-2, methods have recently been proposed for fabricating highly conducting and transparent carbon nanotube networks. Our group has been in the forefront of teams that

have acquired the necessary know-how for finally making carbon nanotube networks interesting for potential applications.

At the end of 2005, the first results on the use of carbon nanotube networks as a transparent anode for photovoltaic cells and OLEDs were published.[40; 42] Even if these prototypes provided the impetus for continuing to explore carbon nanotubes as an alternative electrode material, the performance of the devices was far from what was already possible with traditional ITO electrodes.[40] The photovoltaic cell exhibited an energy conversion efficiency of only 1% compared to 5% for similar devices on ITO anodes. The polymeric LED device displayed light output of only 100 cd/cm$^2$ compared to 10 000 cd/cm$^2$ for the same devices on ITO. [42] The first OLED device displaying performances comparable to state-of-the-art OLED devices on ITO were fabricated as part of this thesis work. Since, our work was published (May 2006),[39] a number of groups have followed and reported similar performances.[37; 94] This work demonstrates that carbon nanotubes electrodes are an alternative to ITO for OLED applications. This will be presented in detail in chapter 7. In chapter 8 we will also demonstrate that carbon nanotube networks can be used to fabricate electrodes for injecting holes in TFT devices.

## 2.4.2 Semiconducting carbon nanotube networks for organic thin-film transistors

Thin film transistors are a particular type of metal-insulator-semiconductor field-effect transistor (MISFET) characterized by the thin semiconducting layers that compose the channel of the device. Unlike the complementary metal-oxide-semiconductor (CMOS) technologies that are used for making integrated circuits, TFTs commonly use amorphous or polycrystalline silicon instead of the monocrystal silicon. Alternatively, the semiconducting layer can be made of organic materials, nanowires, carbon nanotubes or any other semiconducting material that is amendable to thin film deposition. The back gated thin film transistor geometry is illustrated in Figure 2-8.
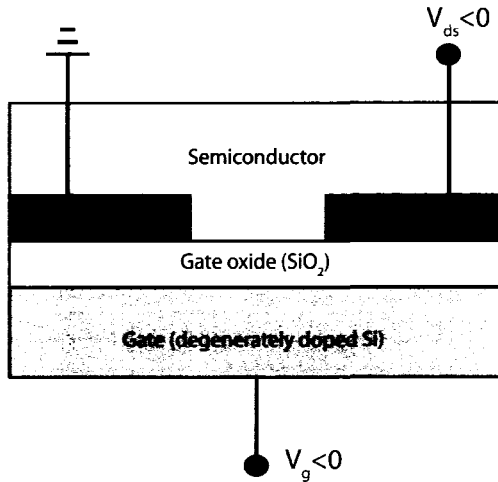
Figure 2-8. Schematic of a TFT device fabricated on a silicon wafer covered a thin thermal oxide. In this configuration the device is in p-channel accumulation or depletion modes. The source is grounded and a potential is applied at the gate and drain. Holes are injected by the source electrode and colleted at the drain.

Both organic and carbon nanotube field-effect transistors operate in the accumulation mode because they are usually undoped. That is, negative (positive) gate voltage ($V_g$) accumulates holes (electrons) at the interface between the semiconductor and the gate oxide inducing a conducting p-channel (n-channel) between the source and the drain electrodes. Charge will then be allowed to flow between source and drain when a voltage is applied between them. The amount of current through the channel will depend on the carrier mobility ($\mu$) times the concentration of carriers of a given semiconductor. On Figure 2-9a we show an example of transfer characteristics displaying modulation of the current between source and drain ($I_{ds}$) as a function of the gate voltage.

Degenerately doped silicon wafers[5] with thin thermal oxide layers having high dielectric constants ($\varepsilon$) are commonly used for fabricating prototypes of these devices. Typically a back-gated geometry, displayed in Figure 2-8, is used as a convenient way to fabricate

---

[5] Degenerately doped Si wafers are commonly used as a replacement of the typical metal gate electrode for prototyping purposes.

many prototypes of these devices over large areas. The use of oxidized silicon wafers also provides a high quality gate insulator having a high dielectric constant ($\varepsilon$). The geometry of TFT devices is defined by the width ($W$) and length ($L$) of the channel, as well as the thickness of the oxide layer ($d$). The behavior of these devices in the diffusive regime is well understood and has been modeled extensively for inorganic devices. An example of the current-voltage ($I_{ds}$-$V_{ds}$) characteristics, also called the output characteristics, is given in Figure 2-9b.
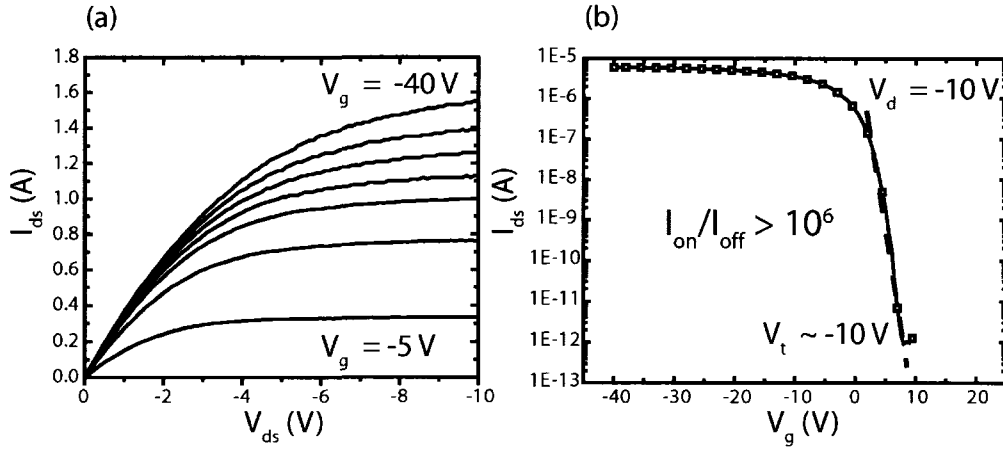


Figure 2-9. Operational characteristics of a thin film transistor device. Output characteristics under negative bias (a) and transfer characteristics (b) of a TFT device. The output curves clearly display both the linear and saturation regions. The transfer characteristics display saturation at high voltages, which is a particularity of carbon nanotube TFTs.

For positive (negative) gate values above the threshold for conduction in the channel ($V_g$ > $V_{th}$), $I_{ds}$ increases linearly with the voltage applied between source an drain ($V_{ds}$) and is given by the following equation (transistor in the linear region):

$$I_{ds} = \mu(W/L)C_{ox}[(V_g - V_t)V_{ds} - V_{ds}^2/2],\qquad(2.4)$$

where $C_{ox}$ is the gate capacitance per unit area. As the value of $V_{ds}$ increases, the carrier concentration at the drain region will decrease for a given value of $V_g$. The current in the

device reaches a saturation regime and the channel is said to be pinched off. The current in the channel (saturation regime) is then given by:

$$I_{ds} = \frac{1}{2}\mu(W/L)C_{ox}(V_g - V_t)^2.$$ (2.5)

The value of the mobility can be extracted from the transconductance $(g_m)$. This can be calculated in the linear regime using:

$$g_m = \left.\frac{\partial I_{ds}}{\partial V_G}\right|_{V_{ds}<V_{sat}} = \mu\frac{WC_{ox}}{L}V_{ds}$$ (2.6)

The mobility can also be extracted from the slope of $|I_{ds}|^{1/2}$ vs. $V_g$ in the saturation regime. Either way of calculating the mobility should yield the same value.

It was however shown that this relation is no longer applicable for devices with injection barriers at the source-semiconductor interface.[22; 95; 96] In fact, this is the case for most of the organic semiconductor devices, where the Schottky barrier contacts limits current injection. Thus, the application of the equations mentioned above to TFT-NTs should be done with caution. First, the carbon nanotube networks are two-dimensional materials and there is a limit to the amount of charge that can be accumulated in the channel.[97] Second, the width and length of the channel are not well defined due to the low fill factor of networks. Thus, the channel capacitance is not known. Therefore instead of calculating a mobility value, which requires knowledge of the capacitance, a normalized transconductance $(g_{normalized})$ can be calculated:

$$g_{normalized} = \left.\frac{1}{W}\frac{\partial I_{ds}}{\partial V_G}\right|_{V_{ds}<V_{sat}}$$ (2.7)

However, it has been demonstrated that the true mobility of carbon nanotube networks differs by less than 50 % from the mobility that is calculated by assuming the full parallel plate capacitance,[98]

$$C = \frac{WL\varepsilon_{ox}}{d_{ox}},\qquad\qquad(2.8)$$

where $\varepsilon_{ox}$ and $d_{ox}$ are the gate oxide permittivity and thickness respectively. Most published results on TFT-NT provide the value of the mobility that is calculated by using this approximation.[38; 43; 76; 99] We will refer to this value as the effective mobility and will use it in order to compare our results to those that are reported in the literature.

Another important aspect of carbon nanotube devices is the sizable hysterisis that is observed in the transfer characteristics. During a 20 to -20 gate voltage scan, the hysterisis has been measured to be more than 10 V. An important consequence is that the threshold voltage cannot be determined as it will shift considerably from one measurement to the next and will depend of the operation history of the device. Also important is that the hysterisis does not allow for the precise measurement of device characteristics. As such, the semiconducting properties of networks, namely the transconductance, the sub-threshold slope and the effective mobility are always underestimated. This behavior is not yet fully understood but various explanations have been proposed.[100-103] However, by using very thin gate oxides or high-k dielectrics, it has been shown that this effect can be eliminated.[104; 105]

Only a handful of groups have explored the use of carbon nanotube networks for TFT applications. As mentioned previously, it is difficult to fabricate networks with well-defined semiconducting properties having both high mobilities and high $I_{on}/I_{off}$ ratios. The researchers at the *Naval Research Laboratory* were the first to publish their results for carbon nanotube network TFTs in 2003.[38] They used the direct growth of carbon nanotubes by CVD on a silicon substrate having oxide thickness ($d_{ox}$) of 250 nm.

They were able to obtain effective mobility values of $\mu_{effective} = 7$ cm$^2$/V.s and $I_{on}/$ $I_{off}$ ratios of $10^5$ for carbon nanotube networks having a density of 1 nt/$\mu$m$^2$. Using C ~ $\epsilon/d_{ox}$ performances are comparable to what is possible with amorphous silicon TFT ($\mu = 1$ cm$^2$/V.s $I_{on}/$ $I_{off} = 10^5$) and are by far superior to any other known organic semiconductor.[6] The group mentioned however that it was difficult to obtain consistent semiconducting behavior. They reported that different semiconducting behaviors were obtained for every synthesis run. Indeed it took them two more years before reporting the fabrication of TFT-NT devices on flexible substrates.[106] Since high temperature CVD methods are not applicable with polymeric substrates, they fabricated the network by self-assembly on a functionalized surface instead. By using this technique they were able to fabricate networks having mobilities of 150 cm$^2$/V.s but $I_{on}/$ $I_{off}$ ratios of only $10^2$. Although the mobility was improved by two orders of magnitude the high current in the on state is not suitable for applications.

The group headed by Prof. George Gruner at the University of California Los Angeles has used a similar surfactant based method for fabricating carbon nanotube transistors on flexible polyethylene teraphtalnate (PET) substrates, but obtained mobilities of only 1 cm$^2$/V.s and ratios of $I_{on}/I_{off} = 10^2$.[43] The agglomeration of carbon nanotubes in surfactant solutions seems to be responsible for the poor performance of these devices. Significant mobility values (>1 cm$^2$/V.s) can be obtained only when sufficient semiconducting carbon nanotubes are on the surface. This occurs when the threshold for metallic percolation is reached.[107]

The best performances to date for TFT-NT have been obtained by Rogers *et al.* The CVD technique developed by this group allows them to grow carbon nanotube networks of controllable densities and alignment on a quartz surface.[56] The process of stamping allows them to transfer these networks onto any type of substrate.[108] Effective mobilities of up to 30 cm$^2$/V.s with ratios of $I_{on}/I_{off} = 10^4$ were measured for these TFT-NT devices. Recently, they have also demonstrated that effective mobilities of

1 000 cm$^2$/V.s are possible by aligning the carbon nanotubes along the channel.[44] In this case the transport is no longer percolating since the current is transported by carbon nanotubes that bridge the entire channel length. As a result $I_{on}/I_{off}$ ratios are low due to the presence of 1/3 metallic nanotubes. Electric breakdown of metallic nanotubes is therefore necessary in order to attain $I_{on}/I_{off}$ ratios of 10$^5$.[109] An inverter having a gain of 2.75 was fabricated from these transistors.[44] This is a higher gain than what has been demonstrated with individual carbon nanotube transistors (gain ~ 1).[110; 111] By performing a numerical simulation coupled to their experimental results, Rogers' group able to explain both the percolating and non-percolating behaviors of their carbon nanotube networks.[52] They have also calculated the optimal degree of alignment and density necessary to obtain the best TFT-NTs. Their work represents a major move forward in the field of carbon nanotube networks. However, the CVD method they used to fabricate the networks requires specialized equipment and complex fabrication steps. We will show in chapters 7 and 8 that it is possible to fabricate high performance TFT-NTs from commercially available carbon nanotube materials by using simple solution based methods.

# CHAPTER 3: Experimental procedures

In order to use carbon nanotubes as building blocks for future electronic devices, researchers have investigated ways to manipulate them effectively in order to incorporate them in different device geometries. Because of their nanoscale dimensions and particular chemistry, working with carbon nanotubes has proven to be a great challenge. As discussed in the previous chapter, a number of different techniques have been developed in order to assemble carbon nanotubes into two-dimensional networks. However, the detailed steps enabling the incorporation of carbon nanotube as passive or active constituents in functional devices were not discussed. In this chapter, a detailed description of the fabrication and characterization techniques that were used during the course of this research will be presented. All experimental procedures relating to carbon nanotube device fabrication and testing will be presented - from the production of electronic grade carbon nanotube materials to the fabrication of thin film transistors and anodes.

## 3.1 Carbon nanotubes and their purification

The carbon nanotube material that was used for the bulk of this work was donated by Dr. Benoit Simard's Group at the *Steacie Institute for Molecular Sciences* at the *National Research Council of Canada*. These nanotubes were fabricated using a variant of the laser vaporization method originally described in 1995 by Prof. Richard E. Smalley and coworkers at Rice University.[112; 113] The rationale for working with this source of nanotubes is: 1) this technique produces nanotubes having a relatively narrow diameter distribution between 1.1 - 1.4 nm.[114] Since all electronic and optoelectronic properties of nanotubes are a unique function of the diameter, a narrow diameter distribution will yield well-defined electronic properties. 2) Laser ablation nanotubes have been

extensively studied and information on their transport properties is readily available in the literature 3) Purified laser ablation carbon nanotubes have to date yielded the best conductivities of any other carbon nanotube source.[63]

The synthesis of carbon nanotubes from the catalytic decomposition of hydrocarbon precursors invariably leads to the production of many impurities.[115; 116] These impurities consist for the most part of amorphous and partly graphitized carbon as well as the metal nanoparticles used as catalyst. The precise composition of as-synthesized samples depends on the exact procedure that was used to prepare the nanotubes. The first step in working with carbon nanotubes thus consists in developing a purification procedure that is unique to a given nanotube sample and eliminates the majority of impurities.

The as-synthesized CNR-nanotubes contain on average between 20-35% of impurities mostly in the form of amorphous carbon and Co and Ni nanoparticles.[117] Figure 3-1 shows both scanning electron microscope (SEM) and transmission electron microscope (TEM) images taken by us from a typical samples of as-synthesized CNR-nanotubes. The purification procedure we developed is adapted from the original procedure described by Liu *et al.*[118] in the seminal 1995 Science paper. It is mainly based on wet chemical oxidation of the as-synthesized carbon nanotube soot by $HNO_3$, that will be described in detail below.
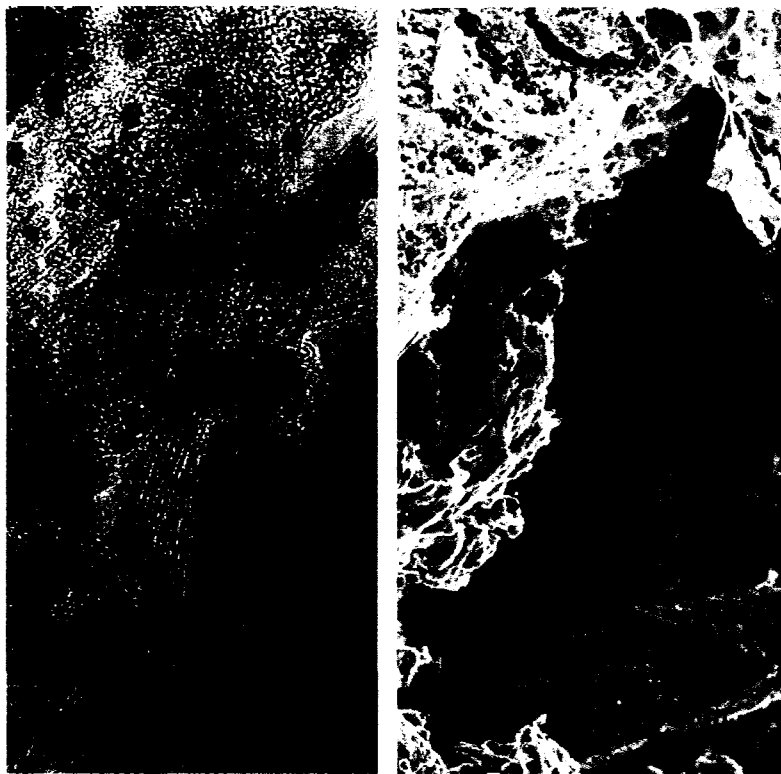
Figure 3-1. TEM image (left) and SEM image (right) of as-synthesized CNR-nanotubes. The TEM image reveals the presence of small metal catalytic nanoparticles (appear black) as well as carbon nanotube bundles (ordered structures). Carbon nanotube bundles are barely visible in the SEM image as amorphous carbon coats most of the samples.

As with most other purification methods, the challenge is to subject the material to an oxidizing treatment in order to "burn" the amorphous and partly graphitized material, while inducing the least amount of damage to the carbon nanotubes.[119] In the present case, the well graphitized carbon nanotubes in our samples allowed us to use an aggressive oxidation treatment without affecting the integrity of the material. This treatment consisted in refluxing the as-synthesized soot in a 0.1 mg/ml of nanotubes in concentrated $HNO_3$ (14M) for 4 hours. The solution was subsequently filtered using a standard filtration apparatus and 1 μm pore PTFE filters. The remaining soot was then refluxed in ultrapure water (Millipore Milli-Q system) for 2 hours in order to remove any remaining nitric acid from the nanotube bundles and rinced. Only well-graphitized forms of carbon (e.g. carbon nanotubes) can survive such harsh oxidative treatments.

Although lower concentrations of $HNO_3$ (4M) could be used in order to yield similar nanotube purities the higher concentration treatment gave the most reproducible results. This procedure was used to purify the as-received CNR-material from five different synthesis runs, all resulting in the same material purity. The impurities consisted in spherical graphitic particles (see Figure 3-1) as determined by TEM micrographs. They accounted for less than 5% by weight of the total material obtained after this step. An additional consequence of this $HNO_3$ treatment is the intercalation of acid groups in the bundles which in turn leads to p-type charge transfer doping of the nanotubes. [120; 121] Also, this purification treatment results in carbon nanotubes having carboxylic groups (-COOH) covalently attached to the side-walls and at their ends.[122; 123]

We also used commercially available carbon nanotube sources for some experiments in order to investigate the impact of different diameter distributions on the electrical and optical properties of carbon nanotube networks. The so-called HiPco-nanotubes purchased from Carbon Nanotechnologies Inc. (Purified Research Grade) were used without further purification. These nanotubes are synthesized using a CVD process that consists in the high pressure catalytic decomposition of carbon monoxide.[124] HiPco-nanotubes have small average diameters between 0.7 and 1.1 nm. The purification process that the company uses is confidential, but they assured us that it does not consist in any kind of oxidative treatments. Thus the nanotube side-walls are most likely not functionalized. Alternatively, we imparted a carboxylic functionalization to these nanotubes by refluxing the as-received soot in a dilute (1M) $HNO_2$ solutions for 2 h followed by our standard filtration and refluxing in ultra-pure water treatments.

A second source of CVD synthesized carbon nanotubes was obtained from Southwest Nanotechnologies and was used, again, without further purification. These so-called CoMoCat[125] carbon nanotubes (from the Co and Mo catalysts that are used during their synthesis) have a diameter distribution broader than both HiPco- and CNR-nanotubes between 0.7-1.4 nm as determined by Raman and luminescence spectroscopy.[49; 126]

However, CoMoCat nanotubes are particularly interesting because the carbon nanotube distribution sharply peaks at specific chiralities. In particular, carbon nanotubes having chiral indexes (m,n) of (6,5) can make up as much as 50% of the distribution.[127]

Finally, a source of double wall carbon nanotubes (DWNTs) was also used. DWNTs were obtained from Prof. Emmanuel Flahaut's group and were used as received. These nanotubes contained few impurities and had an average diameter twice as large as CNR-nanotubes (> 2 nm).[128] As discussed later in this chapter, electrical contacts to nanotubes having larger diameters are better and offer lower contact resistances.

## 3.2 Separation and suspension of carbon nanotubes in solutions

In 2D percolation networks, the conductance of each percolation path will be defined by either the metallic or semiconducting character of the carbon nanotube (or bundle). As we have seen in the previous chapter the relative number of conducting and semiconducting paths will define the "bulk" behavior of the network. It is thus crucial to separate carbon nanotubes from the bundle in order to obtain individual paths with well-defined metallic or semiconducting properties. The separation or unbundling of carbon nanotubes in solution is made difficult by their high surface area and the Van der Waals forces that bind them together along their length.[129; 130] One of the most effective strategies to exfoliate carbon nanotubes from bundles (or ropes) is to intercalate them with a chemical species. Furthermore, by chemically modifying the side-walls of the carbon nanotubes, it is possible to impart them with an added solubility with organic solvents.[131]

### 3.2.1 Strategies for making aqueous carbon nanotube suspensions

In general, surfactant micelles are used to encapsulate and stabilize the highly hydrophobic carbon nanotubes in $H_2O$. Sodium cholate solutions (1% concentration)

have been used to individually suspend purified CNR-nanotubes. Other surfactants such as sodium dodecyl sulfate,[49]triton-X,[132] and others[133; 134] have also been used to make carbon nanotube solutions. In particular cholate biosurfactants, such as sodium cholate, are particularly efficient in stabilizing individual carbon nanotubes in aqueous suspentions.[135] Solutions of 0.1 mg/ml of purified CNR-nanotubes were made by subjecting the nanotubes in sodium cholate solutions to a mild sonication treatment in a bath sonicator for 1 h (45W, Crest Tru-Sweep$^{TM}$ 275). This was followed by a more intense sonication treatment in a high intensity (50 W) cup-horn for 10 min (Branson S450). Sonication is necessary in order to separate carbon nanotubes from the bundle and allow for surfactant encapsulation. This treatment however is known to shorten the nanotubes.[136] Since the threshold for percolation in 2D networks is a function of the carbon nanotube length,[52; 137] shortening the carbon nanotubes is not desired. This, although unintended, is an unavoidable consequence of sonication treatments. The use of a low intensity sonication, prior to aggressive cup-horn treatment, is done in order to minimize damage. Finally, the solutions are centrifuged at 5 000 g and subsequently decanted. To remove the nanotube material that was not adequately dispersed the supernatant was collected and consisted in individual carbon nanotubes and only small (~5 nm) carbon nanotube bundles having on average 2 µm in length, as determined by AFM imaging.

### 3.2.2 Organic carbon nanotube suspensions

The fabrication of carbon nanotube networks by self-assembly onto functionalized substrates requires that carbon nanotubes be individually suspended in amide solvents.[65; 66] Dimethylformamide (DMF) was chosen in our case as it led to the most stable dispersions. It is known that carbon nanotubes have a finite solubility in different organic solvents.[138] For example, carboxylic functionalized carbon nanotubes, as the ones resulting from our purification treatment, easily exfoliate and suspend in DMF. A small amount of water was found to be necessary in order to make stable suspensions. Carbon nanotubes in anhydrous DMF tend to agglomerate and fall to the bottom of the

vial. The carbon nanotubes were suspended in DMF at a concentration of 0.1mg/ml by both the mild and high-intensity sonication treatments. AFM microscopy images revealed that the vast majority of the nanotubes in these solutions are individually segregated.

## 3.3   Optical spectroscopy

Optical absorption spectroscopy can be used as a simple yet powerful technique for the characterization of bulk carbon nanotube samples. It is known that the excitonic transitions of individual carbon nanotubes will give rise to peaks in the near-infrared absorption spectra. The positions and shapes provide a measure of the quantitative composition of carbon nanotubes in the solutions.[139] Figure 3-2 shows the absorption spectra from solutions of the three single-wall carbon nanotube sources used during the course of this work. Peaks corresponding the $1^{st}$ and $2^{nd}$ excitonic transitions of semiconducting nanotubes as well as analogous transitions from metallic nanotubes can be resolved. Well-resolved peaks are seen for solutions containing a large proportion of individualized carbon nanotubes and this is due to the suppression of broadening effects that usually takes place in bundles.[140] Note in figure 3-7 that the different positions of the peaks in the optical absorption spectra reflect the different diameter distributions of the nanotubes contained in the sources. Optical spectroscopy thus provides essential information about the structure of carbon nanotubes contained in a given sample. The application of Beer's law [141] was found to follow the relative concentrations of carbon nanotubes in both solutions and films. Thus, the carbon nanotube film thickness can be determined using the amplitude of the signal. The amplitude of the signal arising from the $1^{st}$ excitonic transition of semiconducting nanotubes is also sensitive to doping.[142] This technique has been used to evaluate the level of doping of both the p-type and n-type doping of carbon nanotubes. For these experiments a Varian Cary 3000 spectrometer covering the 175 to 3000 nm wavelength range was used. Solutions from the different sources of carbon nanotubes were characterized using optical absorption

spectroscopy. The optical transparency of dense carbon nanotube films and their level of doping was thus evaluated.
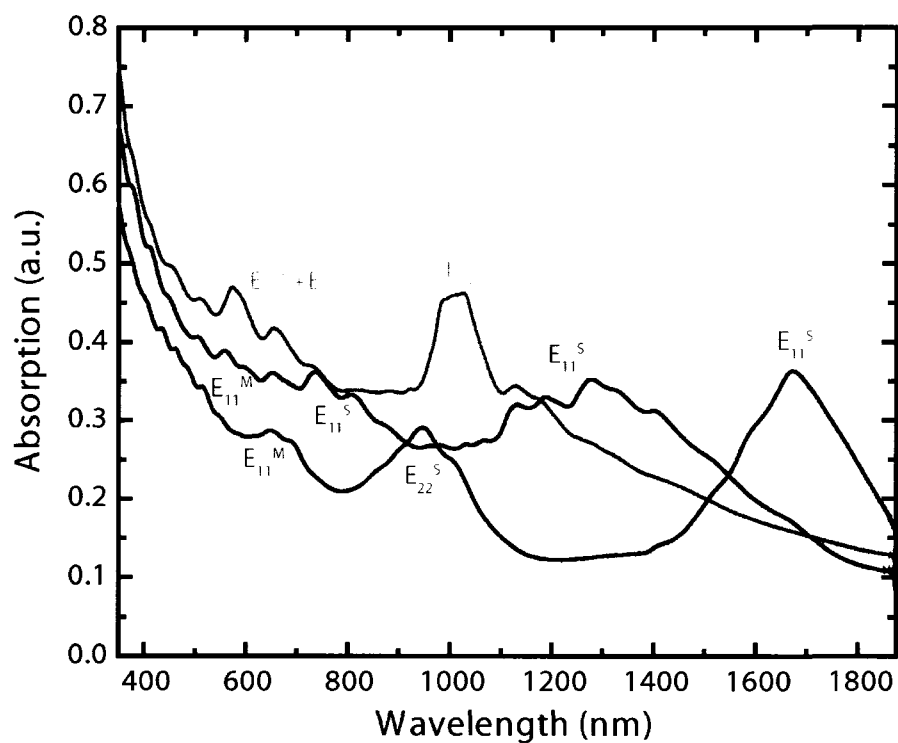


Figure 3-2. Absorption spectra from purified laser ablation nanotubes (blue), HiPCO nanotubes (red) and CoMoCat nanotubes (green) in aqueous surfactant solutions. Peaks from the first two semiconducting transitions as well as the first metallic transition are indicated.

## 3.4 Protocols for fabricating carbon nanotube networks

### 3.4.1 Fabrication of carbon nanotube networks using the filtration method

Sparse and dense carbon nanotube networks were fabricated using the technique described by the Rinzler's group.[41] Although the technique is very simple, special care must be taken during the fabrication of the networks in order to achieve high homogeneity and better smoothness. As will be described in Chapter 4, the homogeneity of the networks is extremely important, particularly for sparse carbon nanotube coverages where the electrical properties of the networks vary rapidly as a function of density. Equally important is the smoothness of the dense carbon nanotube films used as electrodes. It is important if electrical shorts are to be avoided in organic thin film devices. Surface roughness has to be kept at a minimum.

All parameters were optimized in order to achieve the homogeneity, smoothness, and conductivity needed for electronic applications such. To do so our fabrication steps had to be modified relative to what was originally described by Rinzler et al.[41] Moreover, in order to avoid contamination during carbon nanotube network fabrication, it is best to work in a clean room environment. The vacuum filtration apparatus (Lab System 2) and filters (MF-Membrane Filters) purchased from Millipore were used for this work. The filtration apparatus consisted in a fitted glass filter support 47 mm in diameter. The filters were based on mixed cellulose esthers with pore sizes of 0.1 µm and 0.2 µm and had a smooth glossy surface. The smoothness of the filter was found to be very important as any inhomogeneity on the filter surface will be transferred onto the networks. Filters with glossy looking surfaces were found to give the best results. Sodium cholate nanotube solutions of 0.1 nanotubes/ml were made following the procedure described above. The solution was filtered in order to form a 2D percolation network on top of the filter surface. Once filtered the nanotube solution was used without subsequent rinsing. The filters were left to dry overnight.

Substrates were cleaned by sonicating them in warm acetone and isopropanol followed by drying under a nitrogen flow. In order to transfer the films on the substrates, the filters are first dipped in chlorobenzene. This solvent does not dissolve the filters nor damages them in any way, but it wets the pores of the filter to avoid air bubbles. If air bubbles are trapped during the dissolution of the filter, they will create holes in the network. Moreover, a thin chlorobenzene film will help fixing the filters onto the glass surface by surface tension and capillary forces. Once the filter is set upon the glass surface (nanotube side down) it can be dissolved by pouring acetone using a squirt bottle. When the filter has started dissolving acetone, the substrates can be transferred into a covered acetone containing 250 ml crystallizer. The filters are then allowed to dissolve during approximately 30 minutes, at which time the samples are rinsed carefully in clean acetone and isopropanol, and at last dried under a $N_2$ flow. Before this first drying step, the networks are not strongly bound to the glass surface and all manipulations are to be done carefully (but quickly) in order not to disrupt the networks. Finally, the filters are immersed in a second clean acetone bath for more than an hour, rinsed again in clean acetone, followed by isopropanol and dried. This process insures that no apparent filter residues remain on the carbon network surface, as determined by AFM.

The exact same procedure can be used on basically any substrate surface. However, it was observed that carbon nanotube networks do not bind strongly to hydrophobic surfaces. Thick carbon nanotube networks deposited onto hexamethyldisiloxane (HMDS) functionalized surfaces that are highly hydrophobic can be pulled off from the surface using the Tape technique. Figure 3-3 shows a free standing dense nanotube network fabricated using this technique.
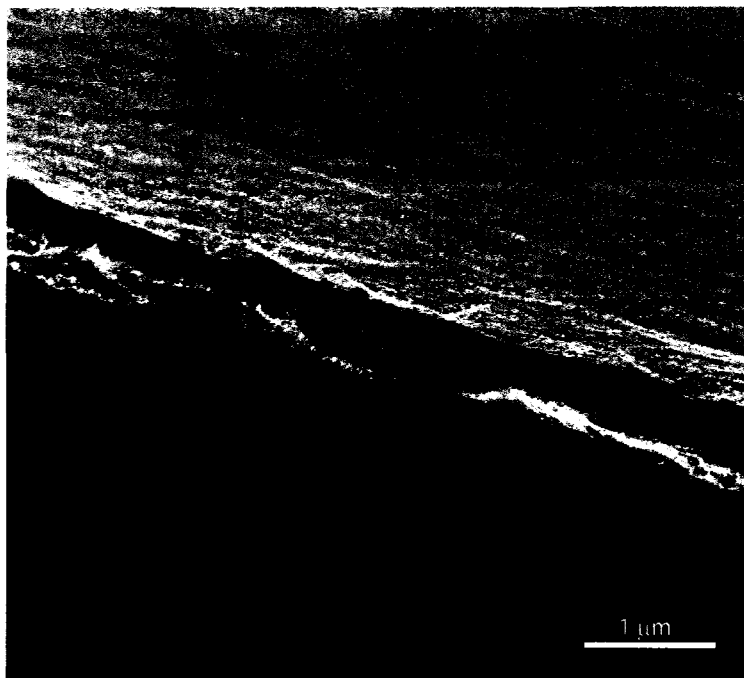
Figure 3-3. SEM image of a freestanding carbon nanotube film fabricated by the filtration method and peeled off from a HMDS treated glass surface.

### 3.4.2 Fabrication of carbon nanotube networks by self-assembly onto a functionalized surface

The self-assembly technique for fabricating carbon nanotube networks on amine functionalized surfaces[65-67] was used in order to make both random and aligned carbon nanotube networks on substrates over 10 cm² in size. The affinity of carbon nanotubes for functionalized substrates drives the self-assembly of the networks. The fabrication technique we developed aimed at maximizing this interaction.

Although different amines can be attached to oxide surfaces from liquid solutions, it has been demonstrated that a monolayer of (3-aminopropyl)triethoxysilane (APTES) deposited by vapor deposition promotes higher bonding to carbon nanotubes.[65-67] Moreover, the vapor deposition method has the advantage of being amendable to work with substrates that have been patterned using lithographic techniques. As described in

Chapter 5, optical lithography can be used to define APTS patterns on a substrate where carbon nanotube networks can be assembled at precise locations.

In order to accomplish high amine monolayer coverages, the surfaces of oxidized silicon wafers were first treated in a 1:3 $H_2O_2$:$H_2SO_4$ solution for 20 min. This so-called piranha solution, in addition to attaching –OH groups to the surface of the oxide, leaves the surface free of any contaminants. Hydroxyl groups (-OH) are necessary for the silane end of the molecule to bind to the surface. The substrates were then rinsed in ultra-clean water and dried suing a $N_2$ gun. Immediately after drying, the substrates were inserted in a home made vapor deposition system illustrated in Figure 3-4.

The APTES process uses a vapor deposition system that was fabricated by adapting a glass desiccator, as illustrated in Figure 3-4. First, a small crystallizing dish containing 1 ml of fresh APTES (99% pure Aldrich) is placed at the bottom of the desiccator flask. The substrates are positioned on top of the dish and the dessicator is sealed. A mechanical pump is used to pump the interior of the dessicator through J. Young PTFE needle valves. The dessicator is left to pump for 1 min and the valve is then closed. An additional 30 s allows for the amino-silane vapor to react with the silicon oxide surface, after which time the vacuum is broken by inserting $N_2$ though a needle inserted in a sleeve stopper PTFE septum. Finally, the substrates are annealed in air at 120 °C for 20 minutes in a laboratory oven. This annealing step is known to condense the APTES and to increase the number of primary amines on the surface of the substrates. All deposition parameters influence the primary amine composition and thus the affinity of carbon nanotubes to the networks. In our case we have optimized the deposition time, annealing temperature, and the annealing time to obtain surfaces having the highest affinity for carbon nanotubes. Random and aligned carbon nanotubes networks were deposited on the substrates no more than 1 h after they were removed from the oven.
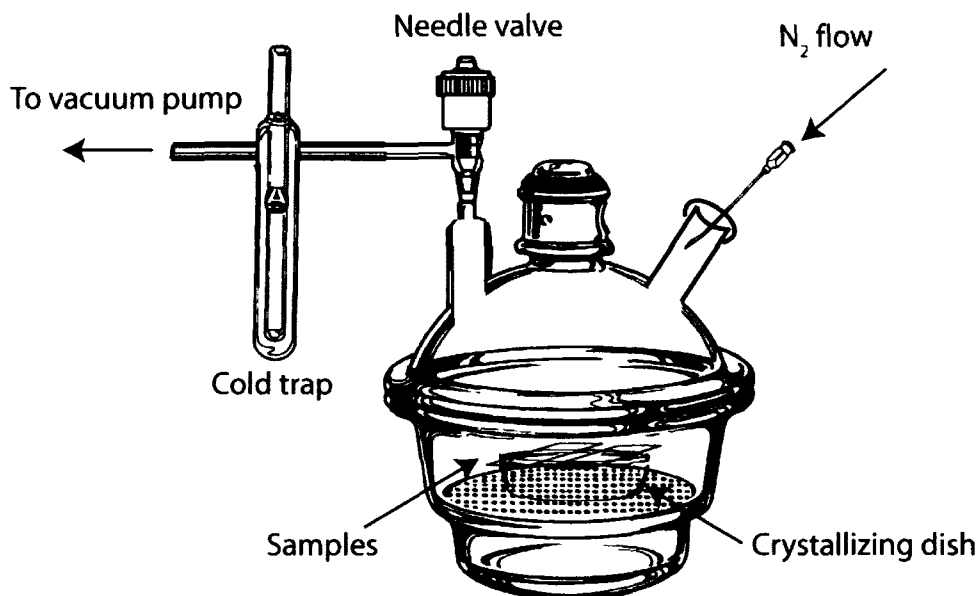
Figure 3-4. Home made vapor phase amino-silane deposition apparatus. This set-up allows the deposition of a single monolayer of (3-aminopropyl)triethoxysilane molecules.

The self-assembly of random carbon nanotube networks on APTES functionalized substrates is done by first covering the surface of the substrates with solutions of carbon nanotubes dispersed in DMF. The substrates are allowed to sit for 10 min after which time the DMF solutions are removed by drying in a spin coater rotating at 3 000 rpm. Random networks can also be deposited by simply immersing the substrates in the solutions for 10 min. The spin coater is used simply as a consistent and convenient way to dry the samples. Carbon nanotubes that are not subjected to the acid treatment, such as the as-purchased HiPco nanotubes, do not attach to the amine surface. It is therefore fair to say that acidic groups covalently attached to the nanotube sidewalls play crucial role in the bonding of nanotubes to the surface.

The self-assembly technique can also be extended to flexible polymeric substrates. This is achieved by oxidizing the surface of the polymer prior to the deposition of the amino-silane layer. The oxidizing treatment is analogous to the piranha treatment described

before. It essentially activates the surface with the -OH groups that are involved with the amino-silane attachment.

### 3.4.3 Alignment of carbon nanotubes

Alignment of the carbon nanotube networks is possible when the deposition takes place while the functionalized substrates are rotating rapidly in a spin coater (8 000 rmp). A single drop of the DMF carbon nanotube solution is let to fall at the center of the spinning substrate, followed immediately by the first DMF solution drop (less than 1 s). While the substrate continues rotating rapidly, 15 μl of 1,2-dichloroethane is sprayed at the center of the substrate using a micropipette. This will dry the substrate rapidly and align the carbon nanotubes radially on the oxide surface. In order to increase the density of aligned nanotubes, this procedure can be repeated until the surface is virtually covered with a monolayer of aligned carbon nanotubes. If lower densities are desired, diluting the solution will decrease by an equal factor the number of carbon nanotubes deposited on the substrate. For example, a 0.1 mg/ml solution that produced a carbon nanotube density of 20 nm/$\mu$m$^2$ will yield a density of 10 nm/$\mu$m$^2$ when diluted by 2.

A variant of this technique has also been used to align DWNTs. DWNTs dispersed in 1,2-dichlroethane (DCE) appear to have an affinity for substrates that have been treated in hot $H_2O_2$-$NH_4OH$-$H_2O$ 1:1:5. Consequently, it was not necessary to disperse the nanotubes in DMF. A single drop of DWNTs dispersed in DCE was dropped on the rapidly spinning substrate (8 000 rpm). Unlike the APTS functionalization, nanotubes in this case are not strongly bound to the surface. The alignment is not as good. Even mild sonication will detach the carbon nanotubes because of the weaker affinity of DWNTs to the surface.

## 3.5 Imaging of carbon nanotube networks

### 3.5.1 Scanning electron microscopy (SEM) imaging

SEM imaging is particularly well-suited for characterizing conducting and semiconducting carbon nanotube networks. Although the inherent resolution of SEM microscopes is limited to a few nanometers (below the average diameter of carbon nanotubes), carbon nanotubes appear bright on an insulating substrate when imaged under low accelerating voltage operation (0.5-2 keV).[74; 143; 144] In fact, the connectivity of carbon nanotubes in a network can be assessed by examining the contrast of the SEM image. Carbon nanotubes that are connected to the network or to metallic electrodes appear very bright. On the other hand, carbon nanotubes that are isolated from the network (not making electrical contact) are dark and are barely distinguishable from the background. The mechanism responsible for contrast during SEM imaging of carbon nanotube networks remains a matter of some debate. Among the explanations that have been proposed we find: voltage contrast,[143] amplified secondary electron emission by an electron beam induced current,[144] and the more recent electric field induced contrast.[74] Regardless of the mechanism, SEM is a powerful technique for assessing carbon nanotube network density and connectivity. We used a Hitachi S-4700 field emission SEM in order to image carbon nanotube networks. The accelerating voltage was between 0.5 and 1 keV and the working distance was set to ~3-5 mm. The microscope has been operated in its high-resolution mode (resolution ~ 2 nm) and only the top secondary electron detector was enabled. The current of the beam was limited to 7 μA in order to prevent excessive charging of the insulating substrate and to avoid beam induced damage to the carbon nanotubes. Figure 3-5 shows a typical image of a partially interconnected carbon nanotube network.

Figure 3-5. SEM image of a carbon nanotube network deposited on a SiO$_2$ surface at coverage below the percolation density and partially connected with Pd electrodes. Nanotubes making close contact to the metal electrodes appear as very bright (orange arrow). Carbon nanotubes that form small network clusters (blue arrow) are less bright but clearly resolved. Individual carbon nanotubes or small bundles that are neither connected to an electrode or part of a larger network (green arrows) can hardly be seen as they are virtually undistinguishable from the background.

## 3.6 Atomic force microscopy (AFM) imaging

In order to estimate the average diameter of carbon nanotubes (or bundles) deposited on a surface, AFM imaging was used in the intermittent (tapping) mode. Although the lateral resolution is limited by the radius of the cantilever probe ($\sim$ 2-20 nm), the height resolution ($\sim$ 0.05 nm) is sufficient to evaluate their average diameter. However, due to the deformation of carbon nanotubes by their interaction with the probe tip, the measured diameter normally underestimates the actual diameter by $\sim$ 0.5 nm. Moreover, impurities deposited on the carbon nanotube surface and the roughness of the substrate

will also contribute to the uncertainty of the measurement. Thus, AFM imaging is only used in order to make rough estimates of the actual diameters. By measuring the diameter of the same carbon nanotube at different positions along its length we estimate that the error is on average $\pm$ 1 nm. For experiments detailed here, we used a commercial AFM microscope (Nanoscope Dimension 3000) in the intermittent tapping mode. Cantilever probes having a force constant of ~ 50 N/m and a resonant frequency centered at ~300 kHz were used.

## 3.7   Electrical contacts to carbon nanotubes

Making electrical contacts to carbon nanotubes has been the subject of numerous experimental and theoretical works.[145-151] Claims of ohmic contacts appear frequently in the literature but this remains a matter of debate whether or not these contacts are Schottky in nature.[148; 150] This complication arises because our understanding of band alignment, Fermi-level pinning, and Schottky barriers developed for bulk semiconductor-metal contacts does not carry over to one-dimensional nanostructures such as nanotubes.[151] However, there are a number of conclusions that can be drawn from the extensive data that has been collected throughout the years. First and foremost, it is clear that contacts play a crucial role in determining the behavior of carbon nanotube devices. [145-147] Secondly, metals such as Pd and Ti appear to form contacts having lower contact resistances (i.e. smaller Schottky barriers) than most other metals.[146; 148] Furthermore, it is easier to make good contacts to nanotubes having larger diameters.[148; 149] Although, the "end bonding" or "side bonding" of carbon nanotubes also plays a role, there is a general agreement that top contacts (metal on nanotube) make better connections than bottom contacts (nanotube on metal) for otherwise similar conditions. We took into account all these considerations when developing the protocol for making electrical contacts to carbon nanotubes. It is our experience however that fabrication protocols and carbon nanotube sources played a primary role in the batch-to-batch behavior of contacts to carbon nanotube devices. Our

protocol allowed us to make contacts exhibiting nearly linear current-voltage characteristics for individual carbon nanotube devices (-2 to 2 V range). The apparent resistance of an individual carbon nanotube device was $\sim$ 250 k$\Omega$[6]. Devices made from carbon nanotubes having larger diameters (e.g. DWNTs) consistently resulted in lowering the resistance to $\sim$ 100 k$\Omega$.

In order to fabricate thin film transistor devices, electrical contacts (top contacts) were made to carbon nanotubes deposited on the surface silicon substrates having a thin oxide layer (100 nm). Electrode patterns were defined by optical lithography using a Karl Suss MA-4 mask aligner. All samples where left in a dehydration oven (120 °C) for at least 1 h prior to the lithography steps. First, a 100 nm layer of LOR A lift-off resist (MicroChem) was deposited by spin-coating at 4000 rmp for 30 s (256 rpm/s). This was followed by a soft-bake at 170 °C on a hotplate for 3 min. A 500 nm layer of photoresist S1805 (Rohm & Haas Electronic Materials) was deposited at 4000 rmp for 30 s (256 rpm/s) followed with a soft bake at 115 °C for 1 min. The samples were then exposed for 3.5 s using light at $\sim$ 5-10 mW/cm$^2$ @ 365 nm and after which they were developed for 1.5 min in MF-319 (Rohm & Haas Electronic Materials), rinsed in pure water and dried. This double layer protocol resulted in devices having resistances one to two orders of magnitude smaller than what was possible using the single S1805 photo resist layer. The difference is probably due to the presence of residues on carbon nanotubes that results by directly depositing a S1805 photo resist on the carbon nanotubes.[152] Patterns having spacings as small as 0.8 μm and dimensions of 1 μm could be defined.

E-beam evaporation (Edwards Auto 306) was used to deposit metal electrodes in a $\sim$1x10$^{-6}$ mbar vacuum. A 0.5 nm Ti adhesion layer was deposited before evaporating 20 nm of Pd. Ti contacts were deposited directly on the samples. Lift-off of the resins was done by immersing the samples in hot (70 °C) PG-Remover (MicroChem) resist

---

[6] The device resistance was calculated from the slope of the Id-Vd characteristics in the transistor On state.

stripper for 30 min. The samples were rinsed in clean, room temperature PG-Remover, isopropanol and water and then dried using a $N_2$ gun. Finally, the samples were annealed in a vacuum oven ($\sim$5x10$^{-6}$ mbar) for at least 1 h at 550 °C. Annealing is known to improve the quality of the contacts.[153] We observed an overall decrease of device resistance and a substantial improvement in the stability of the devices after the annealing step for both Ti and Pd contacts. Also, it is possible that at 550 °C the reaction of Ti with the carbon nanotubes forms a carbide.[154] TiC is known to produce electrodes having good contacts for both electrons and holes injection.[146]

## 3.8 Patterning carbon nanotube networks

One of the main advantages of carbon nanotube networks compared to traditional organic semiconductors is the possibility to pattern them using conventional optical lithography techniques. This is possible because they are chemically inert and can withstand any of the lithography steps without impacting in anyway their electrical properties. Moreover, carbon nanotubes can be easily etched away using a $O_2$ plasma,[87; 152] allowing the construction of complex patterns on a substrate.

In order to define the channel region of thin film transistor devices, once the carbon nanotube networks had been deposited on the substrate and electrical contacts were defined. Patterns were defined by optical lithography using the same equipment and general procedure that was described for patterning electrodes (see section 3-5). Areas that have been covered by the thick photoresist layer are protected, while all other nanotubes will be etched away using a $O_2$ plasma. In our experiments a 1.5 μm layer of photo resist S1813 (Rohm & Haas Electronic Materials) was deposited at 4000 rmp for 30 s (acceleration = 256 rpm/s) and a soft bake at 115 °C for 1 min followed. The samples were then exposed for 7 s using light $\sim$ 5-10 mW/cm$^2$ @ 365 nm. They were then developed for 2 min in MF-319 stripper (Rohm & Haas Electronic Materials), rinsed in pure water, and dried. The samples were baked at 550 °C in order to remove

leftover residue. In order to etch away the carbon nanotubes, the samples were inserted in a home made reactive ion etching system and exposed for 30 s to an 75-100 mbar $O_2$ plasma etch at 80 mW/cm$^2$ (100 W). The photoresist layer is stripped in hot 70 °C PG-Remover for 30 minutes, rinced in clean PG-Remover, isopropanol, water and dried. This procedure can completely etch networks up to 20 nm in thickness, while not etching the photoresist layer. Thicker photo resist layers should be used in order to etch thicker networks. A rigid shadow mask (e.g. aluminum mask) can also be used instead if very thick networks not requiring micrometer resolutions are to be etched.

## 3.9   Deposition of organic semiconductors

Organic semiconducting layers can be deposited using various techniques. In general small molecule semiconductors are deposited by vacuum sublimation, while semiconducting polymers are drop-cast or deposited by spin coating. Solution-based methods are particularly interesting since they are inexpensive and can be easily scaled up for industrial production. Moreover, semiconductors that can be solution cast are amendable to printing using specialized jet printing equipment.

### 3.9.1   Deposition of organic thin films by vacuum sublimation

For the experiments detailed in this thesis, small molecule organic layers were in general deposited by vacuum sublimation. A home made vacuum deposition system able to reach 5x10$^{-6}$ torr was used. The apparatus consisted in a bell jar ~40 cm in diameter and ~60 cm in height where vacuum was achieved using an oil diffusion pump. Although contamination is usually a major concern with organic semiconductors, for our experiments the optimization of individual semiconducting layers was not required given that we were comparing two devices fabricated using the same materials. Consistency and reproducibility important for our work were readily achieved with our system. Seven different organic evaporation sources are located at the bottom of the bell jar along its circumference (approx. 10 cm from the center). The source material is

placed in a cylindrical alumina crucible (radius ~25 mm, height ~30 mm) and heated using a W filament. An eighth evaporation source consisting in a W evaporation filament was used in order to deposit Al contacts. All semiconducting materials were used without any type of purification. Between runs organic materials were kept in sealed vials but are frequently exposed to air. Samples were mounted at a ~45 cm distance from the sublimation sources and covered using a manually operated shutter. Sublimation of organic molecules proceeded by slowly applying current to the filaments until arriving at a deposition rate of ~0.2 nm/s (this took approx. 10 min) monitored using a quartz microbalance.

Small molecule thin films were used to fabricate both OLED and TFT devices. Since the purpose was to evaluate the performance of carbon nanotube based electrodes, we chose the materials that are commonly used as the gold standard in order to fabricate these devices. Our OLED devices were based on the tris(8-hydroxyquinoline) aluminum (alq3) stack structure originally described by Tang and VanSlyke in their seminal paper.[155] The p-type semiconductor pentacene was used in order to fabricate organic TFTs. Pentacene exhibits one of the highest mobilities among all the organic semiconductors (~ 1 cm$^2$/V.s) and is perhaps the most widely studied small molecule organic semiconductor for TFT applications.

### 3.9.2 Deposition of pentacene islands

Small molecules such as pentacene are insoluble in most organic solvents and are thus not amenable to solution based deposition methods (e.g. spin-coating). It is for this reason that pentacene is normally deposited by vacuum sublimation as described above. Recently, however, Afzali *et al.* synthesized the pentacene adduct 13,6-N-Sulfinylacetamidopentacene which is highly soluble in chlorinated solvents. By heating spin-coated films of this precursor to 120-200 °C, it is possible to convert the adduct film into pentacene.[156] These pentacene films exhibited field-effect mobilities of ~ 0.8 cm$^2$/V.s which are comparable to their vacuum sublimated counterparts. We

found that if a very thin film (~ 10 nm) of this precursor is heated, the conversion will lead to small pentacene crystals (islands) instead of a continuous film. Moreover, it was observed that crystallization is promoted by the presence of carbon nanotubes. When thin spin-coated adduct films were deposited onto substrates decorated with carbon nanotubes, the conversion resulted in small pentacene islands (radius ~ 200 nm) attached to carbon nanotubes. This technique was used in order to make the pentacene nanoscale transistors that will be presented in Chapter 8.

All chemical used were purchased from Sigma-Aldrich and used without further purification. Thin adduct films were deposited on clean, degenerately doped silicon wafers having 100 nm thick thermal oxide layer. A 0.2 mg/ml solution of 13,6-N-Sulfinylacetamidopentacene in choloform was spin coated on a substrate rotating at 2800 rpm. The substrates were immediately annealed at 200 °C atop a heating plate for 90 s. The deposition and conversion of the adduct took place in a $N_2$ filled glove box. An image of the resulting pentacene islands attached to carbon nanotubes is shown in Figure 3-6.
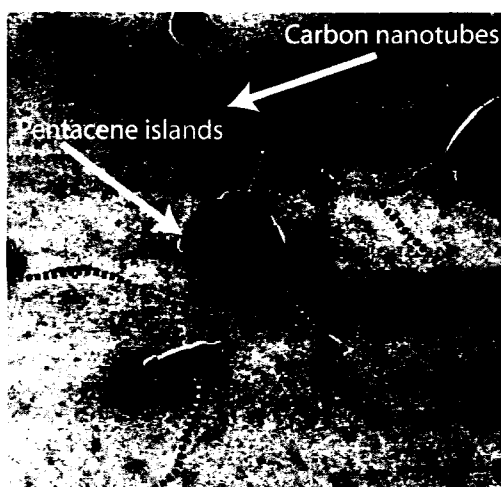


Figure 3-6. Pentacene islands deposited on carbon nanotubes from the conversion of of pentacene precursor 13,6-N-Sulfinylacetamidopentacene at 170 °C.

## 3.10 Electrical characterization

The electrical characterization of carbon nanotube network devices was done using either an ambient atmosphere microprobe station or vacuum microprobe station (Lake Shore Desert 6 probes) coupled with an Agilent A1500B semiconductor parameter analyzer. No difference was observed for measurements conducted in the dark versus under direct illumination from the microprobe station {high intensity (80W) white light at 5X magnification}. Measurements in vacuum allowed us to asses the impact of the environment on the transport properties of carbon nanotube networks. The vacuum station also allows measurements of the transport properties down to 77 K. For all measurements Berylium-Copper alloy probes having fine 10 μm diameter tips from Metal Specialty Co. were used.

In order to measure the sheet resistance of thick carbon nanotube networks, a standard four-point probe measurement apparatus coupled to a Keithley 2010 multimeter and a Keithley 236 current source was used. A Probex probe head having a 1.2 mm spacing and tungsten carbide needles, 0.5 mm in diameter, was used.[7] This measurement however is destructive as small holes are pierced into the networks. No more than 3 measurements where done on an individual film.

---

[7] Although osmium alloy needles, which are more ductile, are recommended for fragile materials such as organic conductors, the measurements with tungsten carbide needles yielded consistent results.

# CHAPTER 4: Evaluating the performance limits of conducting and semiconducting carbon nanotube networks for thin-film applications

## 4.1 Introduction

Single-wall carbon nanotubes (SWNT) have been widely studied for their unique electrical properties.[35] Individual semiconducting carbon nanotubes exhibit outstanding effective mobilities, while metallic carbon nanotubes have shown current carrying capacities that exceed $10^9$ A/m.[31-33] As such they have been envisioned as a possible alternative to traditional Si-based technologies for high speed devices.[34; 157] However, most of these applications call for well-ordered arrays of individual SWNT of a given helicity and length to be positioned at precise locations between metallic contacts. The difficulty this entails is what has stalled the widespread implementation of carbon nanotube electronics. Although a number of approaches have been proposed for the large scale fabrication of individual carbon nanotube devices,[65; 158] a viable solution has not yet emerged.

Increasingly, materials composed of a mixture of carbon nanotubes have been drawing attention as they exploit the properties of individual SWNT while avoiding the processing drawbacks of individual nanotube applications. In particular, metallic and semiconducting films can be made from an entangled two-dimensional percolation network of nanotubes having different diameters and chiralities.[38; 77] The metallic and semiconducting behaviors of the networks can be controlled by adjusting the number of nanotubes per unit area ($\rho$). TFT devices made from nanotube networks having densities in the vicinity of the percolation threshold typically exhibit effective mobilities of 0.5-50 cm$^2$/V.s and $I_{on}/I_{off}$ ratios of $10^2$-$10^5$.[38; 43; 52; 68; 76] Although the mobility figures cannot be linked directly to the intrinsic properties of the network, these device

performance values far exceed those of any other known organic-based TFT. Devices such as diodes,[36] inverters,[44] and light emitting TFTs[51] have been demonstrated with semiconducting carbon nanotube networks. For densities above the percolation threshold (> 30 nanotubes/$\mu m^2$), carbon nanotube networks are metallic with conductivities typically in the 100 to 1000 S/cm range.[41; 63; 77] These networks can be made into flexible electrodes having sheet resistances as low as 100 $\Omega$/sq. for optical transmittance values over 50%. Conducting carbon nanotube sheets have been incorporated in organic light emitting diodes,[37; 39; 42] photovoltaic cells,[40; 159-161] and electrochromic devices.[162] These devices showed performances rivaling that of devices fabricated with the traditional transparent conducting oxide ITO. Since a control of the electronic properties of the network material is directly linked to the nanotube network coverage, it is of utmost importance that a detailed study of the metallic-semiconductor transition as a function of network density be made.

Different fabrication techniques have been used for making carbon nanotube networks. The filtration method developed separately by Rinzler *et al.*[41] and Gruner *et al.*[68] has been adapted to fabricate networks of controllable densities. In addition to allowing the fabrication of networks from any of the commercially available carbon nanotube sources, this technique is also compatible with essentially any rigid or flexible substrate. In this report, we show how this method can be exploited for fabricating high quality carbon nanotube networks with well-defined metallic or semiconducting properties. By precisely controlling the carbon nanotube density, we fabricated semiconducting networks TFT having high transconductance and $I_{on}/I_{off}$ ratios. Even better On state currents are observed at larger nanotube densities, but this is also associated with a significant degradation of the device Off state due to metallic percolation pathways. So far, the selective removal of metallic paths using electrical breakdown or selective functionalization has failed to improve the overall device characteristics. Finally, we studied the impact of doping on the conductivity of the networks. We developed a

reliable method of doping the semiconducting nanotubes and investigated the stability of the dopant.

## 4.2 Experimental

Purified laser ablation synthesized carbon nanotubes have consistently given the best conductivities for metallic carbon nanotube networks.[63] The material used in this study was donated by Dr. Benoît Simard from the Steacie Institute of Molecular Sciences.[117] They consist of a statistical distribution of 1/3 metallic and 2/3 semiconducting single-walled carbon nanotubes.[46] A standard purification procedure involving a wet oxidation treatment in concentrated nitric acid was used to eliminate amorphous carbon and metal catalyst impurities from the as-synthesized sample.[118] All other chemicals were obtained from Sigma Aldrich, and unless otherwise noted, were used without further purification.
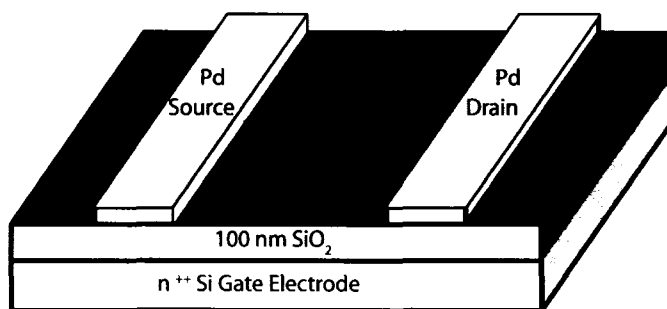


Figure 4-1. Device layout for the carbon nanotube network thin film transistor (NN-TFT). The degeneratively doped Si wafer acts as the back electrode.

The thin film field-effect transistor (TFT) configuration was used in order to evaluate both the conducting and semiconducting behavior of the carbon nanotube networks. Figure 4-1 illustrates the top contact/bottom gate geometry used for our devices. First,

carbon nanotube networks were deposited on clean $n^{++}$ Si substrates having a 100 nm SiO$_2$ oxide layer (WaferNet, Inc.) using the procedure described by Wu et al.[41] The concentration of the carbon nanotube solution used to prepare the network was $5\times10^{11}$ nanotubes/ml, as determined statistically by counting the number of nanotubes deposited on a surface within a given area using AFM imaging. The density of the deposited carbon nanotube networks was controlled by filtering different volumes of the solution. This allowed us to make networks having densities from 1-100 nanotubes/$\mu m^2$ from nanotubes bundles $2.3 \pm 1$ $\mu m$ in length. Electrical contacts were made by depositing 0.5 nm of Ti and 25 nm of Pd using an e-beam evaporator. Finally, the devices were defined by protecting the channel region using a 1 $\mu m$ thick Shipley 1813 layer and etching the unprotected regions using an oxygen plasma (30s, 100 mTorr, 80 mW/cm$^2$).[8] All devices were annealed in vacuum ($1\times10^{-6}$ Torr) at 500 °C for at least one hour prior to electrical measurements and chemical treatments. This insures reliable electrical contacts, removes residues leftover from the deposition process, and eliminates unintended doping by prior chemical treatments.

The covalent functionalization of carbon nanotube networks was conducted by immersing the TFT devices in a 1.3 $\mu M$ 4-bromobenzenediazonium tetrafluoroborate aqueous solution (NaOH x $10^4$ M) for 5 min. The substrates were then rinsed in water and dried in a N$_2$ flow. Raman spectra of the nanotubes were collected before and after the reaction. Two different laser lines at 514.5 and 633 nm were used in order to probe both the covalent attachment of functional groups to the sidewalls of semiconducting and the metallic nanotubes (not shown).

The p-type charge transfer doping of networks by the mild oxidant FeCl$_3$ and the charge transfer complex 2,3-dichloro-5,6-dicyano-1,4-benzoquinone (DDQ) were studied. Doping was conducted by dipping the networks in solutions of the reactants for 30

---

[8] The photoresin was stripped following the etching step.

minutes followed by blow drying using a Nitrogen flow. Acetone and aqueous solutions of and of DDQ (0.7 mg/ml) and $FeCl_3$ (5 mg/ml) respectively were used.

The optical properties of both doped and undoped carbon nanotubes networks were measured using a Varian 5000 UV-Vis-NIR spectrometer. For these measurements, carbon nanotube networks were deposited on clean microscope slides following the procedure described above.

Electrical measurements were conducted both in ambient atmosphere and in vacuum. In both cases using an Agilent B1500A semiconductor parameter analyzer.

## 4.3    Results

### 4.3.1    Electrical characterization of carbon nanotube networks

The TFT configuration was used to determine the channel conductance as a function of the gate voltage for different carbon nanotube network densities. Figure 4-2 shows the typical transfer characteristics for carbon nanotube TFTs (NN-TFTs) having fixed channel widths of 100 μm and lengths of 50 μm and densities of ~3, 8 and 30 nanotubes/μm$^2$. As expected, these NN-TFTs operate in air as standard p-type TFTs, typical of carbon nanotube devices.[163] Also evidenced from these curves is the higher channel conductance in both the On and Off states as the nanotube density increases.[9]

---

[9] The ratio of On and Off state currents was evaluated from the maximum and minimum value of the transfer characteristics evaluated at $V_d = -10$.
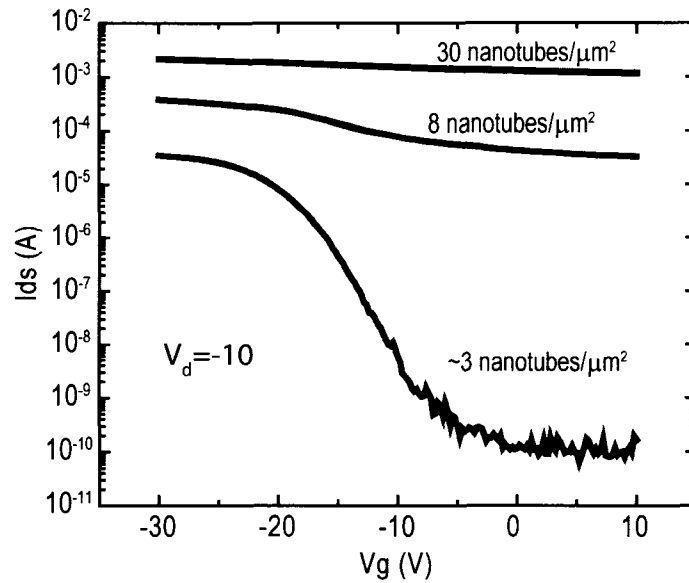
Figure 4-2. Transfer characteristics for NN-TFTs fabricated from networks having three different carbon nanotube densities and the same channel length (50 μm) and width (100 μm). Networks having densities near the percolation threshold ($\rho L_{NT}$ = 16) exhibit high $I_{on}/I_{off}$ ratios. The On/Off ratio drops by 4 orders of magnitude for slightly denser carbon nanotube networks.

The Off state current presents no conduction from semiconducting nanotubes and it is therefore a measure of the density of purely metallic percolating paths. Thus, one can compare DC TFT results with other published data by simply considering the conductivity in the Off state. This requires however to know the effective network thickness. It is known that the optical thickness commonly used as the effective thickness is proportional to the carbon nanotube density.[77] On one hand, the density of the carbon nanotube network is controlled in our case simply by controlling the volume of the filtered solution. On the other hand, the density can be linked to the thicknesses of the networks by considering atomic force microscopy (AFM) measurements in the 20 - 300 nm range. This allows us to derive effective thicknesses for thinner networks by taking into account the filtered volume. Note that thicknesses below 1.8 nm (i.e. the average carbon nanotube diameter) are simply indicative of submonolayer coverage. Figure 4-3 shows the conductivity as a function of the carbon nanotube density. As can

be seen, the conductivity ($\sigma$) varies by over 5 orders of magnitude over a very narrow carbon nanotube density range before saturating at a value of ~ 250 S/cm. This is the "bulk" conductivity of our carbon nanotube networks.

The conductivity behavior in Figure 4-3 can be fitted using the power law dependence $\sigma \propto (\rho - \rho_c)^\alpha$ that is expected from classical percolation theory.[52; 68; 77] Here $\rho_c$ is the critical nanotube density and $\alpha$ is the critical exponent related to the dimensionality of the system. An exponent $\alpha$ of 1.3 and 1.9 are expected for 2D and 3D percolation, respectively. From the fit to our data, we find a critical nanotube density of $3.7 \pm 0.7$ nt/$\mu$m$^2$ and a critical exponent of $1.4 \pm 0.2$.[10] This value of $\alpha$ is within the error of what we expect for an ideal 2D system ($\alpha = 1.3$). For carbon nanotubes having an average length of $L_{NT} = 2.3 \pm 1$ $\mu$m (measured by AFM), a theoretical critical density can also be estimated from the relation $\rho_c L_{NT}^2/3 \sim 4.236^2/\pi$.[52] Taking into consideration the relative fractions of metallic to semiconducting carbon nanotubes in a sample, the density is predicted to be ~ 3 nanotubes/$\mu$m$^2$ for the average length measured, which is remarkably close to the value measured from the curve fit ($\rho_c \sim 3.7$).

Note that we obtain a remarkably good fit to our data using an unconstrained fitting routine, even if the values vary by more than three orders of magnitude. The calculated R-square parameter, which is a measure of the "goodness" of our fit, was 0.96. Thus 96% of the variation measured for $\sigma$ can be accounted for by the scaling relation predicted by classical percolation theory.

---

[10] Note that we obtain a remarkably good fit to our data using an unconstrained fitting routine, even if the values vary by more than three orders of magnitude. The calculated R-square parameter, which is a measure of the "goodness" of our fit, was 0.96. Thus 96% of the variation measured for $\sigma$ can be accounted for by the scaling relation predicted by classical percolation theory.
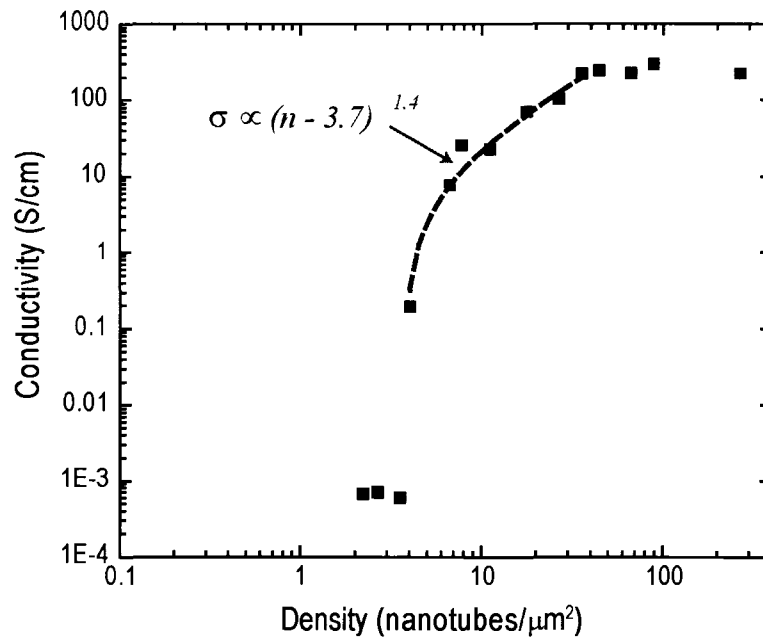
Figure 4-3. Carbon nanotube network conductivity as a function of the carbon nanotube density taken in the Off state. The unconstrained fit to the power scaling law governing the conductivity in percolation systems is also shown (dashed curve) with the corresponding parameter. This behavior is typical for percolation in 2D systems of carbon nanotube sticks.

In the On state, current will flow through the various percolation paths formed by both metallic and semiconducting nanotubes. This is why we are able to measure in Figure 4-2 considerable currents in the On state, even if the conductivity of the networks falls towards zero for carbon nanotube coverages under 3 nanotubes/$\mu m^2$. This indicates that although no purely metallic paths are able to bridge the NN-TFT channel, there exist paths composed of both metallic and semiconducting carbon nanotubes. An increase of the gate voltage toward negative values promotes carrier accumulation in the semiconducting segments of the channel, thereby allowing the current to flow between source and drain.
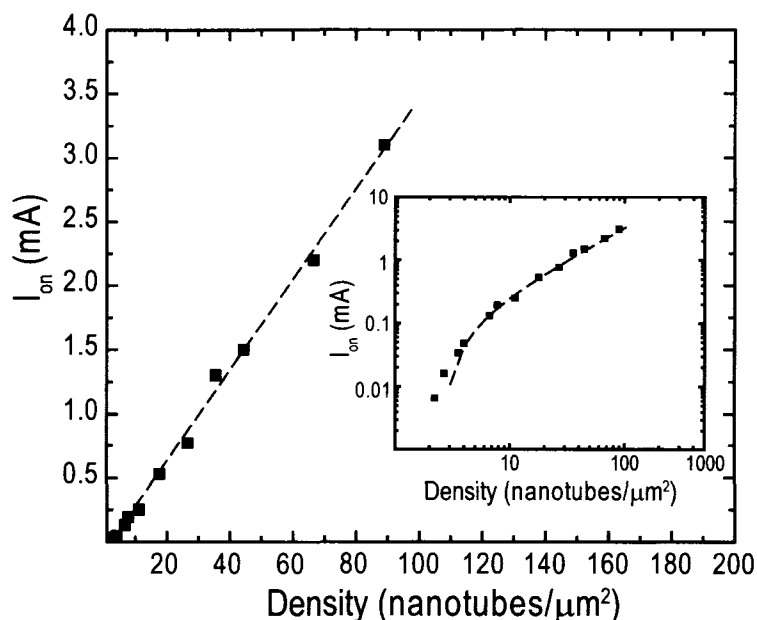
Figure 4-4. On state current measured at 1 V drain bias as a function of the carbon nanotube density. The nearly linear behavior for networks above 3 nanotubes/$\mu m^2$ indicates a scaling that is similar to "bulk" semiconductors.

The On state current can also be plotted as a function of carbon nanotube density (Figure 4-4). The behavior is nearly linear in the range measured which is a clear indication that the critical density for carrier percolation through the semiconducting paths (i.e. the ohmic limit) has already been reached. A small deviation is nevertheless observed at low densities (see inset), but the expected exponential increase seen in the Off state is not observed. By filtering smaller volumes of the solution, we attempted to fabricate networks with densities below 2 nt/$\mu m^2$, but no measurable currents were observed in those cases. We believe this is due to the inhomogeneity in the network density. This can be seen in AFM images of the films, such as shown in Figure 4-5. Indeed, some degree of clustering always occurs in the nanotube films and this seems inherent to the filtration method used to fabricate the devices. Networks having densities below 2 nanotubes/$\mu m^2$ are simply not uniform enough to present well-defined device characteristics.
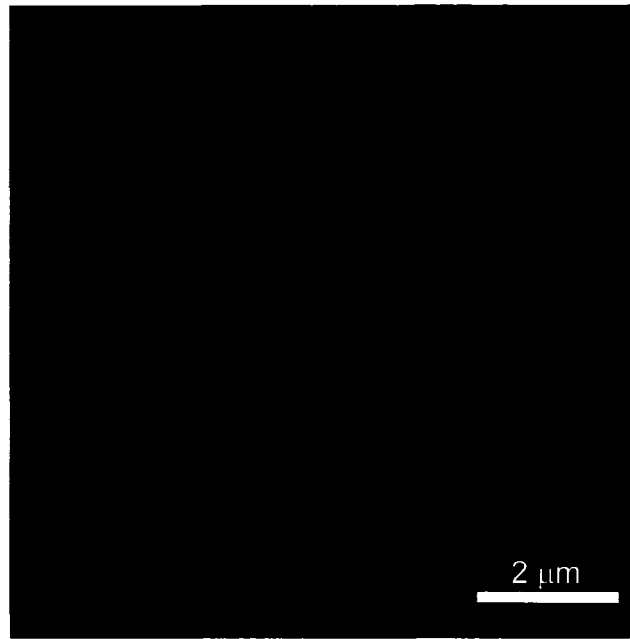
Figure 4-5. Atomic force microscopy image of a 5 nanotubes $/\mu m^2$ carbon nanotube network deposited on a $SiO_2$ surface. The fabrication of the networks by vacuum filtration leads to a small degree of aggregation of the nanotubes. Small clusters of nanotubes are clearly seen in the image.

In order to evaluate the semiconducting properties of our carbon nanotube networks, the device output characteristics and the $I_{on}/I_{off}$ ratios were evaluated at different densities across the available range. Typical device characteristics for networks near and above the critical percolation density are shown in Figure 4-6 with their corresponding SEM images. As the network density increases, the On state current and transconductance will be greater. However, the Off state current also becomes important with a corresponding decrease of the $I_{on}/I_{off}$ ratio.
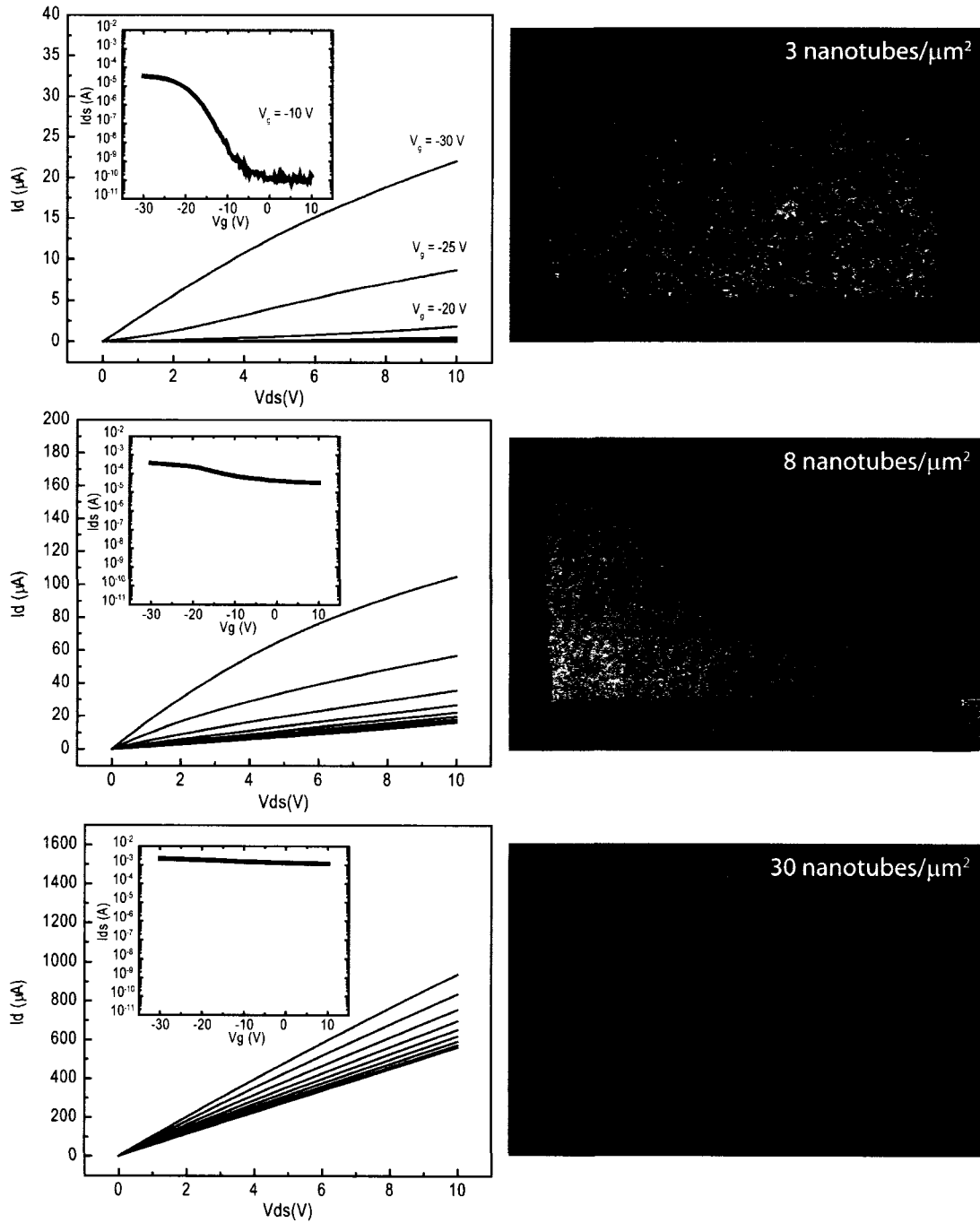
Figure 4-6. Electrical characteristics of NN-TFTs and their corresponding scanning electron microscopy images for nanotube densities (a) below, (b) near and (c) above the critical density for metallic percolation.

From these $I_{ds}$-$V_{ds}$ curves, the scaled transconductance ($\Delta I_{ds}/\Delta V_g.W$), where W is the width of the channel, was evaluated at $V_d = 4V$. The results as well as the On/Off ratios for different network densities are displayed in Figure 4-7. The effective mobility was also calculated using a parallel plate capacitance approximation ($C = \varepsilon/d$). Please note that fringing fields and electrostatic screening influence the capacitance estimate and the true capacitance is lower by as much as $\sim 40\%$.[98] Consequently, our mobility results are probably underestimated and serve only as a basis for comparing with previously reported values.

Below the density for metallic percolation, it is possible to increase the device transconductance without decreasing the $I_{on}/I_{off}$ ratio. Above the critical density ($\rho > 4$ nanotubes/$\mu m^2$), the transconductance continues to increase linearly as the number of semiconducting paths are added until reaching a saturation value. At this point the networks appear to behave as a bulk semiconductor having a fixed effective mobility value of $\sim$40 $cm^2/V/s$. The $I_{on}/I_{off}$ ratio however, increases dramatically near the percolation threshold due to the fast increase of the Off state conductivity from the metallic percolation. Devices having $I_{on}/I_{off}$ ratios over $10^5$ and effective mobilities of up to 5 $cm^2/V.s$ are possible only below the density for metallic percolation. These values far exceed that of any other organic semiconductor and are among the best ever reported for 2D carbon nanotube networks. Although effective mobility values as high as 45 $cm^2/V.s$ are measured in denser networks, the associated $I_{on}/I_{off}$ ratios are low and the networks are not really suitable for device applications.
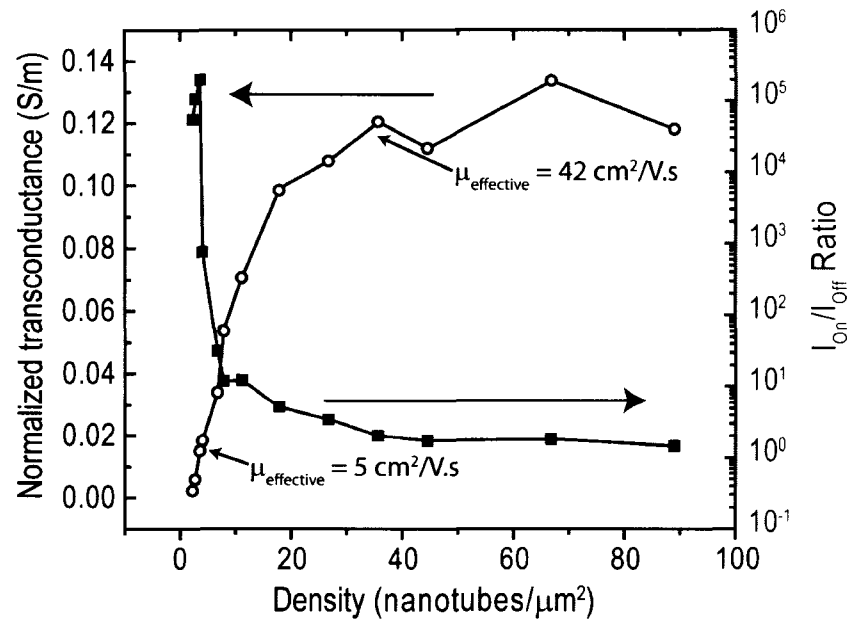
Figure 4-7. Normalized transconductance (open circles) and $I_{on}/I_{off}$ ratio (filled square) for NN-TFTs of different density. The width and length of the devices are 100 and 50 μm respectively.

## 4.3.2 Improving the semiconducting behavior of carbon nanotube networks

From the results in Figure 4-7, NN-TFTs having a bulk transconductance as high as 0.13 S/m and large $I_{on}/I_{off}$ ratios could be in principle attainable, if metallic paths are eliminated completely. Any process leading to the separation or enrichment of the semiconducting carbon nanotubes species prior or subsequent to the deposition of the networks would be an efficient strategy for further improvement. Unfortunately, current methods of enrichment shorten the carbon nanotubes down to ~100 nm and produce materials with only low yields.[164] Two alternative approaches are known to eliminate the metallic percolation paths subsequent to the deposition. The first involves the electrical breakdown of the metallic percolation paths while conduction through semiconducting paths is inhibited by the gate voltage.[44; 109] The second involves the selective functionalization (or destruction) of the metallic nanotubes using a chemical reaction.[165-167]

We attempted to "burn" metallic percolation paths using the first method, but we did not observe breakdown for any of our NN-TFTs after applying up to 100 V between source and drain, irrespective of the nanotube density. It appears that electrical breakdown is only effective when individual metallic carbon nanotubes are directly connected between source an drain, which is not the case here. In percolation networks, the higher resistances at nanotube-nanotube junctions do not seem to allow for the high current densities that are necessary for electrical breakdown to take place.

The second method for eliminating metallic percolation paths was previously demonstrated using diazonium salts as reactants.[165; 167] The introduction of defects to metallic carbon nanotubes though covalent functionalization appears to take place at a higher rate compared to semiconducting species. The result is a marked decrease in the conductance of the metallic nanotubes. There should be a window of reactant concentrations at which mainly the metallic carbon nanotubes are attacked while the semiconducting behavior should remain intact. We attempted, without success several diazonium reactions concentrations cited in the literature and for different network densities. An example shown in Figure 4-8 illustrates a typical transfer characteristic before and after the diazonium reaction. We consistently obtained only a decrease of the overall current density. There does not appear to be a universal set of parameters for which only the metallic species are affected.
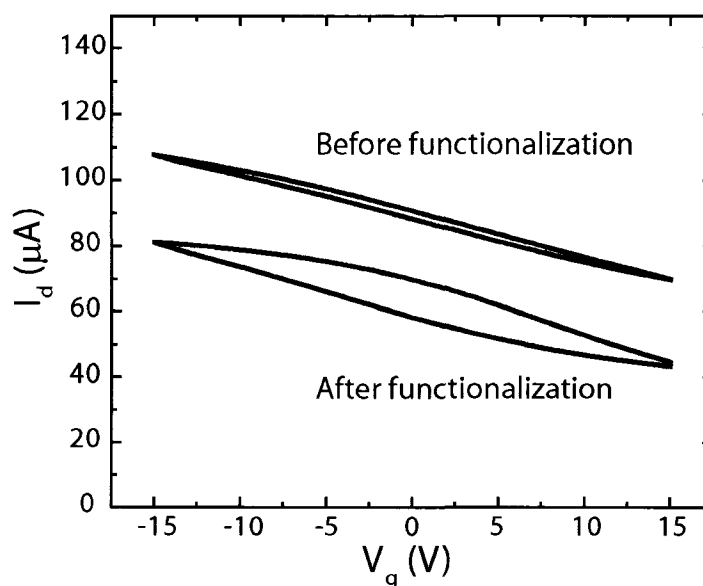
Figure 4-8. Transfer characteristics of a NN-TFTs taken before and after functionalization reaction using diazonium salts. The width and length of the devices are 100 and 50 μm respectively.

### 4.3.3 Optimization of conducting properties through doping

As will be presented in chapter 7, thick (~130 nm) conducting carbon nanotube networks can be used as transparent electrodes in organic light emitting diodes.[39] The performance of these devices could be greatly improved if the sheet resistance is reduced without affecting the transparency of the layers. A convenient approach is to chemically dope the semiconducting carbon nanotubes in the network. This in principle triples the number of metallic paths that participate to the DC conductivity. Doping increases the density of charge carriers and renders semiconducting nanotubes more conducting. Both p-type and n-type charge transfer doping has been demonstrated with electron donors such as potassium and lithium[168] and electron acceptors such as bronsted acids[169] and small organic molecules[170], respectively.

We investigated two different dopants that are known to be strong acceptors for p-type doping the carbon nanotube networks: 2,3-dichloro-5,6-dicyano-1,4-benzoquinone (DDQ) in acetone and $FeCl_3$ in deionized water. On one hand, DDQ forms non-covalent bonding with the carbon nanotubes and interacts strongly with the sidewalls of the nanotubes.[171] Calculations have shown that the hybridization between the DDQ molecular level and the nanotube valence bands charges the semiconducting nanotubes with p-type carriers.[11] Moreover, DDQ is commonly used to dope organic semiconductors and is thus compatible with these materials.[173-175] On the other hand, $FeCl_3$ is a well-known oxidizing agent with a redox potential of $E_0$=0.77V for the $Fe^{3+}/Fe^{2+}$ couple. This value is well above that of carbon nanotubes, which is $E_0$=0.5V. Consequently, $FeCl_3$ acts as an electron acceptor in the presence of carbon nanotubes and leads to p-type charge transfer doping.

In order to assess the degree of doping by either of these two acceptor species, we evaluated the depletion of the states in the valence band (p-doping) using the intensity of the first optical transition in the absorption spectra of thick carbon nanotube films.[168] Although Raman spectroscopy can also be used to evaluate charge transfer doping in carbon nanotubes,[176] the nearly linear relation between the decrease of the absorbance and the four-point resistance of carbon nanotube films was found to be more convenient in our case (results not shown). Figure 4-9 shows the absorption band for a 80 nm thick network in the region of the first optical transition taken before and after doping. This network was conducting (sheet resistance 450 $\Omega$/square) and displayed an optical transparency of ~80% at visible wavelengths. A ~7 fold decrease in the network resistance was measured for both $FeCl_3$ and DDQ. This value is among the highest ever reported for p-type doping of carbon nanotube networks.

---

[11] There is some controversy however as to the validity of DFTs' ability to calculate the interaction between weakly bound systems.[172]
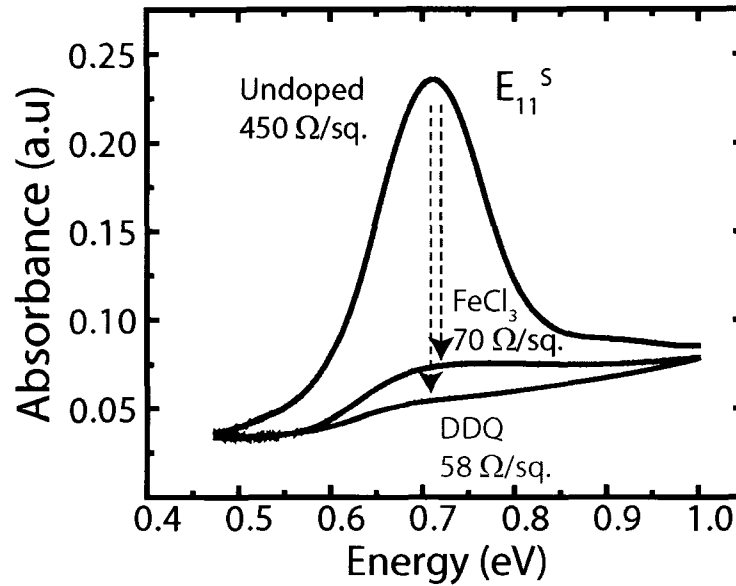
Figure 4-9. Doping of a 80 nm thick carbon nanotube network. First optical transition of semiconducting carbon nanotubes for a 80 nm network taken before and after a 30 minute exposure to DDQ and $FeCl_3$. The suppression of the absorbance, due to p-type charge transfer doping, correlates with a marked decrease in the sheet resistance.

Doping by DDQ is more effective and leads to the complete depletion of the valence band, as evidenced by the near total suppression of the first optical transition. A sheet resistance of only 58 $\Omega$/square at 80% transparency can be achieved in this way.

These doping results are very promising for improving the electrical properties of nanotube networks. We further investigated the effectiveness of DDQ doping by conducting the same experiment but for the semiconducting carbon nanotube networks (i.e. at density below the metallic percolation density). The transfer characteristics of the corresponding TFT device taken before the doping treatment are shown in Figure 4-10. The intrinsic networks behave as a typical semiconductor channel with a ratio of $I_{on}/I_{off} \sim 10^7$. After doping, the conductance can no longer be modulated by the gate voltage and the networks are metallic. Note that the overall channel conductance corresponds, at any gate field, to the On state conductance taken before doping. We can therefore conclude that: 1) DDQ is able to convert the majority of the semiconducting

carbon nanotubes into metallic and 2) any doping strategy will lead to no more than an order of magnitude improvement of the conductivity of carbon nanotube electrodes. This result also suggests that only a nominal decrease in the sheet resistance can be gained using exclusively metallic carbon nanotubes. Since the resistance of the networks is dominated by the nanotube-nanotube junction resistance, strategies that target minimizing or eliminating the number of junctions should be explored.
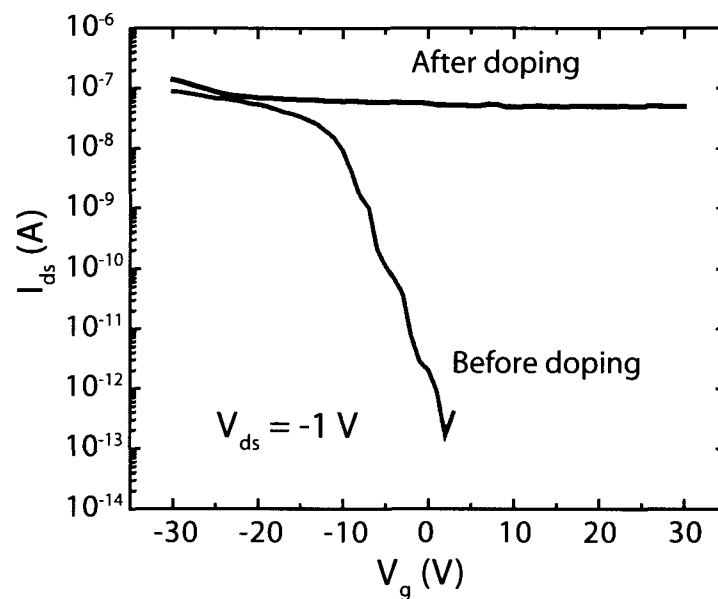
Figure 4-10. Transfer curve for a semiconducting carbon nanotube TFTs having channel width of 50 μm and length of 100 μm. (density ~ 2 nanotubes/μm$^2$) before (green) and after (blue) charge transfer doping with DDQ.

Finally, it is important that the chemical species that is used as the dopant for thin film applications is stable in air or in vacuum. We measured the sheet resistance over a long period of time after doping nanotubes with DDQ for networks kept in vacuum and in air. The evolutions are presented in Figure 4-11. The increases in resistance with time is less important in air than in vacuum, which is likely due to the dependence of partial

pressure of DDQ with pressure. Less than 10% change is observed in the sheet resistance after 10 days in air. In vacuum, the resistance gains approximately 100 % from the original value over the same period of time. The non-covalent bonding of DDQ to carbon nanotube allows the desorption of the molecule from the carbon nanotube network and this results in a reduction of the carrier concentration. Thus, for planar transparent electrode applications, the doping stability after deposition of organic semiconducting layers should be evaluated.
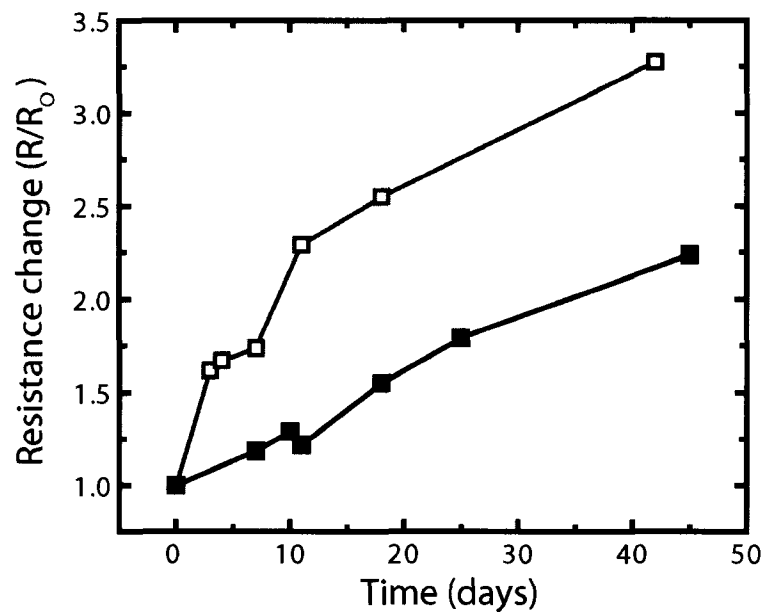


Figure 4-9. Evolution of the sheet resistance over the course of 45 days for networks kept in air (blue curve-filled squares) and vacuum (orange curve-empty squares).

## 4.4 Conclusion

We have investigated the semiconducting and metallic properties of carbon nanotube network devices fabricated using the vacuum filtration method. This study demonstrates for the first time the fabrication of networks having controllable densities and predictable electronic transport properties. This control allowed us to explore the

percolation behavior of nanotube networks. The evolution of the electrical characteristics as a function of the density of deposited networks revealed that this material behaves as two-dimensional conductor. By merely doubling the carbon nanotube network density from 4 to 8 nanotubes/$\mu m^2$, it was observed that the conductance varies by more than four orders of magnitude. This DC conductivity saturates at a value of 250 S/cm for networks having densities above ~ 30 nanotubes/$\mu m^2$. We were also able to increase the conductivity of the networks by a factor 7 using charge transfer doping by DDQ acceptor molecules. The doping of thick carbon nanotube networks lead to a thin carbon nanotube films (~80 nm) having a sheet resistance of 58 $\Omega$/square for optical transmittance values of 80%. This result is among the best ever reported for thick carbon nanotube networks. Also, this performance is equivalent to ITO the transparent conducting oxide currently used commercially as the transparent electrode for display devices and photovoltaic cells.

At the low density end (below the metallic percolation threshold) networks having pure semiconducting properties were obtained. A very narrow window of 2-4 nanotubes/$\mu m^2$ allows for purely semiconducting networks exhibiting very large $I_{on}/I_{off}$ ratios (> $10^5$) to be fabricated. The effective mobilities of these networks were of the order of 5 $cm^2$/V.s, which are among the best ever reported for random carbon nanotube networks. A maximum value of 45 $cm^2$/V.s was measured, but metallic percolation paths must be eliminated in order to attain suitable $I_{on}/I_{off}$ ratios. Electrical breakdown and selective functionalization strategies were assessed but neither eliminated selectively the metallic percolation paths. It thus appears that controlling the density of the networks remains the most effective strategy for controlling the semiconducting properties.

This is the first systematic study to date of the transition from insulating to semiconducting to metallic behavior near the percolation threshold of carbon nanotube networks. By determining the precise densities for which the different electrical

behaviors can be observed, we have been able to determine the bulk limit of both conducting and semiconducting performances.

# CHAPTER 5: The fabrication and scaling characteristics of aligned and random carbon nanotube network thin film transistors

## 5.1 Introduction

Thin film transistors (TFT) made from organic materials, such as polymer and small molecule semiconductors and carbon nanotube networks, have been gaining acceptance as an alternative to amorphous silicon (a-Si) based TFTs. In addition to exhibiting field-effect mobilities that rival those of a-Si, the low-cost fabrication methods that are used to fabricate organic TFT devices make them particularly attractive for large area applications. Organic thin film materials can be used in place of a-Si for the fabrication of TFT backplanes for flat panel displays[177], TFT array x-ray detectors[178; 179], and large-scale complementary circuits.[180]

It is key to establish the parameters that dominate the transport characteristics of these materials in order to unlock the potential of this revolutionary technology. Transport in carbon nanotube networks and amorphous organic semiconductors is governed by hopping conductivity. In this framework, percolation models have been formulated in order to explain their electrical transport properties.[181; 182] However, whereas scaling has been extensively studied and exploited in bulk semiconductor devices (e.g. a-Si TFTs), little is known about scaling in percolation systems. Recent theoretical studies have investigated the conductance scaling in 2-dimensional stick percolation systems as a function various geometrical parameters such as the density, stick length, and degree of alignment.[44; 52; 183-186] Because it is difficult to control these parameters experimentally there is limited data on the scaling behavior of realistic devices.

The present experiments were specifically designed to investigate the scaling properties of devices in the percolation regime. Carbon nanotube networks were used since they behave as a quasi-ideal 2-dimentional stick percolation system and thus can be easily modeled. In order to circumvent the intrinsic limitations associated with the vacuum filtration method, an alternative fabrication protocol was developed. Indeed we saw in Chapter 4 that the vacuum filtration method produced networks that did not display predictable electrical properties below a certain density. The scaling of the devices to shorter channel lengths will only amplify the detrimental effects due to the non-ideal uniformity. In this chapter we will show that highly uniform networks can be fabricated using a self-assembly chemical approach. Moreover, it is possible to impart alignment to the nanotubes that compose the network. This allowed us to investigate for the first time the scaling laws of carbon nanotube network TFT (NN-TFT) devices in the percolation regime for various configurations and geometries. The detailed electrical characterization of NN-TFT, devices having channel lengths and widths ranging from 1 to 100 μm, allowed us to extract the scaling characteristics of this new thin film material. The channel conductance followed a power law dependence as a function of the channel length. We show that the power law exponent is considerably different for random and partially aligned carbon nanotube networks.

## 5.2 Experimental

The general procedure we have developed to fabricate the carbon nanotube arrays is illustrated in Figure 5-1. The chemical assembly consists in functionalizing a silicon oxide substrate with an aminosilane self-assembled monolayer. Amino ($-NH_2/-NH_3^+$) terminated surfaces have a strong affinity to the carbon nanotubes dispersed in amide-based solvents [65; 66] and induce the chemical bonding of the nanotubes on the substrate. The van der Waals interaction between the substrate and the carbon nanotubes provides the initial driving force enabling the attachment of carbon nanotubes to the suface. To gain better alignment, a drop of nanotube solution is first placed at the center of the

rapidly rotating substrate. Then, a second solution of dichloroethane (DCE) is placed immediately following the release of the initial carbon nanotube solution drop. As will be discussed later, the fast spreading of this rapidly evaporating solvent pins down the carbon nanotubes to the substrate and the liquid flow allows the nanotubes to be "combed" along the radial direction.
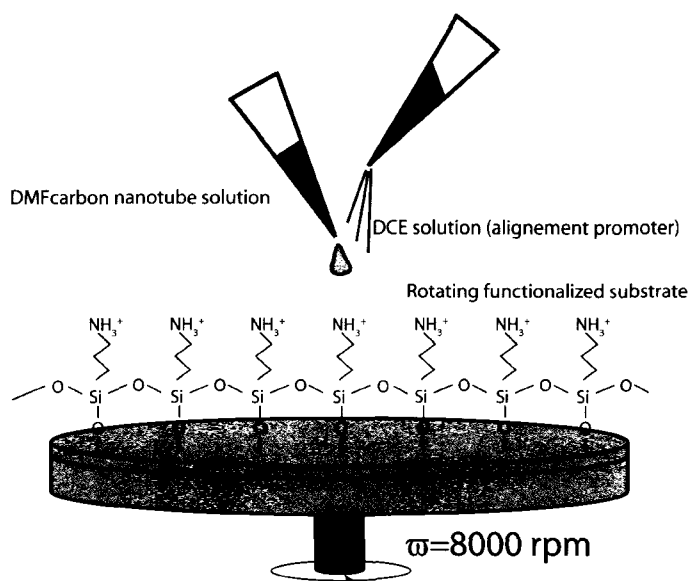


Figure 5-1. Schematic of the anchor-and-array setup for fabricating aligned arrays of carbon nanotubes on an aminosilane functionalized substrate.

In order to demonstrate the universality of our approach to carbon nanotube assembly, two sources of single-wall carbon nanotubes were used. The first consisted in carbon nanotubes synthesized by a laser ablation method (LA-nanotubes). The second source, which we will refer to as HiPco nanotubes, was purchased from Carbon Nanotechnologies (Purified Research Grade). The LA-nanotubes were subjected to a wet oxidation treatment in concentrated $HNO_3$ (reflux 4h, 14 M). This treatment removes 90% of the impurities from the sample and leads to the covalent attachment of carboxylic moieties to the nanotube sidewalls.[118] A milder oxidation treatment was used to impart the HiPco nanotubes with a carboxylic functionalization ($HNO_3$, reflux 4

h, 1M). It is known that –COOH functionalized carbon nanotubes form stable, individualized, dispersions in amide solvents.[187]

A self-assembled monolayer of (3-aminopropyl)triethoxysilane (APTES) was deposited on degenerately doped silicon substrates having a 100 nm thermal oxide layer. The vapor deposition method developed by Choi *et al.*[65] was used in order to obtain substrates having a high affinity to -COOH functionalized carbon nanotubes. Following the APTES deposition the substrates were annealed in an oven at 120 °C for 20 min. Dimethlylformamide (DMF) solutions having carbon nanotube concentrations of 0.1 mg/ml were made by sonication in a high intensity cup horn[12] (10 min, Branson 500) and centrifugation (1h, 10 000 g). The supernatant was collected and this solution was used for the carbon nanotube deposition.

Random carbon nanotube networks could be fabricated by simply immersing the functionalized substrates in the DMF-carbon nanotube solutions for 10 min. The substrates were then rinsed in isopropanol and dried in a $N_2$ flow. The affinity of these carbon nanotubes to the substrates is sufficient for a sub-monolayer network to deposit on the surface. Alternately, the substrates were positioned in the spin coater and, while remaining immobile, the surface was covered with the DMF-carbon nanotube solution. After 10 min the substrates were spun dry at 3 000 rpm and rinsed with isopropanol. The use of the spin coater to dry the samples reduces the number of manipulations and yielded more consistent results. In order to align the carbon nanotubes and obtain arrays, the deposition took place while the substrates were rotating at 8 000 rpm. The placement of a single drop of DMF-carbon nanotube solution (~7 μL) was followed (immediately after the appearance of the first Newton ring) by a 15 μl spurt of DCE at the center of the substrate using a micropipette.

---

[12] The preparation of DMF-carbon nanotube solutions is done by sonication in a high intensity cup-horn as explained in Chapter 3. This leads to short carbon nanotubes.

Drain and source electrical contacts consisting in 0.5 nm Ti and 20 nm Pd layers were deposited through lithographically defined patterns by e-beam evaporation. The channel region of the devices was defined by protecting the carbon nanotubes with a 1.5 μm photoresist layer (Shipley 1813) and etching unprotected regions using a $O_2$ plasma. Finally the devices were annealed in vacuum ($1 \times 10^{-6}$ mbar) at 550 °C for at least 1h. Electrical measurements were conducted using an ambient probe station coupled to a semiconductor parameter analyzer (Agilent A1500B).

## 5.3  Self-assembly of carbon nanotube networks

### 5.3.1  Results

Figure 5-2 displays atomic force microscopy (AFM) and scanning electron microscopy (SEM) images of a typical random network fabricated using LA-nanotubes from a 0.1 mg/ml DMF solution. The carbon nanotubes assemble as straight sticks having diameters between 1 and 2.5 nm[13] as measured by AFM. The images also indicate that the majority of the nanotubes are individualized or in the form small bundles. The mean length of the carbon nanotubes ($L_{NT}$) was 0.75 ± 0.4 μm, which is typical of purified laser ablation carbon nanotubes that have been shortened by sonication and acid treatments. The density of the carbon nanotube coverage was approximately ~ 26 nanotubes/μm² as determined from SEM images. The density did not increase further after longer exposures to a given DMF-nanotube solution. The self-limiting nature of the deposition results in networks having uniform densities over the entire surface (~10 cm²). Repeated depositions resulted in networks having the same densities (within 10%). It was observed, however, that the affinity of carbon nanotubes to APTES functionalized substrates varied according to sonication time, water content in the solution, and acid treatment. By subjecting the carbon nanotubes to different sonication

---

[13] Height measurement was used to determine the approximate carbon nanotube diameter. The apparent width is not significant when measuring features in the order of the cantilever tip diameter (~ 20 nm). In general, AFM imaging underestimates the diameter by ~ 0.5 nm.

and oxidation treatments a control of the density of random carbon nanotube networks could be achieved.
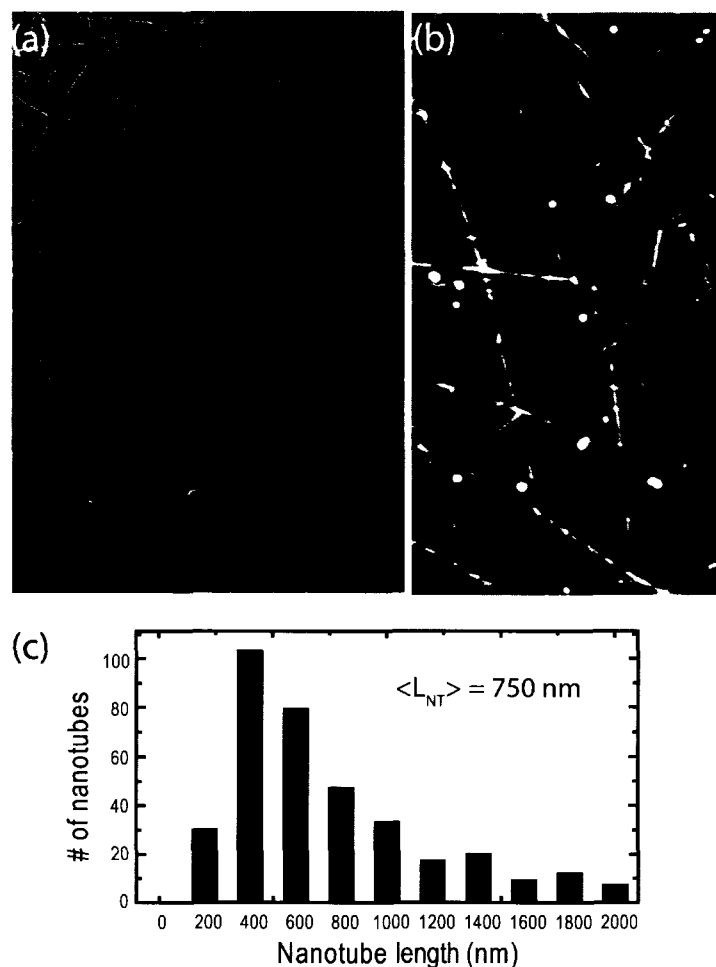


Figure 5-2. Random carbon nanotube networks assembled on aminosilane functionalized surfaces. (a) The SEM and (b) AFM images are shown with the corresponding histogram (c) of the measured lengths of the carbon nanotubes (taken from SEM images).

Carbon nanotubes made from HiPco process also lead to the assembly of networks on functionalized substrates. This demonstrates the versatility and robustness of our fabrication protocol. Figure 5-3 displays an AFM image of a typical random -COOH functionalized HiPco carbon nanotube networks. The networks are substantially denser than those made from LA-nanotubes. We believe the difference arises from the different

degrees of nanotube -COOH functionalization introduced by the oxidation step. Indeed, carbon nanotubes not subjected to the carboxylation treatment did not attach to the functionalized substrate with significant yields (this lead to network densities of less than 0.01 nanotubes/$\mu m^2$). The affinity of amino groups to carboxylic groups is central to the deposition of carbon nanotubes.
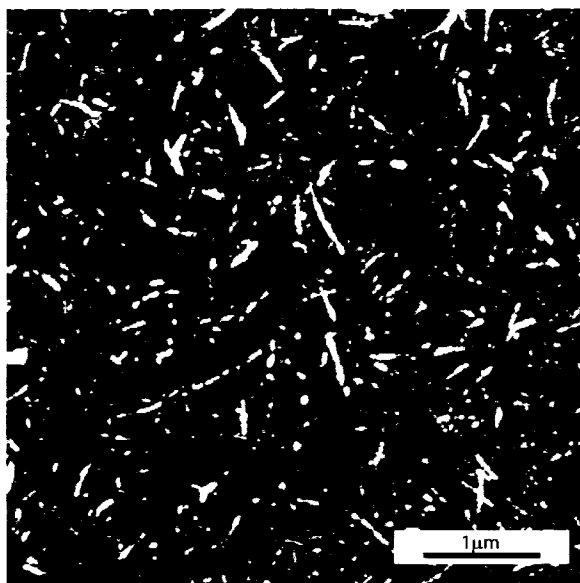


Figure 5-3. Self-assembled random carbon nanotube network fabricated using HiPco nanotubes on a aminosilane functionalized surface.

We will now describe the results for aligned LA-carbon nanotube arrays. Figure 5-4a displays an array of carbon nanotubes deposited from a single drop of the 0.1 mg/ml DMF-carbon nanotube solution followed by DCE. The histogram summarizing the distribution of angles (Figure 5-4e) shows the high degree of alignment that can be obtained. Depositing several drops each followed by a spurt of DCE in a subsequent manner increases further the density of the carbon nanotube coverage. Our results for denser carbon nanotube networks obtained from the deposition of 2, 3, and 4 drops are shown in Figure 5-4 b, c, and d, respectively. For a given DMF-carbon nanotube solution, we noted that the number of carbon nanotubes deposited follows a linear relation with the concentration of nanotubes in the solution (results not shown). Unlike

the deposition of random networks, two ways therefore exist to control the density of the arrays. Finally, for both random and aligned networks the density saturates when there is no longer enough functionalized surface area in order to further attach carbon nanotubes.
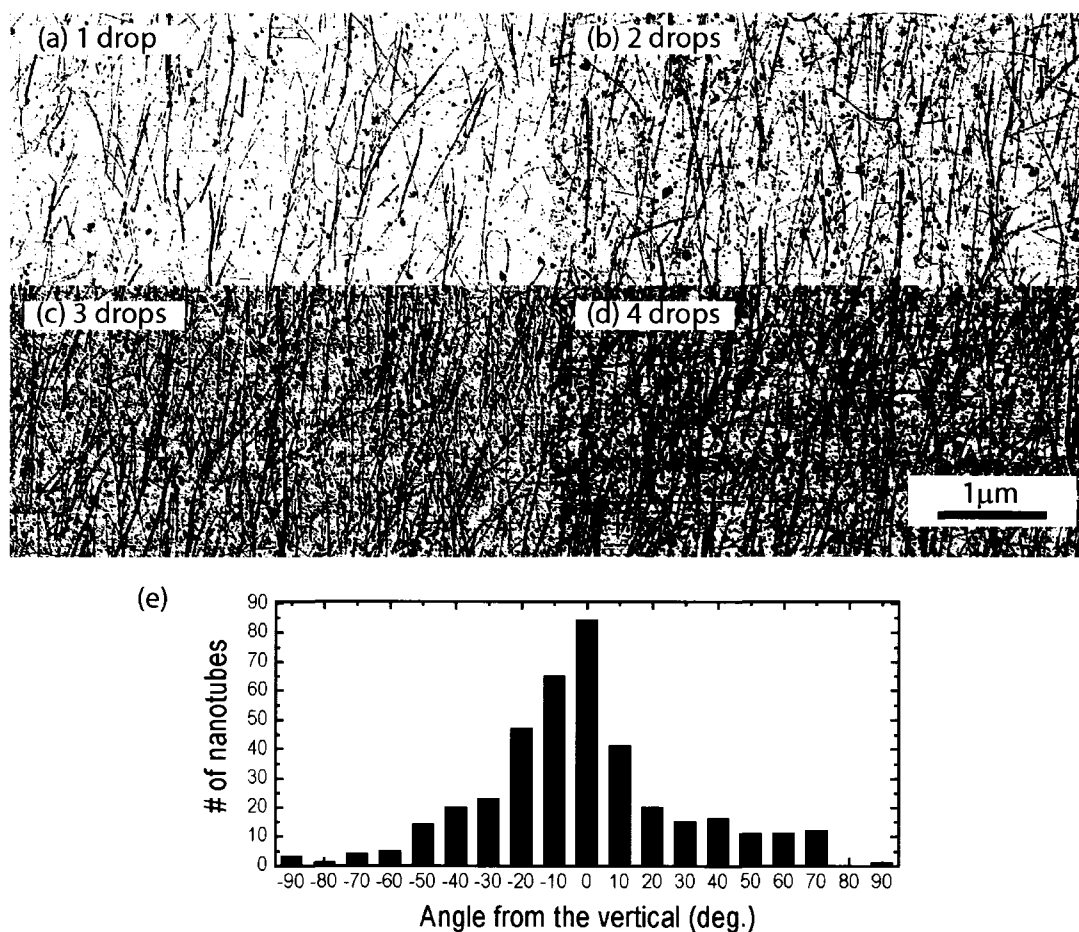


Figure 5-4. (a)-(d)AFM images of LA-carbon nanotube arrays deposited by the anchor-and-comb method. The images correspond (clockwise) to the self-assembly from a single drop (a) to four consecutive drops (b-d). (e) Histogram of the measured angles for arrays of carbon nanotubes showing a high degree of alignment. Data are taken from the deposition of one drop.

## 5.3.2 Discussion

In order to explain the high degree of alignment obtained from our deposition protocol, we propose an anchor-and-comb mechanism (illustrated in Figure 5-5) similar to what has been described for aligning strands of DNA.[188; 189] Initially the DMF-carbon nanotube drop spreads individual carbon nanotubes uniformly across the surface in the direction of the fluid flow. On one hand, this solvent has a very low vapor pressure and no significant evaporation takes place during this process <evaporation rate = 0.17 (BuAc = 1)>[14]. On the other hand, DCE evaporates relatively quickly <evaporation rate = 6.5 (BuAc = 1)> and is miscible in DMF. When dropped above the substrate, a drying front spreading across the surface is observed. The expanding meniscus induces the pinning of one end of the carbon nanotubes to the substrate. The centrifugal spreading of the solution then aligns the carbon nanotubes along the radial direction of the liquid flow. The anchoring to the substrate must be strong enough so that the receding air-liquid contact line will extend the carbon nanotubes, without detaching them from the surface. It is for this reason that the amino functionality is essential to the alignment procedure that we have described. Substrates had not been functionalized resulted in arrays having poor alignment and low carbon nanotube densities.
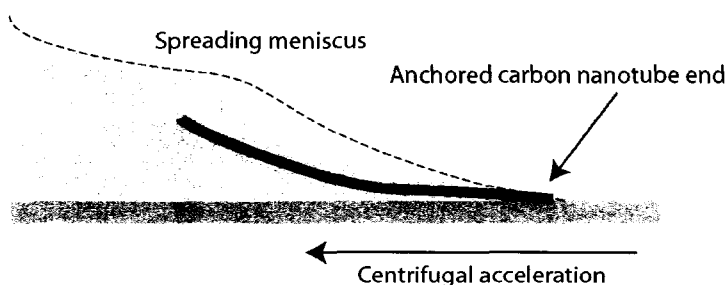


Figure 5-5. Schematic of the anchor-and-comb mechanism used to align carbon nanotubes on a functionalized surface in order to obtain parallel carbon nanotube arrays.

---

[14] The evaporation rate of Butyl Acetate (BuAc) is used as a relative reference.

The proposed mechanism also provides a good explanation to the linear relationship observed between the number of deposited carbon nanotubes and the concentration of the DMF-carbon nanotube solutions. All carbon nanotubes encountered by the advancing meniscus will be pinned and aligned on the substrate surface. As such, higher nanotube concentrations yield higher number of carbon nanotubes deposited. Once the surface is saturated, the interaction between the substrate and the nanotubes becomes insufficient to keep them in place and the density has reached its maximum. Finally, we note in the protocol described here that the laminar flow supplied by the spin coater allows us to comb the carbon nanotubes along a preferential direction.

In principle, other means of producing laminar thin-film flows can be used. For example, laminar flows along microfabricated channels are known to align carbon nanotubes and other one-dimensional nanostructures.[190] The remarkable electrical characteristics of these networks will now be addressed.

## 5.4 Electrical properties of carbon nanotube network thin film transistors

### 5.4.1 Results

First, we present our results for random carbon nanotube networks. We chose a carbon nanotube solution that had been optimized in order to obtain NN-TFT devices with high $I_{on}/I_{off}$ ratios and large On-state currents (network density $\sim 26$ nanotubes/$\mu m^2$). Figure 5-6 displays a typical SEM image of a random network TFT fabricated using the back gated geometry described in Chapter 4.
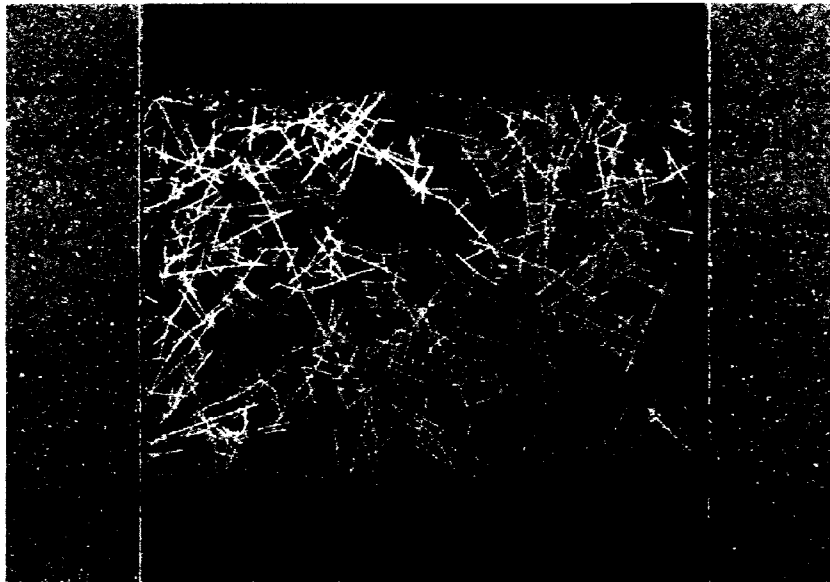
Figure 5-6. SEM image of a typical random network TFT device on a SiO₂ surface. This particular device imaged here had a device length of 10 µm and width of 7 µm.

Output characteristics for a typical device having 30 µm wide channel ($W_C$), 20 µm in length ($L_C$) are displayed in Figure 5-7. This device displays the p-type conducting behavior that typically characterizes carbon nanotube FETs on SiO₂ surfaces. Very high $I_{on}/I_{off}$ ratios (> $10^6$) and considerable on state currents ($I_{ds} \sim 2$ µA) can be measured for this device without having to eliminate the metallic percolation paths, as described in other studies.[44; 165; 167] The normalized transconductance of the network was measured to be 0.005 S/m, corresponding to an effective mobility of 1.2 cm²/V.s. This value compares favorably with a-Si ($\mu = 1$ cm²/V.s). So far, we are not aware of any other process published in the literature giving similar results.
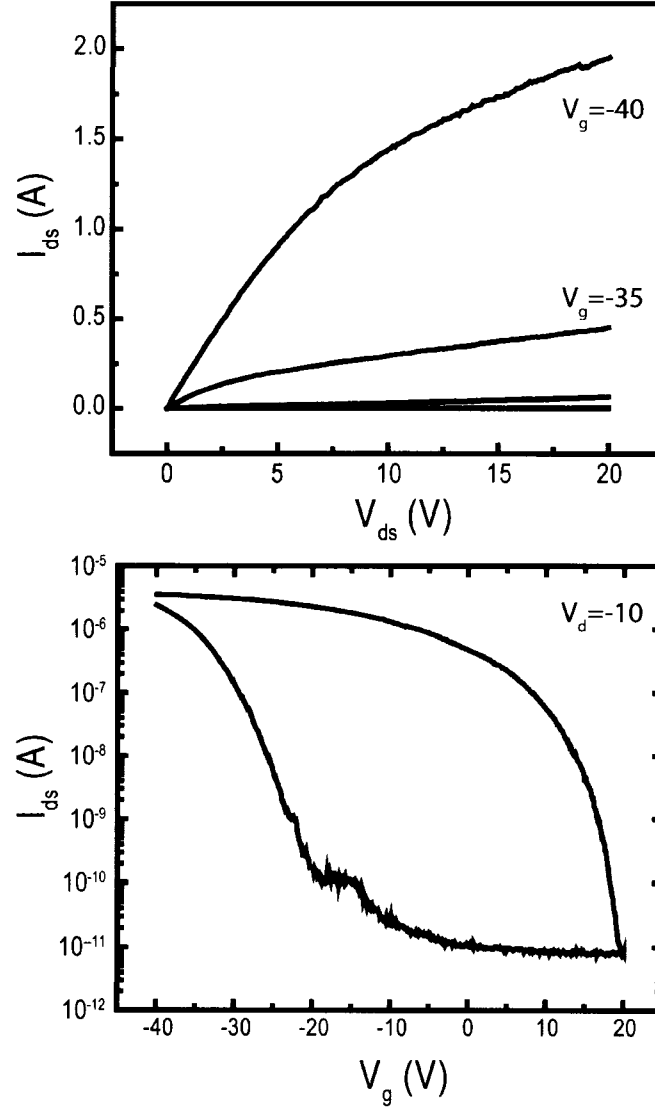
Figure 5-7. Typical output (top) and transfer (bottom) characteristics of random carbon nanotube TFTs. The device has a width W = 30 μm and a length L = 20 μm and operated in the hole accumulation mode. the transfer characteristics indicate over 6 orders of magnitude modulation of the current.

To study of the scaling behavior of these random carbon nanotube network devices, we fabricated a series of TFTs with channel lengths ranging from 1 μm to 100 μm and widths of 30 μm. The results are displayed in Figure 5-8. The On state current follows a

power law dependence and deviates only at long channel lengths. The Off state current, for its part, also follows a power law dependence until the current falls down below the resolution limit of the measurement apparatus (~ 1 pA). This behavior results in very high $I_{on}/I_{off}$ ratios, even for devices having channel lengths as short as 6 $\mu$m. Below this limit, the individual metallic carbon paths begin to bridge the entire channel and contribute substantially to the Off state current. As will be discussed in the next section, the exponent from the power law dependence defines the percolation behavior of carbon nanotube networks.
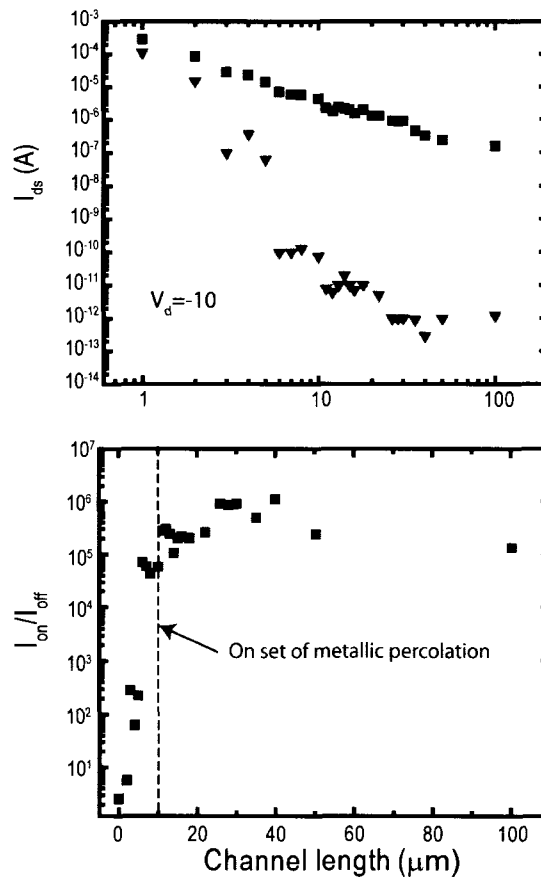


Figure 5-8. Scaling characteristics of a 26 nanotube/$\mu$m$^2$ random carbon nanotube network. (Top) The evolution of the On (squares) and Off (triangles) state current of carbon nanotube TFTs having widths of 30 $\mu$m and lengths ranging from 1 to 100 $\mu$m. (Bottom) Corresponding $I_{on}/I_{off}$ ratios showing the onset of metallic percolation.

It is expected that the power law behavior of the networks can be controlled by adjusting the density of carbon nanotubes and by conferring them with some degree of alignment. To test this, we measured the scaling characteristics of aligned network TFTs fabricated from 2 and 3 consecutive drops.[15] The results for devices having channel widths of 30 μm and lengths varying from 1 to 100 μm are displayed in Figure 5-9. Again, the current for the On and Off states follows a power law dependence as evidenced from the log-log plots similar to random networks. As will be discussed in the next section, the power law exponents, however, are significantly different.
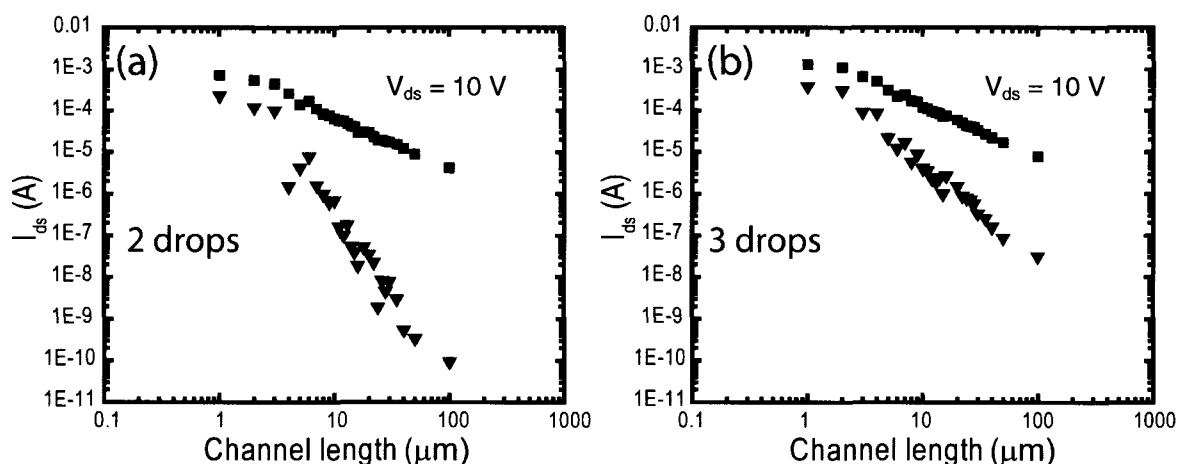


Figure 5-9. Scaling characteristics of aligned arrays of carbon nanotubes from the depositon of (a) 2 and (b) 3 drops of a 0.1 mg/ml DMF-nanotube solution. The devices are 30 μm wide and between 1 and 100 μm long. Both the On (squares) and Off (triangles) states are displayed.

## 5.4.2 Discussion

It is useful to interpret our results in the framework of classical percolation theory. Rogers et al.[52; 182] have recently published a theoretical model that accounts for the percolation behavior of random carbon nanotube networks. They have shown that the current satisfies the following scaling relationship:

---

[15] NN-TFT made from the deposition of 1 and 4 drops are currently being characterized.

$$I_{ds} \sim \frac{k}{L_{NT}} \left( \frac{L_{NT}}{L} \right)^m \tag{4.1}$$

The constant *m* is the scaling exponent that depends on the carbon nanotube length, coverage and alignement, *k* is a constant that depends on the resistivity of the networks (junctions + nanotubes), and $L_C$ and $L_S$ are the average lengths of the channel and the nanotubes, respectively. For networks that are well above the percolation density, the scaling constant is m = 1 and the On state current is simply inversely proportional to the channel length, as in a standard diffusive conductor (Ohmic limit). For random networks having densities at the percolation threshold, given by the relation $\rho_c L_{NT}^2 \sim 4.236^2/\pi$, the scaling factor is m = 1.9. [52] Below the percolation threshold, higher values for the scaling constant are found. Scaling parameters for the series of devices described in the previous section were determined using unconstrained curve fits. The R-square parameter for all the displayed fits was over 0.96, indicating that over 96% of the current dependence can be accounted for from the scaling function above. The result for the random network is displayed in Figure 5-10.
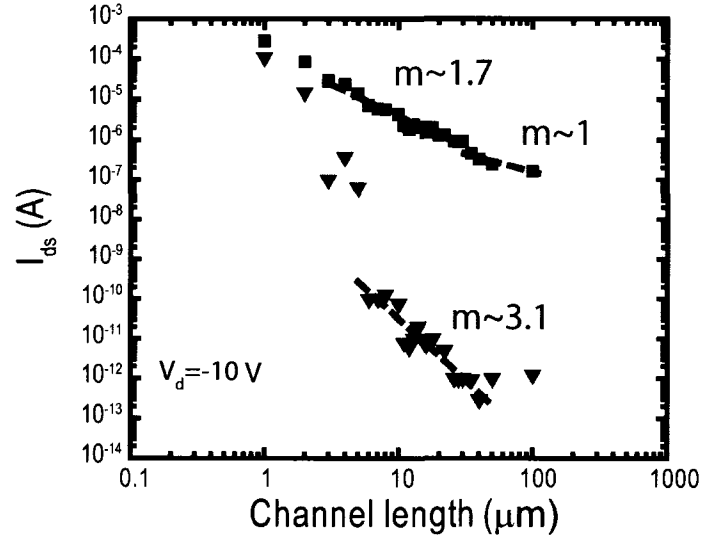
Figure 5-10. Power law fits to the On (squares) and Off (triangles) state currents of the random carbon nanotube network.

Various regimes can be extracted from this plot. First, the devices display in the long channel limit ($L_C > 40$ μm) an ohmic behavior with a scaling exponent that tends towards $m \sim 1$. In this regime, the Off state current is nearly zero owing to the complete absence of metallic percolation. This leads to an On/Off ratio of $\sim 10^6$. For shorter channel lengths, the exponent is found to be m = $1.7 \pm 0.05$. By fitting this data to the theoretical dependence of $m$ on the coverage $\rho L_{NT}^2$ reported by Rogers et al.,[52; 182] we find $<\rho L_{NT}^2>_{calculated} \sim 7.5$, which is below the value we had estimated from the density and carbon nanotube length $<\rho L_{NT}^2>_{measured} \sim 14$. This discrepancy simply reflects the fact that the distribution of carbon nanotube lengths does not follow a normal distribution function. If instead of taking 0.75 μm in the calculation above the maximum value of the distribution was used instead (0.44 μm), $<\rho L_{max}^2>_{measured} \sim 5$. Thus the calculated value falls within the measured value when the dispersion in carbon nanotube lengths is taken into account. In the Off state, the scaling parameter is found to be m = 3.4, indicating that the density is indeed below the metallic percolation density. From the above results, we can therefore conclude that the random self-assembled

networks exhibit favorable scaling behavior. Devices with 6 μm long channels exhibit On state currents exceeding 1 μA, while having $I_{on}/I_{off}$ ratios $\sim 10^5$. This is highly reproducible, which is an excellent result considering the difficulty and compromises imposed by the presence of metallic percolation.

Next, we have extracted the scaling parameters for aligned carbon nanotube networks in the same manner as for the random networks. The results are presented in Figure 5-11.
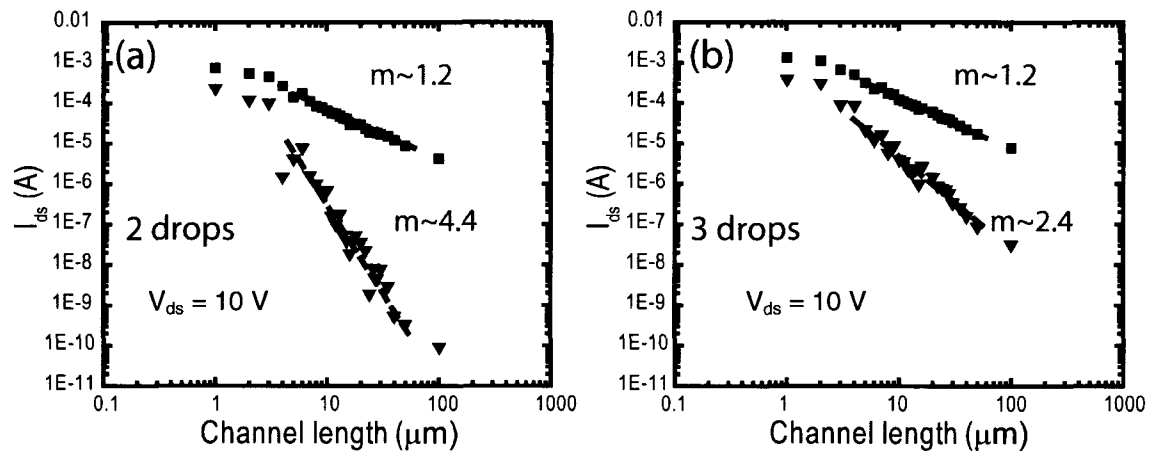


Figure 5-11. Power law fits to the On (squares) and Off (triangle) state currents for aligned networks fabricated using (a) 2 drop and (b) 3 drops of a 0.1 mg/ml DMF carbon nanotube solution.

It is interesting to note that the scaling parameter for the denser networks is the same as for the networks having lower densities (m = 1.2). This reflects the slow variation of the scaling parameter for densities that are above the critical percolation density.[52] Also, the current for the 10 μm long devices doubles, from 63 μA to 120 μA, although the density of the networks was increased by less than a factor of 2. This contrasts with the variation observed for the Off state current, where the scaling parameter passes from m = 2.2 to m = 4.4 by going from the denser to the sparser coverage. Since the purely metallic carbon nanotube network is one third less dense than the semiconducting network (metallic + semiconducting nanotubes), a fast variation of the scaling parameter is observed. Note however, that this model was developed for random carbon nanotube

networks. A model that takes into account the degree of alignment must be developed in the future in order develop strategies to improve NN-TFT device characteristics. Nonetheless, we have demonstrated that the deposition method provides an independent control over the scaling characteristics of the TFTs. We are currently exploring the tradeoff that is required between higher current densities and higher $I_{on}/I_{off}$ for different carbon nanotube alignments.

## 5.5 Conclusion

We have shown that both random and aligned carbon nanotube networks can be readily made from bulk carbon nanotube sources. The density of the networks can be precisely controlled over the entire wafer scale. This process allows us to look into the scaling behavior of carbon nanotube thin-film transistors of various configurations. Previously reported methods to align carbon nanotubes relied on other driving forces for orienting the nanotubes during their growth. For example, through the use of magnetic, and electric fields[55] of by growing nanotubes along the step edges of sapphire or quartz substrates.[56] Such guided growth techniques have a number of important drawbacks. The need to transfer the networks from the growth substrate to a target substrate imposes a number of relatively complex fabrication steps. Also, these techniques rely on the CVD synthesis of carbon nanotubes and result in large distributions of diameters leading to various optoelectronic properties. We show that by using a combination of forces, it is possible to produce networks over large areas having a high degree of alignment and controllable densities. Prior to this work, no solution-based technique had been developed that provided such control over the nanotube arrays.

The scaling characteristics of network devices having various configurations were studied. By using individualized carbon nanotubes to assemble the networks, both high mobilities and very large $I_{on}/I_{off}$ ratios were achieved reproducibly for devices having short channel lengths. We also showed that it was possible to control the intrinsic

percolation properties of the network, as expressed in the critical scaling parameter by controlling the density and by conferring alignment to the networks.

The characteristics of these devices demonstrate conclusively that scaling of carbon nanotube TFTs leads to predictable behaviors, demonstrating the potential of carbon nanotube networks as a technologically relevant organic thin film material. This new class of materials can be easily pattered to make integrated circuits and complex device architectures. In addition to exhibiting electronic performances equivalent to amorphous silicon and far superior to any other organic semiconductor, this material is flexible and transparent. We believe that carbon nanotube networks constitute an important building block for future microelectronic applications.

# CHAPTER 6: Substrate vs. environment - What suppresses electron conduction in field-effect transistors?

## 6.1 Introduction

The field-effect transistor (FET) configuration has been crucial for elucidating the electronic transport properties of organic and nanoscale systems.[191-193] A degenerately doped silicon wafer with a thin oxide layer is the ubiquitously used substrate since it also functions as the gate electrode. Because of the chemical inertness of the $SiO_2$ surface, it was widely assumed that the substrate did not influence the measurement of the intrinsic properties of the material under study. However, Friend at al.[21] recently demonstrated that by changing the chemical functionality of the substrate, organic semiconductors that were thought to be exclusively p-type conductors in fact exhibit ambipolar behavior. They singled out silanol groups at inorganic oxide surfaces as the culprits for generating electron traps responsible for suppressing electron conduction.

Carbon nanotube field-effect transistors (CNFETs) are the most extensively studied nanoscale field-effect transistors to date.[192; 194] Given that their behavior is well described by detailed theoretical models, they provide an ideal system for investigating fundamental transport mechanisms at the nanoscale.[145; 147] Much like organic semiconductor FETs, a distinctive characteristic of carbon nanotube devices has been their almost exclusive p-type character in air.[163] Ambipolar transport can be observed only under certain conditions, for example, in large diameter/low bandgap nanotubes, [163] devices annealed in vacuum[163] and devices fabricated on very thin gate oxides (<5 nm). The similarities between the electrical behavior of CNFETs and organic semiconducting FETs provided the impetus for investigating the influence of substrate on the measured electronic properties carbon nanotube devices.

## 6.2 Experimental
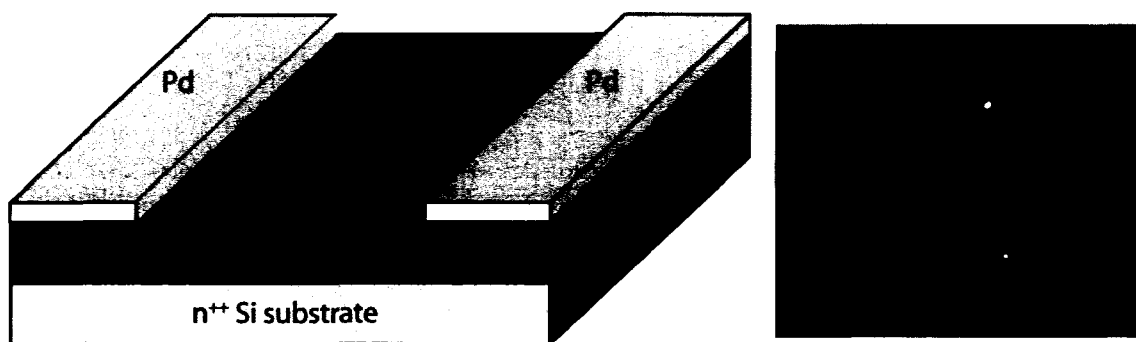


Figure 6-1. Individual carbon nanotube field effect transistor. A schematic of the back gated geometry of the device on a SiO2 substrate (left). A AFM image of a typical device (right).

Laser ablation synthesized carbon nanotubes were used for all the experiments detailed here. The electrical characteristics of both individual carbon nanotubes and carbon nanotube network FETs were assessed. The device fabrication procedures have been detailed in previous chapters.[16] We first considered devices fabricated on the traditional $n^{++}$ doped silicon substrates with a 100 nm thermal oxide layer (Figure 6-1.). The second substrate consisted of a bilayer structure in which we deposit 100 nm parylene-C films (Cookson Electronics) on a silicon substrate with a 20 nm thick thermal oxide layer. Parylene is an oxygen free, hydrophobic polymer that forms conformal pin-hole free coatings on $SiO_2$ surfaces. Electrical contacts were made by depositing 20 nm thick metal layers by e-beam evaporation through lithographically defined patterns. Prior to electrical measurements, the devices were annealed in vacuum ($1 \times 10^{-6}$ torr) at 550 °C and 260 °C for devices fabricated on silicon oxide and parylene substrates, respectively. Electrical measurements were conducted using a semiconductor parameter analyzer (Agilent B1500A) either in ambient atmosphere or in a vacuum probe station.

---

[16] Individual carbon nanotube transistors are made by depositing very sparse aligned carbon nanotubes on a surface as described in Chapter 5. Electrical contacts having 1 μm spacings are patterned and probed in order to find devices connected by a semiconducting carbon nanotube.

## 6.3 Results and discussion

Figure 6-2a shows a typical transfer characteristic for a 1 μm long individual CNFET fabricated on a $SiO_2$ surface. This curve highlights the unipolar p-type conduction behavior that is usual for carbon nanotubes on oxide substrates. We have measured over 500 CNFETs from our laser ablation source and observed similar behaviors independent of the metal used as the source and drain electrodes (Au, Ti, Pd, Co). These results are consistent with numerous published results on the electrical behavior of CNFETs. However, these results are in sharp contrast to what we observe for CNFETs fabricated on parylene substrates. From Figure 6-2b it can be seen that the conductance can be modulated with both negative (holes) and positive (electrons) gate voltages. This ambipolar behavior was a persistent observation for more than 30 CNFETs on parylene substrates measured in air. These results unambiguously demonstrate that electron conduction in carbon nanotubes is influenced by the chemical nature of the gate dielectric. It was believed that large Schottky barriers to electron injection present at the metal-nanotube interface were responsible for the exclusively p-type character of these devices.[163] While Schottky barriers indeed play a significant role in the transport properties of CNFETs,[147] it is clear that they are not the dominant factor in limiting n-type conduction.
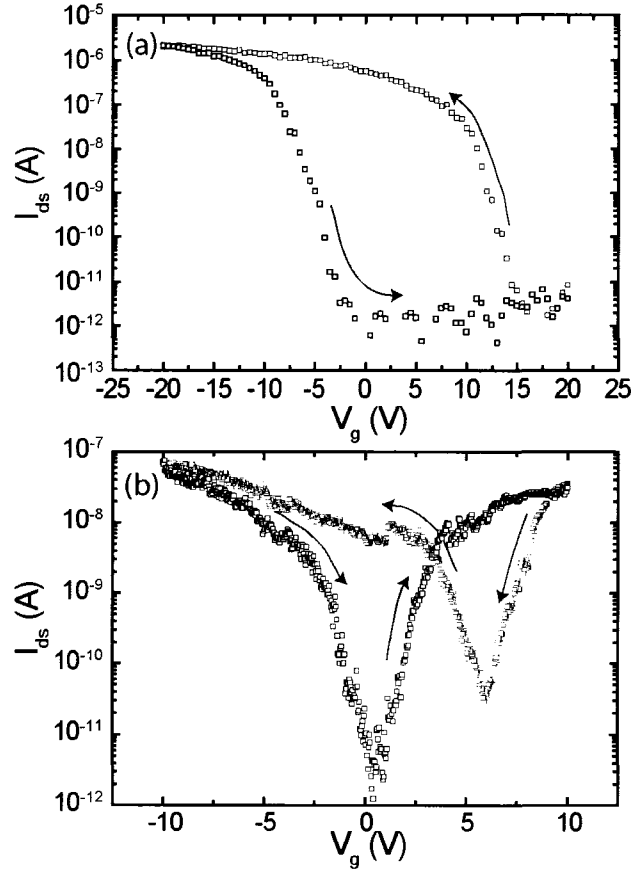
Figure 6-2. Typical transfer characteristics for 1 µm long individual CNFETs fabricated on (a) a silicon oxide surface and (b) on a parylene-C surface. In red is the first voltage scan and black the reverse scan with the arrows indicating the direction of the voltage sweep.

Previous studies have demonstrated that it is possible to transform unipolar p-type CNFETs fabricated on $SiO_2$ surfaces to ambipolar by annealing in vacuum.[163] By sealing the devices in glass before exposing them to the atmospheric environment, they maintained stable ambipolar behavior in air. In a similar experiment we have evaluated the transport characteristics of CNFETs encapsulated in a 200 nm thick parylene-C layer. Parylene is known to be an efficient humidity and oxygen barrier. Encapsulated devices showed transport behavior equivalent to un-encapsulated devices. It was only after annealing in vacuum for 24 h at 260 °C, aimed at desorbing trapped chemical species through the semi-permeable parylene capping layer, that significant electron

currents could be measured. The transfer characteristics of parylene coated devices fabricated on $SiO_2$ substrates after the vacuum annealing step are shown in Figure 6-3. Together these results show that the silanol groups at the oxide surface cannot alone be the origin of electron trapping. Clearly an absorption of a molecular species from the ambient atmosphere at the dielectric interface is responsible for suppression n-type conduction in these devices.
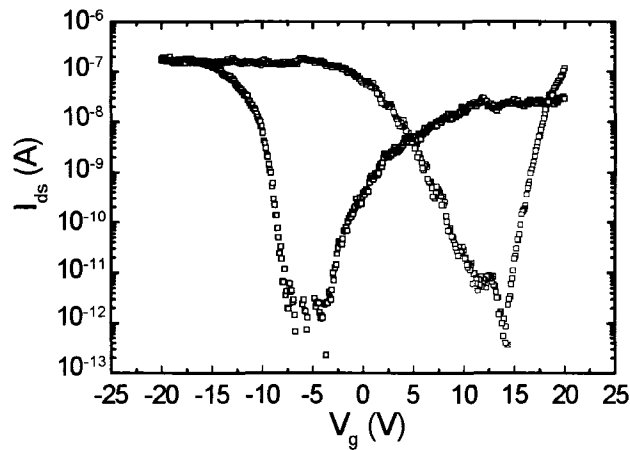


Figure 6-3. Typical transfer characteristics for 1 μm length individual carbon nanotube FET fabricated on a silicon oxide surface and encapsulated in 200 nm parylene layer after vacuum annealing at 250 °C.

It is known that a layer of molecular water will physically adsorb to $SiO_2$ surfaces through hydrogen bonding to silanol (-OH) groups.[195] Under an electric field the water molecule can dissociate into $H_3O^+$ and $OH^-$ groups.[196] Because the mobility of $OH^-$ is significantly lower than that of the proton, a net negative charge will accumulate on the surface upon any gate voltage increase thereby screening the electric field. The accumulation of surface bound $OH^-$ groups has been evidenced during the field-induced local anodization of silicon surfaces.[197] The availability of a monolayer of water is essential for the accumulation of electron traps at the dielectric surfaces. Substrates having a strong affinity to water such as oxygen containing dielectrics will thus lead to a higher density of trapped negative charges.

The mechanism we propose for electron trap generation by ionized surface bound water reconciles our observations of the electrical transport behavior of carbon nanotubes and those reported for organic semiconductors. The hydrophobicity of parylene-C coatings results in a sufficiently low concentration of water generated charge traps so that n-type transport in individual carbon nanotube devices can be readily observed. There is, however, still a considerable amount of water adsorbed on parylene-C surfaces exposed to air. In order to highlight this fact, we fabricated long channel (L = 50 μm) carbon nanotube network thin film transistors on parylene substrates[17]. The transfer characteristics of one of these devices are shown in Figure 6-4. Although n-type conduction is still observed the results are less striking than those for individual carbon nanotube FETs. The probability of electron traps inhibiting transport is exacerbated in long channel devices. In vacuum, the desorption of this lightly bound water layer resulted in carbon nanotube network devices exhibiting almost symmetrical electron and hole conduction characteristics (Figure 6-4, filled squares). Similar devices fabricated on SiO₂ did not display significant n-type transport unless they were annealed in vacuum by passing current through the devices for prolonged periods (several days). This reflects the fact that the adsorbed species on these surfaces (most likely water) require considerable annealing temperatures in order to desorb.

---

[17] The filtration method, described in Chapter 4, was used in order to deposit semiconducting networks (density $\sim 3$ nanotubes/$\mu m^2$) on parylene substrates. Electrical contacts were deposited as previously described.
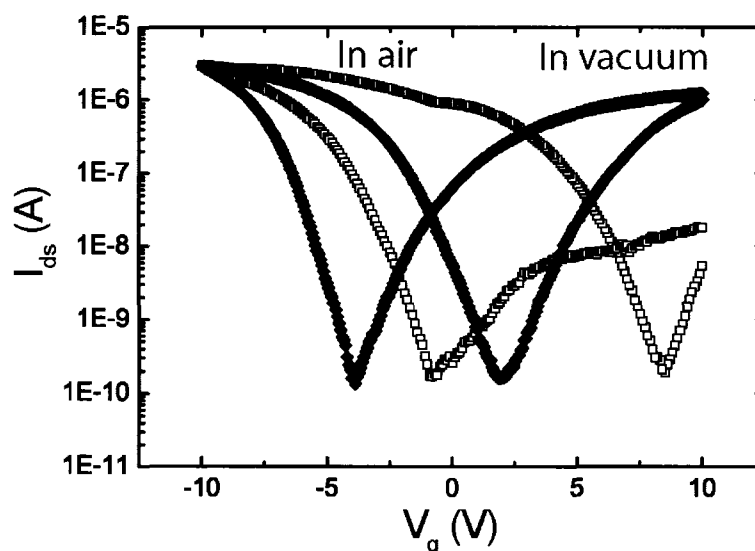
Figure 6-4. Transfer characteristics for the same carbon nanotube network FET having channel length of 50 μm and width of 100 μm fabricated on parylene substrates. The hollow (black) squares are for the device measured in air and the filled squares (blue) are for the same device measured in vacuum. Electron conduction increases by orders of magnitude while there is no change observed to the overall p-type conductivity. Both currents are nearly symmetrical with p-type conduction favored by the Pd contacts.

## 6.4   Conclusion

A detailed study of the electrical characteristics of the devices fabricated on $SiO_2$ and parylene substrates has, on one side, enabled us to fabricate devices that exhibit ambipolar devices in air and, on the other side, to clearly reveal that adsorption of molecules from ambient causes this behavior. Based on the known properties of the selected substrates and the temperatures required for obtaining ambipolar behavior after vacuum annealing, we propose that water vapor in air is the most probable species responsible for the loss of the n-branch in carbon nanotube field effect devices. This investigation, carried out for both individual and network carbon nanotube devices, is of direct and immediate interest for the organic electronics community that is currently facing the same problem.

# CHAPTER 7: Carbon nanotube sheets as electrodes in organic light emitting diodes[18]

## 7.1 Introduction

Light emitting diodes made from thin organic and polymeric layers are generating much excitement due to their applicability in large area flat panel displays and solid state lighting.[11] It is known that the performance of organic light emitting diodes (OLEDs) is largely dominated by charge injection from the anode and cathode.[22] In addition to influencing the overall brightness and power efficiency, improving charge injection increases the lifetime and stability of these devices.[198] The choice of the appropriate electrode material is thus paramount to obtaining reliable and efficient OLED.

Up to now only transparent conducting oxides, such as indium tin oxide (ITO), display both the transparency (>80% in the 400 – 700 nm region) and resistance (~ 20 Ω/sq.) needed for the electrodes through which light is extracted.[199] However, in spite of all the work that has been done towards optimizing devices implemented on ITO anodes, their use poses important limitations. Indium migration from the ITO surface is a known cause of premature device failure.[198; 200] Furthermore, ITO does not lend itself well to deposition onto flexible substrates.[201] The low temperature deposition techniques that are compatible with polymeric substrates lead to higher sheet resistances and surface roughness values. Moreover, repeated bending of ITO layers inevitably leads to cracking and delamination. Finally, the fabrication of top emitting devices using ITO anodes is limited as the ITO deposition process often damages the underlying organic semiconducting layers.[202]

---

Thin and flexible carbon nanotubes sheets exhibiting excellent optical transparencies (40-90%) and electrical conductivities (~1 x $10^4$ S/cm) have recently been fabricated using a room temperature deposition technique.[41] Their intrinsic work function (4.5 - 5.1 eV)[91; 92] is similar to that of ITO (4.4-4.9 eV)[203] and can be tailored through both n–type and p-type charge transfer doping,[204] allowing, in principle, double-sided charge injection in transparent OLEDs. Recently, a polymer LED[42] and an organic solar cell[40] that used multiwall carbon nanotube and single wall carbon nanotube (SWNT) anodes respectively, were demonstrated.

In this chapter, we show for the first time that SWNT sheets can be used as hole injecting anodes for high performance small molecule OLEDs. The luminance efficiencies of our devices are comparable to conventional geometry ITO-based OLEDs made under the same experimental conditions. Our results convincingly demonstrate that novel carbon nanotube anodes are a viable alternative to transparent conducting oxides.

## 7.2    Experimental

The SWNTs used in these studies were produced by a pulsed laser vaporization technique[117] and purified following a standard procedure.[118] This involves the refluxing of the as-received soot in concentrated nitric acid (60%) for four hours followed by filtration and subsequent refluxing in ultrapure water for two hours in order to remove any excess acid. These purification steps eliminate amorphous carbon and metal catalyst impurities from the sample and result in the p-type charge transfer doping of carbon nanotubes.[41]

Carbon nanotube sheets are made following the procedure recently described by Wu et al.[41] The purified SWNTs are dispersed in a 2% sodium cholate solution and centrifuged at 5 000 g for two hours in order to remove undispersed particles and large nanotube bundles. Carbon nanotube sheets of increasing thicknesses are made by filtering increasing volumes of a 1 x $10^{-4}$ mg ml$^{-1}$ sodium cholate solution through a

0.2 μm cellulose filter. Finally, the sheets are transferred onto clean glass slides by dissolving the filters in acetone.

OLEDs were fabricated on carbon nanotube electrodes as well as on commercial ITO-coated glass substrates (Colorado Concept Coatings LCC, 20 Ω/sq.). The carbon nanotube electrodes are patterned through a shadow mask from a $130 \pm 12$ nm thick carbon nanotube sheet (60 Ω/sq.) by reactive ion etching using an RF oxygen-plasma (30 s, 75 mTorr, 80 mW/cm$^2$). Patterning the electrodes in this manner is done in order to avoid the rough edges that would result from cutting the sheets using other methods, e.g. scissors. Finally, electrical contacts are made by evaporating a 50 nm thick Ti layer to one end of the nanotube electrodes.

Traditional OLED devices were fabricated on oxygen-plasma treated ITO anodes. The organic stack structure was optimized for maximum luminance efficiency and consisted in a 10 nm copper phthalocyanine (CuPc) hole injection buffer layer (HIL), a 50 nm N,N'-bis-(1-naphthyl)-N,N'-diphenyl-1,1-biphenyl-4,4'-diamine (NPB) hole transport layer (HTL) and a 50 nm tris-(8-hydroxyquinoline) aluminum (Alq$_3$) electron transport and emissive layer deposited at $\sim 0.1 - 0.2$ nm s$^{-1}$ in a thermal evaporator with a base pressure of $5 \times 10^{-6}$ Torr. The cathode was made by evaporating 1 nm of lithium fluoride and 50 nm of aluminum immediately following the organic layer deposition (i.e. without breaking vacuum). As will be discussed below, thicker organic layers and an alternative buffer layer material were determined to be necessary in order to achieve high performance OLEDs on SWNT electrodes. The buffer layer consisted in a $\sim 1$ nm parylene-C coating (Cookson CVD deposition system) applied onto the carbon nanotube sheets prior to organic stack deposition. OLED devices were then made by depositing NPB and Alq$_3$ layers of equal thicknesses followed by the same bilayer cathode. Although both 50 nm and 100 nm organic layer thicknesses were attempted, devices consisting of thicker layers displayed the best performance. The emissive area of all devices shown is 10 mm$^2$.

The device measurements were carried out under a nitrogen atmosphere using a semiconductor parameter analyzer (HP 4145A) and a photometer (Delta-Ohm HD9021) controlled by data acquisition software.


## 7.3   Results and discussion

The four-point probe sheet resistance of the SWNT electrodes is plotted in Figure 7-1 as a function of their transmittance at $\lambda = 520$ nm, i.e. the peak emission wavelength of our devices. As expected, an increase in transmittance is obtained at the cost of an increase in sheet resistance. The corresponding conductivity ($\sim1.2 \times 10^3$ S/cm) is constant across the thickness range indicating that, in spite of the high surface roughness of 12 nm (rms) measured for all sheets (determined by AFM), a continuous percolative carbon nanotube network is formed even for the thinnest sheets fabricated. This conductivity value, which depends sensitively on carbon nanotube source and doping treatments, falls within the range of reported values.[40-42]
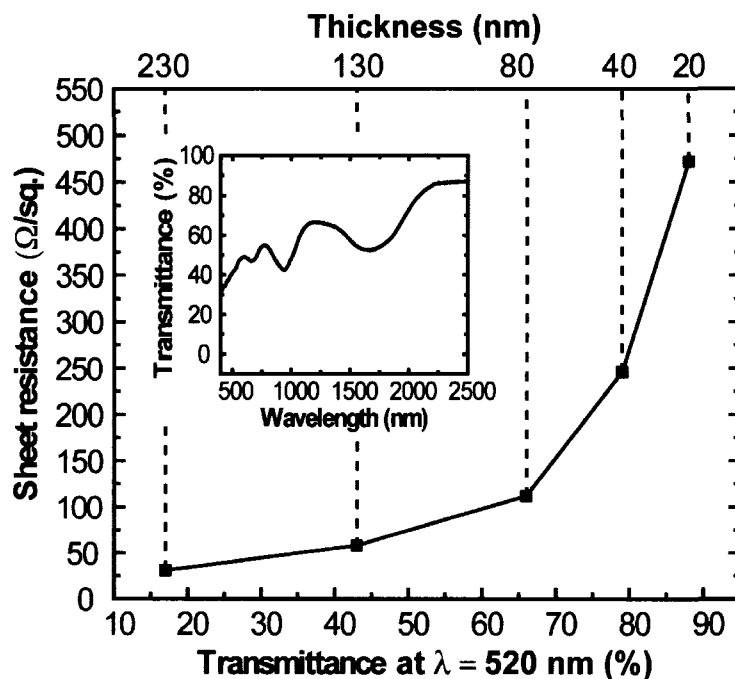
Figure 7-1. Sheet resistance of carbon nanotube sheets versus the transmittance in the visible range ($\lambda = 520$ nm) for different thickness. The transmission spectrum for the 130 nm thick carbon nanotube sheet is given in the inset.

The quality of the small molecule/SWNT interface is a key element for the successful fabrication of OLED devices on SWNT electrodes. The considerable roughness of the SWNT sheets imposes a lower limit to the thicknesses of the organic layers. AFM images (not shown) immediately following the deposition of 100 nm thick NPB layers on bare SWNT electrodes revealed the presence of large pinholes ($\sim$ 100 nm) arising from inappropriate organic layer coverage. This in turn led to devices that were electrically shorted. A parylene buffer coating dramatically improved the wetting and adhesion of the organic layer and led to essentially complete electrode coverage.
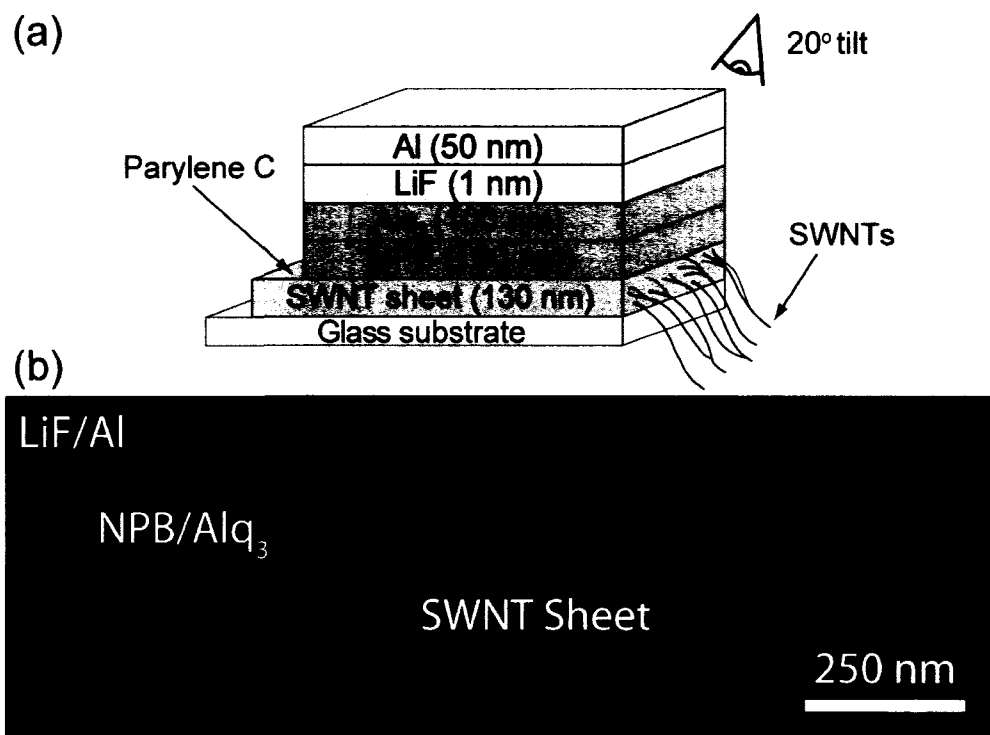
Figure 7-2. (a) Schematic of the SWNT OLED device and (b) corresponding cross-sectional scanning electron microscopy image at a broken edge taken at a 20o angle from the surface normal. Color was added to the image for clarity.

A cross sectional image (~20° inclination) of the complete SWNT-OLED device is shown in Figure 7-2. The sample was prepared for scanning electron microscope (SEM) imaging by cleaving the glass substrate at the center of the emissive area. Given the flexible, fabric quality of the interconnected carbon nanotube network, the sheet does not break at the substrate edge. It can be seen that the SWNT sheets are torn and fold onto the glass substrate.
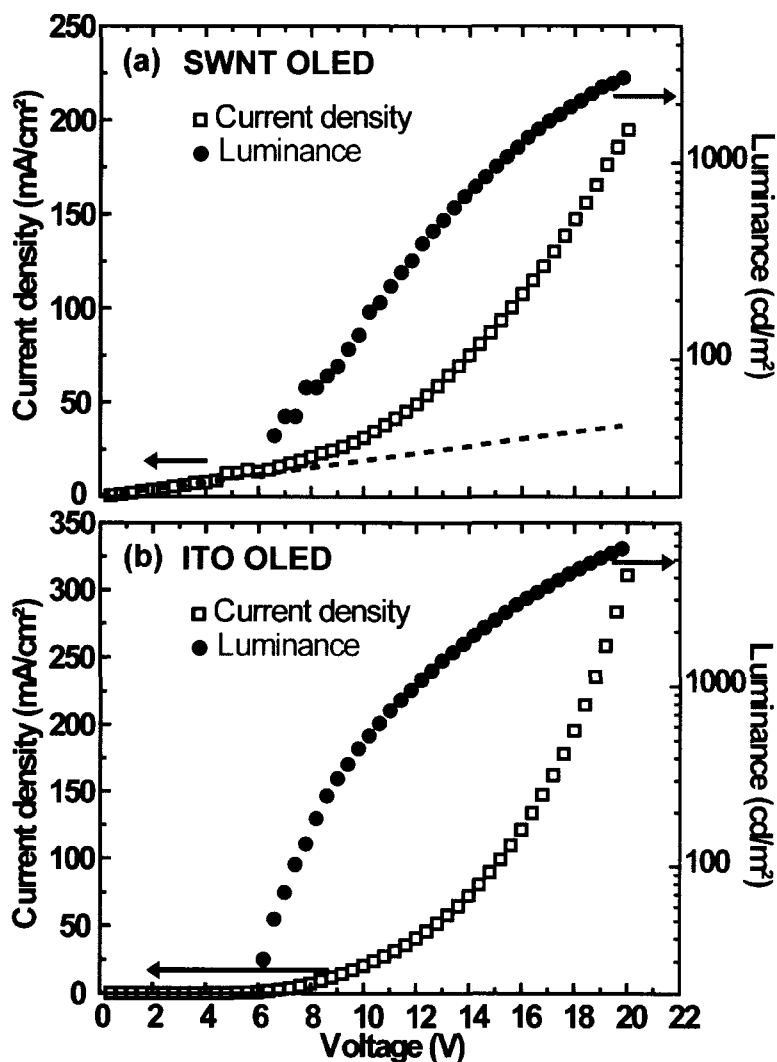
Figure 7-3. Current density (squares) and luminance (circles) as a function of applied voltage for OLEDs fabricated (a) on carbon nanotube anodes (SWNT-OLED) and (b) on oxygen-plasma treated ITO anodes (ITO-OLED).

The current density and luminance characteristics of the devices as a function of voltage, displayed in Figure 7-3, are similar for both devices and are typical of OLEDs.[11; 199] Despite the thicker organic layers used, the measured turn on voltage (6.6 V) for our SWNT-OLED is only slightly higher than that measured for the thinner ITO-OLED (6.2 V). The maximum achieved brightness is 6 000 cd/m$^2$ for the ITO-OLED compared to roughly half, 2 800 cd/m$^2$, for the SWNT-OLED. This is remarkable given that the

carbon nanotube anode displays a transmittance at the peak emission wavelength that is approximately half that of the ITO/glass substrate (i.e. 44% and 90% respectively). After accounting for optical absorption losses, both devices exhibit similar emission performances.

As shown in Figure 7-3a in the case of the SWNT-OLED, below the device turn-on, the current increases linearly with voltage indicating the presence of leakage currents. By extrapolating this curve (dotted line in Figure 7-3a) we estimate that, at the maximum achieved brightness, 20% of the current does not participate to the electroluminescence. Nevertheless, in spite of observed current and optical absorption losses, the luminance external efficiencies achieved are significant. At the maximum light output (20 V) they are comparable at 1.9 and 1.4 cd A$^{-1}$ for the ITO-OLED and SWNT-OLED respectively. We can therefore expect that, by improving the conductivity/transparency ratio and by eliminating all current losses, the performance of SWNT-OLED devices will exceed that of ITO-OLEDs.

Buffer layers between the ITO anode and the HTL are routinely used in order to increase the overall performance of ITO-based OLEDs. The exact role of this layer is, however, not well understood.[13] Parylene, in our case, was chosen for its ability to form thin conformal coatings on carbon nanotubes.[43] Its presence dramatically improved the morphology of the SWNT-HTL interface leading to devices having lower leakage currents. The introduction of this insulating layer between the anode and the HTL does not appear to have a detrimental effect on the carrier injection efficiency. As observed earlier, the turn-on voltages of both our SWNT-OLED and ITO-OLED devices are similar although greater organic layer thicknesses generally result in higher turn-on voltages. Thus, as a first approximation, our results suggest that hole injection barriers for both ITO and SWNT anodes are similar. This was expected given the similar work function of SWNTs and ITO. However, it is clear that in addition to hole injection barriers, the adhesion and wetting characteristics of the deposited organic layers is central to the performance of SWNT-OLEDs.

## 7.4 Conclusion

In summary, we have implemented carbon nanotube anodes in small molecule OLED devices. Using this new electrode material it is readily possible to achieve performances comparable to established ITO-based OLEDs. Our work opens new technological avenues for OLED devices. Unlike ITO, which is brittle, subject to cracking and delamination, carbon nanotube anodes are entirely flexible. Secondly, their room temperature processing renders them suitable for use with a wide range of substrates for both top and bottom emission devices. Finally, the nanoscale morphology of our electrode may yield alternative light out-coupling pathways. By optimizing the SWNT-HTL interface and increasing the carbon nanotube anode transparency, we believe that devices exhibiting performances superior to traditional ITO-based devices will soon be demonstrated.

# CHAPTER 8: Carbon nanotubes as injection electrodes in organic thin film transistor devices

## 8.1 Introduction

The study of the electrical transport properties of organic semiconducting materials has been hindered by the lack of suitable electrical contacts. The main problem is the significant contact barriers due to large band offsets between the metal Fermi level and the energy levels (HOMO and LUMO) of the organic materials.[81; 205] Attempts to reduce this Schottky barrier were essentially unsuccessful because charge transfer involves primarily the local interface states and produces strong dipoles that oppose to further shifting of the organic energy levels.[206] Moreover, the local environment, the impact of adsorbents on the metals, and other processes due to complex surface chemistries further contribute to reinforce the band offsets.[83; 207] It is therefore important to investigate different injection strategies in order to overcome the limitations posed by the electrodes studied to date. Owing to their high surface area and the possible field-enhancement related to the 1D electrostatics,[146; 147; 208] carbon nanotubes may provide alternative injection pathways into organic semiconductors.

We saw in Chapter 7 that carbon nanotube sheets could successfully be implemented as the anode in organic light-emitting diodes (OLEDs). Remarkably, the performance of our carbon nanotube electrode was comparable to the established, state of the art, transparent conductive electrodes. Charge injection efficiency could not be investigated in detail due to the disordered nature of the electrode. In the stacked OLED geometry, the interface is buried and it is thus difficult to determine the area of carbon nanotubes participating to charge injection.

Drawing upon previous work that has pioneered the possible use of metallic carbon nanotubes for making contacts to small pentacene islands[88; 89] and individual

molecules,[87] we have investigated charge injection by carbon nanotube tips in different device configurations. Initially, individual carbon nanotube electrodes were investigated. By placing a semiconducting island between the nanoscale gap separating two carbon nanotubes, a nanoscale field-effect transistor was fabricated. The total amount of current that can be injected from carbon nanotube tips was then measured. We found that the On state current of carbon nanotube contacted islands were two orders of magnitude greater than traditional metal electrodes. Furthermore, we demonstrate that our strategy can be implemented in larger OTFT geometries. The fabrication techniques described in Chapters 3 through 5 allowed us to attach carbon nanotube arrays to metal electrodes. By using these arrays to inject charge into a pentacene based OTFT channels, we show that injection barriers can either be significantly reduced or trimmed down by electrostatic effects.

## 8.2 Experimental

### 8.2.1 Fabrication of nanoscale field-effect transistors

Field effect transistors consisting of a single pentacene island placed between the tips of two carbon nanotubes were investigated. The back gated device configuration illustrated in Figure 8-1 is fabricated as follows: first, carbon nanotubes were deposited by spin coating a dichloroethane carbon nanotube solution onto a degenerately doped $n^{++}$ silicon wafer having a 100 nm thermal oxide layer.[19] Electrical contacts were then patterned by optical lithography, followed by e-beam evaporation of a 0.5 nm of Ti and 20 nm of Pd layers without breaking vacuum. The devices were annealed in vacuum ($1 \times 10^{-6}$ torr) at 550 °C for 1 h in order to decrease the metal-carbon nanotube contact resistances.

The electrical characteristics of the connected carbon nanotubes were initially probed in order to identify devices exhibiting purely metallic behavior (i.e. no conductance

---

[19] $SiO_2$ surfaces suppress electron conduction in organic thin film devices, as discussed in Chapter 6. Here we are probing the injection of holes into pentacene and thus the substrate should have no influence.

dependence of the gate voltage). Nanoscale gaps at the center of the metallic carbon nanotubes were opened by electrical breakdown.[109] The available gap length was measured to be in the range of ~ 20-200 nm. Each end will serve respectively as the source and drain electrodes of the nanoscale transistor.

Carbon nanotube electrodes

Pd

Pd

n++ Si substrate
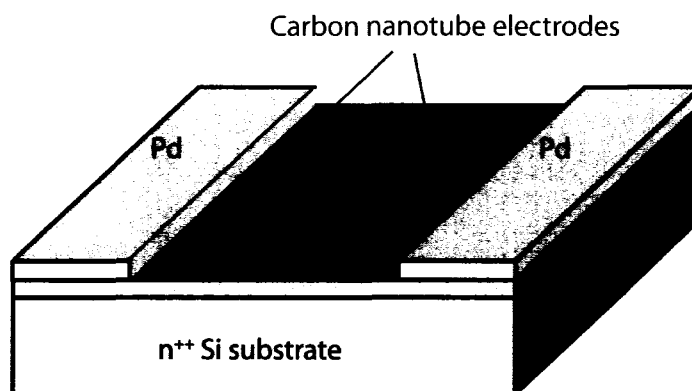
Figure 8-1. Schematic of a pentacene nanotransistor. An individual pentacene island is contacted by two metallic carbon nanotube electrodes that act as source and drain electrodes. The gap is generated by the electrical breakdown of a metallic nanotube.

Pentacene islands were deposited using a soluble pentacene precursor route. The pentacene adduct 13,6-N-Sulfinylacetamidopentacene was purchased from Sigma-Aldrich and used without further purification. Spin-coated films of the precursor undergo a solid-phase conversion to pentacene when heated at 170-200 °C. These pentacene films have been shown to exhibit a field-effect mobility (~ 0.8 cm$^2$/V.s) that is comparable to vacuum sublimated pentacene films (~ 1 cm$^2$/V.s).[156] We spin coated a 2 mg/ml chloroform solution of the precursor onto the wafer containing the carbon nanotube electrodes (after breakdown). These very thin adduct films (~ 10 nm) form pentacene islands a few hundreds of nanometers in diameter and height during their conversion into pentacene. Moreover, we observed that carbon nanotubes promote the

nucleation of pentacene, whereby the islands were found to grow preferentially in the gaps between the carbon nanotube tips.

## 8.2.2    Fabrication of OTFTs having carbon nanotube array electrodes

The implementation of carbon nanotube electrodes to OTFT devices having realistic dimensions was done by attaching arrays of carbon nanotubes to source and drain metal electrodes as illustrated in Figure 8-2.
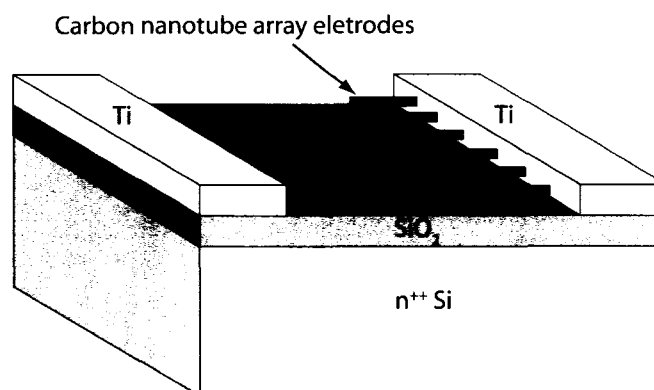


Figure 8-2. Schematic of a carbon nanotube array electrode in the configuration used to fabricate the pentacene OTFT devices. Carbon nanotubes stick out from the titanium electrodes.

A subtractive technique was developed for the fabrication of these "hairy electrodes". A dense carbon nanotube network ($\sim 45$ nt/$\mu m^2$) is first transferred using the vacuum filtration method described in the chapter 4 onto thermal oxide layer (100 nm) on a degenerately doped $n^{++}$ silicon wafer. Titanium contacts (20 nm) are then defined using conventional optical lithography and lift-off techniques. Electrode patterns made for the OTFT devices have channel widths of 200 $\mu$m and lengths of 20 $\mu$m. Finally, the carbon nanotubes that are not directly attached to the metal electrodes were removed by subjecting the structures to a sonication treatment, while immersed in a

n-methylpyrrolidone based resin stripper (AZ300T Clariant). In order to benchmark our nanotube electrodes, standard Au electrodes not connected with carbon nanotubes arrays were also used for making equivalent OTFT devices.

## 8.3 Results and discussion

### 8.3.1 Electrical characterization of individual carbon nanotube electrodes

A typical pentacene nanotransistor connected by carbon nanotube source and drain electrodes separated by ~ 40 nm is displayed in Figure 8-3. Also displayed are the output and transfer characteristics for this device. We measured for this device a ratio $I_{on}/I_{off} = 10^2$ and On state currents of the order of a 2 nA at a drain voltage $V_d = 8V$. Given that the width of the channel is about the average carbon nanotube diameter, i.e. only 2.7 nm in width, this is a truly remarkable result. The characteristics present however severe short channel behaviors, which are most likely due to the thick gate oxides used (compared to the length of the channel). That is, the superposition of the drain and gate fields provide poor control on the field at the source. This problem could be solved by simply reducing drastically the thickness of the gate dielectric down to 1-nm range.

Thirteen such devices were fabricated and characterized for this study. All provided similar p-type transport characteristics with $I_{on}/I_{off}$ ratios between $10-10^4$ and average On state currents between 2-10 nA. The subthreshold slope was S ~ 1.3 V/dec, which is typical for Schottky barrier FETs. [209] The origin of device to device variability is yet unknown. We speculate that this is most likely related to the morphology of the pentacene-nanotube interface.
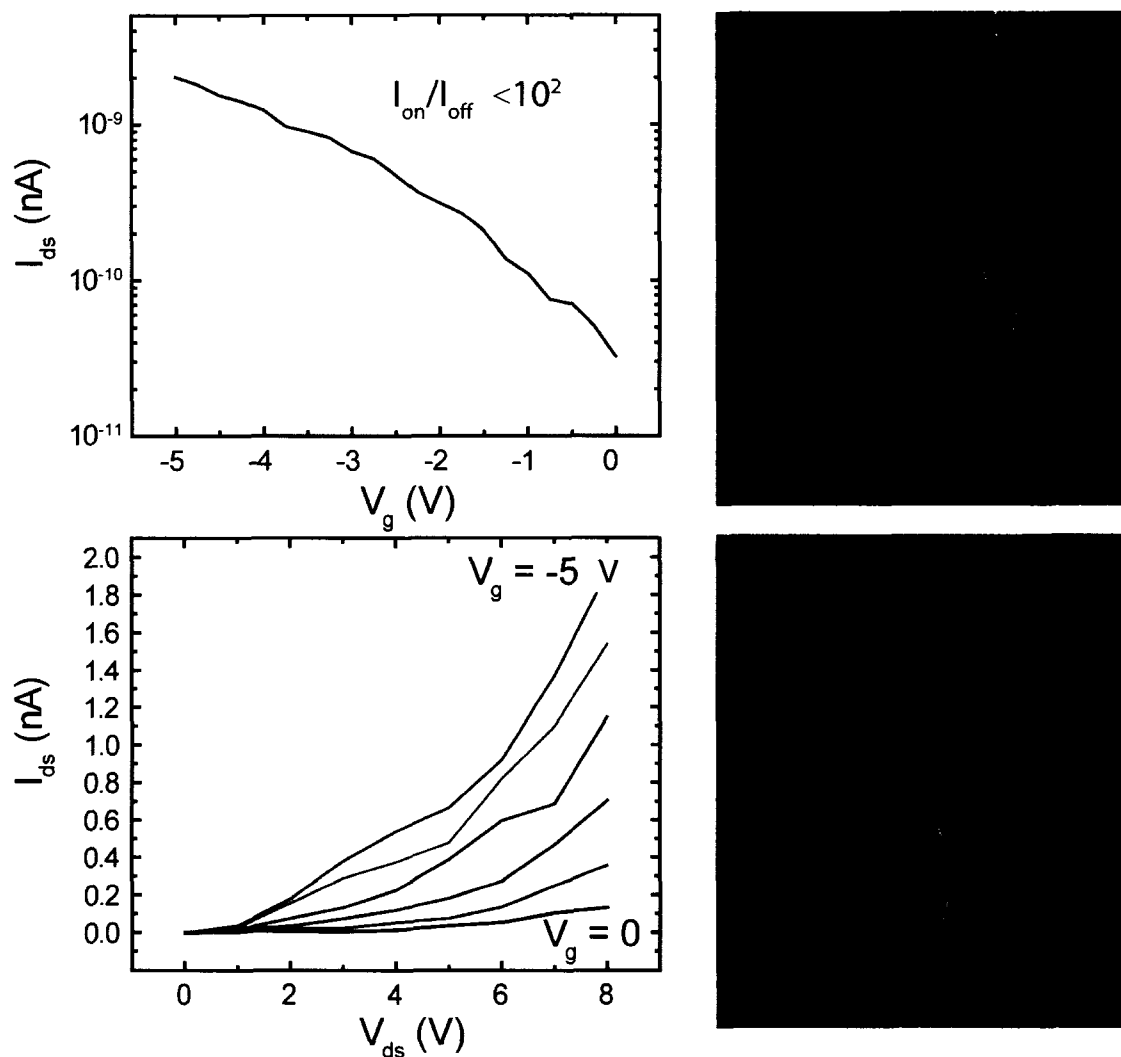
Figure 8-3. Transfer (top) and Output (bottom) characteristics of a pentacene nanotransistor made using metallic carbon nanotubes as source and drain electrodes. Carbon nanotubes stick out from Ti electrodes. The transfer characteristic is shown using Vd= 5 V. An AFM image of the nanotransistor (top right panel) is overlaid with the SEM image (image below) to present the geometry of the device.

It is interesting to compare these results with Au contacted pentacene-based nanoscale transistors reported recently in the literature by Kagan and coworkers.[210] This field effect transistor was built on a 2 nm thick silicon dioxide layer and presented very small channel dimensions: L ~ 20 nm and W ~ 250 nm. In principle, this aspect ratio should

provide good FET characteristics, but the device had a typical short-channel behavior, which could be linked to large contact barriers. Ratios $I_{on}/I_{off} \sim 1 \times 10^2$ and On state currents of 2 nA at $V_d = -4$ V were measured with a subthreshold slope of $S \sim 1$ V/dec. These values are similar to the characteristics observed for the nanotube-pentacene transistors. The width of the channel is however larger by about 2 orders of magnitude. Consequently, the normalized On state current of the nanotube-pentacene FETs is roughly 100x higher than for metal electrodes of similar width. This value alone clearly indicates considerably better injection performance with the nanotube contacts. Either the injection barriers at the organic-nanotube interface are lower or the contact geometry induces electrostatic effects that enhance the shift of the molecular energy-level (band-bending) nearby this interface. Field-enhancement related to the 1D electrostatics at the nanotube apex is expected and could account for the latter mechanism. [146; 147; 208]

The characteristics of our nanotube-pentacene FETs offers the most promising scaling possibilities compared to its metal-contacted analogue. Indeed, both pentacene FETs have similarly bad short-channel characteristics and both will require further scaling of the dielectric oxide thicknesses. In the Au contacted FET reported by Kagan, the gate oxide (only 2nm) can not be much further scaled, but this is not a problem for the nanotube-pentacene FET which has a gate oxide 10x thicker. The performance assessment of the nanotube-pentacene devices will therefore require further experiments but the results, so far, are promising.

Some of the devices fabricated lead to islands contacted on one end to a carbon nanotube electrode and the opposite end to a Pd electrode (Figure 8-4a). The behavior of these devices highlights further the contact improvement achieved with carbon nanotubes. An order of magnitude difference in the current is measured at $V_g = -8V$, when the injection electrode is carbon nanotube. This is measured in spite of the much greater contact area between the Pd electrode and the organic layer. For comparison, devices having symmetrical carbon nanotubes electrodes (Figure 8-4b) exhibited On state currents that differed by no more than a factor of 2.

(a)

$V_g = -8V$

Nanotube electrode

Pd electrode

$I_{ds}$ (nA)

6
5
4
3
2
1
0

-5    -4    -3    -2    -1    0

$V_{ds}$ (V)

(b)

$V_g = -8V$

Symmetric nanotube electrodes

$I_d$ (nA)

8
7
6
5
4
3
2
1
0
-1

-5    -4    -3    -2    -1    0

$V_{ds}$ (V)
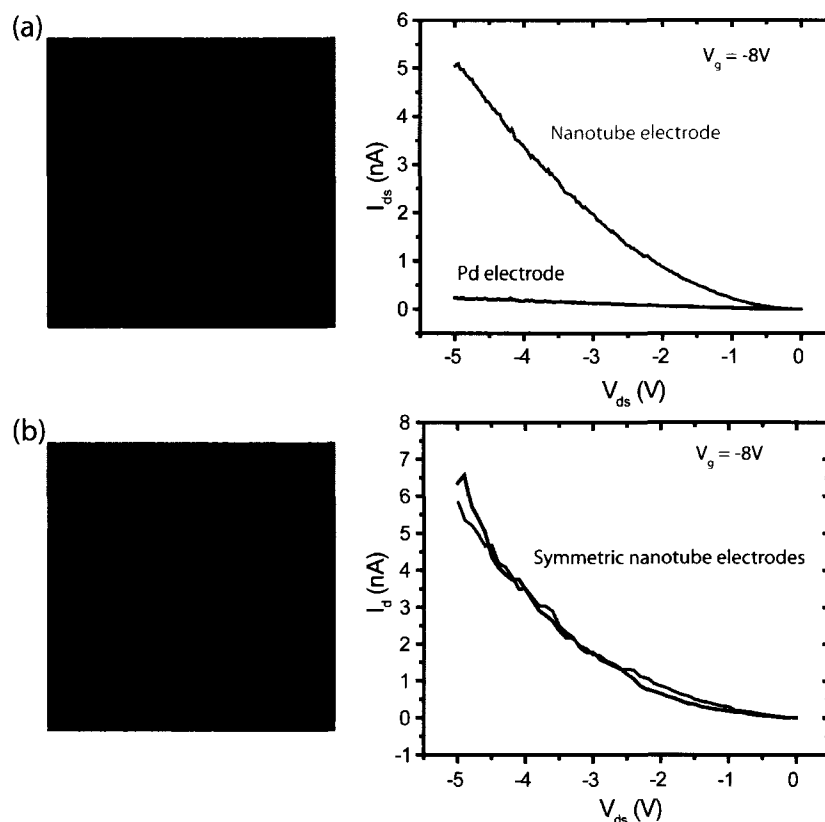
Figure 8-4. Output characteristics of pentacene nanotransistor made using a metal and a carbon nanotube as injection electrodes. Top panel: overlaid AFM and SEM (left) and IVs (right) of a transistor having asymmetrical nanotube and Pd contact electrodes. Bottom: AFM/SEM images (left) and IV characteristics (right) of a transistor having symmetrical nanotube contacts. The electrode defined as the source is labeled in the I-V characteristics.

## 8.3.2 Characterization of OTFT devices that use carbon nanotube arrays

Figure 8-5 presents results for an OTFT fabricated using an array of carbon nanotubes attached to Ti contacts. An SEM image of the arrays covered by a 50 nm thick pentacene layer is shown in the Figure 8-5a. The image reveals that the structure of the interface is slightly disordered because of the poor alignment of the nanotube array, but the pentacene layer appears to be nicely conformal to the structure. Similar devices (not

shown) were fabricated simultaneously (same evaporation) with Au and Ti electrodes. Au is known to provide good contacts to pentacene OTFTs,[211] while Ti is a poor contact metal due to the insulating oxide present at its surface. All the devices have channel widths and lengths of 200 μm and 20 μm, respectively. The differences in performance are highlighted in the low bias regime shown in Figure 8-5b. The current-voltage characteristics for the carbon nanotube array contacted OTFT displays linear I-Vs and ideal injection behavior. This is compared to the highly nonlinear injection by Au electrodes. Nonlinear charge injection is a typical sign that large contact barriers are present at the metal-organic semiconductor contact.[212] To make sure the current measured does not originate from the Ti contacts, we also performed measurements on devices made with Ti contacts (only). The current was more than anv order of magnitude lower without the carbon nanotubes array. The improvement is therefore clearly related to the presence of the nanotubes.
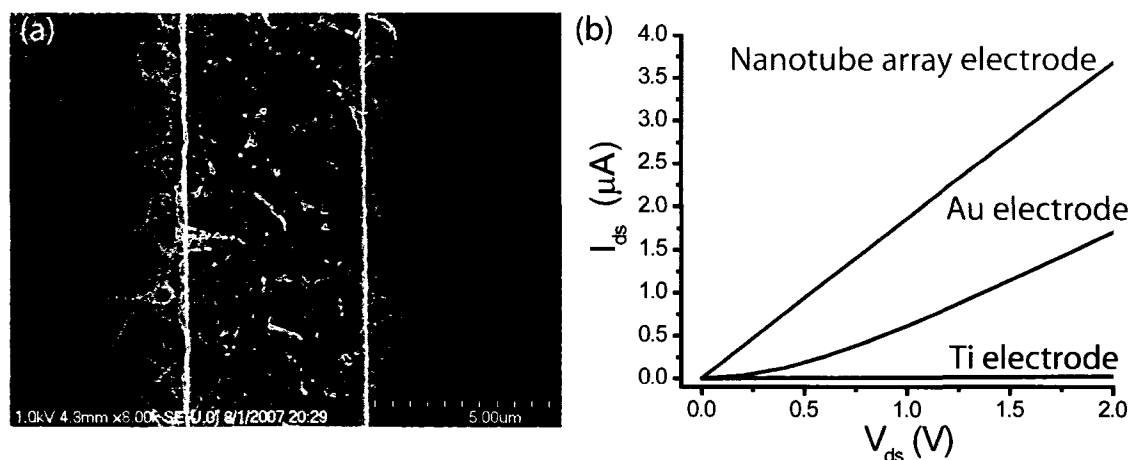


Figure 8-5. (a) SEM image in the contact region of the device with the nanotube arrays covered by the pentacene layer. (b) Comparison of the I-V characteristics at low bias for pentacene thin-film transistors made with Au, Ti or carbon nanotube contacts. The source electrode material is labeled in the I-V characteristics.

The geometry of the nanotube array is non-uniform and should present a larger contact area with the pentacene layer. It is therefore expected that nanotube contacts offer higher currents, even in the absence of improvement. However, the effect of the contact area

should not affect the linearity of the output curve and only improve the overall current throughput, which is not the case. It is therefore safe to say that the contact, even for the same area, is overall better with nanotubes.

The reason for the improvement is not clear yet, but the linearity in the current-voltage characteristics clearly suggests barrier-free like contacts. One possibility to explain the improvement is to consider the presence of 1D electrostatic field at the nanotube-organic junctions. It was shown in Chapter 3 that the effect is to sharpen the field distribution at the nanotube apex, which should shift the energy levels in the contact region and enhance carrier tunneling. This behavior is analogous to what has been described in the case of nanotube-metal contacts.[146; 147; 213] However, not much is known about the interface property and the energy level alignment at this junction. Further studies will thus be required before a better understanding of the improvement and of the physical parameters that define this junction.

## 8.4   Conclusion

We have shown that carbon nanotubes can inject considerable current into organic semiconducting layers by using individual and nanotube array electrodes. The results from individual nanotube-pentacene FET provide two order of magnitude better current than for the traditional metal electrodes. We demonstrated that the approach was scalable to realistic devices where the nanotubes also offer better performances. We propose that field enhancement may be taking place at the contacts enabling better injection.

# CHAPTER 9: Conclusions, General Discussion, and Perspectives

## 9.1 Summary of the results

The primary objective of this thesis was to demonstrate that the unique electrical, mechanical, and optical properties of carbon nanotubes could be put to use in thin film devices by adding functionality and improving their performance. In particular, we wanted to demonstrate that metallic carbon nanotube networks could be used as efficient electrodes in OLEDs. We also wanted to reveal the potential of semiconducting carbon nanotube networks as an alternative material for the fabrication of TFTs. Our main results can be summarized as follows:

*Solution-based approaches:* We have developed and optimized two solution-based processing techniques for the fabrication of carbon nanotube networks. Inspired by the work of Rinzler, we perfected a vacuum filtration technique for the fabrication of random nanotube networks. By controlling the volume of nanotubes used in the solution, we were able to reproducibly fabricate both semiconducting and conducting films with predetermined electronic properties. The process intrinsically leads to an excellent lateral uniformity for networks thicker than 15 nm. Taking advantage of the affinity of carbon nanotubes with aminosilanes, we have also devised a self-assembly process which, when combined with the use of a spin-coater, enabled us to prepare networks in which carbon nanotubes are well aligned. The uniform carbon nanotube coverages that are possible using the self-assembly approach are amendable to the fabrication on a wafer scale of NN-TFT devices exhibiting excellent performances reproducibly.

*Transparent, flexible electrodes:* The vacuum filtration method is well adapted for the fabrication of relatively thick metallic carbon nanotube networks. We have systematically investigated the relationship between film thickness, optical transmission, and electrical conduction. The best compromise for OLED applications is a 130 nm-

thick film having 44% transmission at a wavelength of 520 nm and a sheet resistance of 55 $\Omega$/sq. OLED devices made using these films exhibit very similar performance characteristics comparable to that of control devices made on ITO anodes. Following this demonstration of the potential of carbon nanotube electrodes for such applications, we have further optimized the optical and electrical properties of the sheets by charge transfer doping the semiconducting nanotubes. The best treatment resulted in a 7-fold increase in the network conductance; doped carbon nanotube sheets exhibiting high optical transparencies (80%) and low sheet resistances (~60 $\Omega$/square) were fabricated.

*Charge injection:* The remarkable performances we observed for the carbon nanotube anode, lead us to question if charge injection was assisted by the nanoscale morphology. The charge injection efficiency was investigated by fabricating nanoscale pentacene-FET consisting of individual carbon nanotubes electrodes. We indeed observed that a single carbon nanotube ~ 2 nm in diameter could inject as much current in a pentacene island as a 200 nm wide metal electrode. Further we showed that this strategy could be scaled by integrating "hairy electrodes" into organic TFTs. It was found that charge injection was more efficient at the carbon nanotube-organic semiconductor interface compared to traditional metal electrodes. These results establish convincingly that carbon nanotubes should be considered as an alternative material for organic electronic applications.

*Carbon nanotube thin-film transistors:* Taking advantage of our unprecedented level of control in the preparation of semiconducting carbon nanotube networks, we have fabricated field-effect transistors. Devices made from optimized carbon nanotube networks were characterized by effective mobilities of 5 cm$^2$/V.s for $I_{on}/I_{off}$ ratios of over $10^5$. Moreover, we demonstrated that carbon nanotube networks could be scaled to channels 6 $\mu$m in length. The scaling characteristics can be further optimized by conferring alignment to the networks.

*Origin of the unipolar/bipolar behavior in CNT devices:* Finally, we have designed an experiment for explaining the origin of the usually observed unipolar behavior of carbon nanotube devices. By making field-effect devices on substrates having distinct chemical functionalities – the usual thermal oxide on silicon and a layer of parylene-C, an oxygen-free insulating hydrophobic polymer – we have conclusively demonstrated that adsorbed species – most probably water – from ambient are responsible for modulating electron conduction in thin film and nanoscale devices.

## 9.2   Discussion of the main contributions

In our thesis, we have made notable contributions to the science and to the engineering of carbon nanotube networks for electronic and optoelectronic applications. We shall now briefly comment on the potential impact of our work.

*From the science of carbon nanotubes to the engineering carbon nanotube networks:* One of the underlying themes during the course of this research is the importance of taking an engineering approach to further our current understanding of nanoscale materials and devices. Most of the literature on carbon nanotubes and, incidentally, on various other nanostructures, is aimed at understanding and exploiting the novel properties of individual structures or small ensembles. Such an approach is clearly required for understanding the fundamental properties of materials. Nevertheless, the fact that the properties of nanostructures vary considerably with dimensions makes these investigations difficult. I hope I have made a convincing case that developing a process for the large scale fabrication of, for example, single nanotube devices is therefore extremely challenging. Instead of trying to solve the issue of the strong variability of nanomaterials properties with size, I have chosen to use their 'bulk-like' ensemble properties. I have shown in my thesis, using carbon nanotube networks as a model system, that such an engineering approach can be extremely beneficial for the development of novel materials and devices with improved properties. I trust that this

approach is currently among the most promising for the rapid introduction of nanomaterials in production facilities.

*The potential of solution-based approaches:* Because of my engineering background, it was especially important for me to work on the development of processes that were easily scalable. For the same reasons, I insisted on developing processes which could be compatible with commercial carbon nanotube sources synthesized in bulk quantities; in other words, I wanted to avoid techniques which rely on the local growth of carbon nanotubes. I was thus naturally drawn towards the use of solution-based techniques as they are certainly the most easily amenable to large scale processes and low processing temperatures. They also have the advantage of being easily compatible with flexible substrates. I believe that I have made a convincing case during my thesis that such relatively simple techniques can be used to produce carbon nanotube networks of very high quality. Another, non negligible, benefit of these low-cost processing techniques is that they are easily accessible to the scientific community. Scientists from other laboratories can thus rapidly learn to reproduce our results and exploit them to pursue new research avenues. The existence of simple processing techniques, which are readily accessible to the vast majority of researchers in a given community, clearly leads to accelerated progress.

*The critical importance of the substrate:* As explained above, one of the most significant contributions of this thesis is to demonstrate that adsorbed species from ambient are responsible for suppressing electron conduction. In the past, the FET configuration has been used for the study the conduction behavior of individual molecules, quantum dots, nanowires, and organic semiconducting films. We demonstrated, using carbon nanotubes, that electron trapping is an important effect not only for organic semiconductors but also for other nanoscale materials as well. Moreover, before this work, it was thought that silanol groups at inorganic substrate surfaces were responsible

for charge trapping. Although n-type conduction was only observed in vacuum, Friend et al. surmised this was due to the lower electron affinities of electron transporting materials. Premature oxidation of the semiconducting layers due to the passage of current was proposed to explain poor electron conduction in air. We showed by using carbon nanotube networks that this can now be explained by the concentration of surface bound species (most likely water) on oxygen free substrates. In air, there are still sufficient charge traps to suppress electron conduction. In vacuum this lightly bound layer is easily displaced.

## 9.3 Perspectives for future work

This thesis work opens a number of interesting possibilities that are too numerous to describe in detail here. I chose to present four projects that I believe can have considerable impact although for very different reasons.

The project having the greatest potential to revolutionize an entire field of research is the study of electron trap generation at the insulator-organic semiconductor interface. During my thesis, I determined that water vapor from ambient is the most probable species responsible for suppressing electron conduction in field-effect transistors fabricated on $SiO_2$ surfaces. The hydrophobic parylene-C surface was effective in attenuating, but not totally eliminating, the generation of these traps. By using carbon nanotubes as the test-bed for probing electron trap generation, substrates having a number of different chemical functionalities could be explored. In conjunction with surface science methodologies, it would be possible to pin-point the substrate chemistry that is most efficient for eliminating this detrimental effect. Ideally, I would explore strategies that aim at passivating the $SiO_2$ surfaces. Glass surfaces are ubiquitous thus an efficient surface treatment would not only impact researchers in academic laboratories investigating the intrinsic electronic properties of materials, but also industrial laboratories interested in bringing organic electronics to the marketplace. I believe this project is also the most challenging because it involves both delicate surface science experiments and the mastery of carbon nanotube device fabrication protocols.

The project that is easiest to undertake and that is an obvious continuation of my thesis work is to integrate semiconducting carbon nanotube networks in different device configurations. I demonstrated that it is possible to fabricate ambipolar carbon nanotube TFTs using simple solution based methods. This allows in principle the fabrication of p-n junctions, inverters, and other complementary logic circuits. The investigation of the performance limits of carbon nanotube networks for different applications could explored. As part of this project, the suitability of carbon nanotube networks for low and medium speed applications could be also addressed.

I showed that carbon nanotube electrodes could be used to efficiently inject charge into organic semiconductors for different device geometries. However, it was not possible to determine if charge injection from carbon nanotubes was assisted by field enhancement at their apex. Our results definitely point towards a property exclusive to carbon nanotubes enabling the charge injection barriers to be less problematic lowered. Moreover, for the experiments detailed in this thesis, only hole injection was demonstrated. It is however known that barriers to electron injection are considerably higher. By changing the work function of carbon nanotubes through charge transfer doping, efficient electron injection could be realized.

Finally, the project most susceptible to making me want to start graduate school all over again is the investigation of the applicability of NN-TFTs as x-ray detectors. Large area TFT array x-ray detectors have to date been exclusively manufactured using inorganic semiconductors. Only a few exploratory experiments have examined the use of organic semiconductors for this application. One of these experiments examined the threshold voltage shift of individual carbon nanotube FETs exposed to ionizing radiation. The higher effective absorption areas and signal to noise ratios attainable with network transistors should provide higher detection limits. Because we can fabricate carbon nanotube networks over large areas, prototype detector devices could be easily implemented.

# REFERENCES

[1]      Chiang, C. K., Fincher, C. R., Park, Y. W., Heeger, A. J., Shirakawa, H., Louis, E. J., et al. (1977). Electrical Conductivity in Doped Polyacetylene. *Physical Review Letters, 39*(17), 1098.

[2]      Shirakawa, H., McDiarmid, A., & Heeger, A. (2003). Twenty-five years of conducting polymers. *Chemical Communications*(1), 1-4.

[3]      Elsa Reichmanis, H. K. C. K. A. M. (2005). Plastic electronic devices: From materials design to device applications. *Bell Labs Technical Journal, 10*(3), 87-105.

[4]      Forrest, S. R. (2004). The path to ubiquitous and low-cost organic electronic appliances on plastic. *Nature, 428*(6986), 911-918.

[5]      Singh, T. B., & Sariciftci, N. S. (2006). PROGRESS IN PLASTIC ELECTRONICS DEVICES. *Annual Review of Materials Research, 36*(1), 199-230.

[6]      Dimitrakopoulos, C. D., & Malenfant, P. R. L. (2002). Organic Thin Film Transistors for Large Area Electronics. *Advanced Materials, 14*(2), 99-117.

[7]      Facchetti, A. (2007). Semiconductors for organic transistors. *Materials Today, 10*(3), 28-37.

[8]      Coakley, K. M., & McGehee, M. D. (2004). Conjugated Polymer Photovoltaic Cells. *Chem. Mater., 16*(23), 4533-4542.

[9]      Ma, W., Yang, C., Gong, X., Lee, K., & Heeger, A. J. (2005). Thermally Stable, Efficient Polymer Solar Cells with Nanoscale Control of the Interpenetrating Network Morphology. *Advanced Functional Materials, 15*(10), 1617-1622.

[10]     Peumans, P., Uchida, S., & Forrest, S. R. (2003). Efficient bulk heterojunction photovoltaic cells using small-molecular-weight organic thin films. *Nature, 425*(6954), 158-162.

[11]     Hung, L. S., & Chen, C. H. (2002). Recent progress of molecular organic electroluminescent materials and devices. *Materials Science and Engineering: R: Reports, 39*(5-6), 143-222.

[12]     Muller, C. D., Falcou, A., Reckefuss, N., Rojahn, M., Wiederhirn, V., Rudati, P., et al. (2003). Multi-colour organic light-emitting displays by solution processing. *Nature, 421*(6925), 829-833.

[13]     Veinot, J. G. C., & Marks, T. J. (2005). Toward the Ideal Organic Light-Emitting Diode. The Versatility and Utility of Interfacial Tailoring by Cross-Linked Siloxane Interlayers. *Acc. Chem. Res., 38*(8), 632-643.

[14]     Zhou, L., Wanga, A., Wu, S.-C., Sun, J., Park, S., & Jackson, T. N. (2006). All-organic active matrix flexible display. *Applied Physics Letters, 88*(8), 083502-083503.

[15]    Kondakov, D. Y., Lenhart, W. C., & Nichols, W. F. (2007). Operational degradation of organic light-emitting diodes: Mechanism and identification of chemical products. *Journal of Applied Physics, 101*(2), 024512-024517.

[16]    Li, D., Borkent, E.-J., Nortrup, R., Moon, H., Katz, H., & Bao, Z. (2005). Humidity effect on electrical performance of organic thin-film transistors. *Applied Physics Letters, 86*(4), 042105-042103.

[17]    Mottaghi, M., & Horowitz, G. (2006). Field-induced mobility degradation in pentacene thin-film transistors. *Organic Electronics, 7*(6), 528-536.

[18]    Popovic, Z. D., & Aziz, H. (2002). Reliability and degradation of small molecule-based organic light-emitting devices (OLEDs). *Selected Topics in Quantum Electronics, IEEE Journal of, 8*(2), 362-371.

[19]    Sony Launches World's First OLED TV. (2007). from http://www.sony.net/SonyInfo/News/Press/200710/07-1001E/index.html

[20]    Kagan, C. R., Afzali, A., & Graham, T. O. (2005). Operational and environmental stability of pentacene thin-film transistors. *Applied Physics Letters, 86*(19), 193505-193503.

[21]    Chua, L.-L., Zaumseil, J., Chang, J.-F., Ou, E. C. W., Ho, P. K. H., Sirringhaus, H., et al. (2005). General observation of n-type field-effect behaviour in organic semiconductors. *Nature, 434*(7030), 194-199.

[22]    Malliaras, G. G., & Scott, J. C. (1998). The roles of injection and mobility in organic light emitting diodes. *J. Appl. Phys., 83*(10), 5399-5403.

[23]    Suzuki, T. (2006). Flat panel displays for ubiquitous product applications and related impurity doping technologies. *Journal of Applied Physics, 99*(11), 111101-111115.

[24]    Hebner, T. R., Wu, C. C., Marcy, D., Lu, M. H., & Sturm, J. C. (1998). Ink-jet printing of doped polymers for organic light emitting devices. *Applied Physics Letters, 72*(5), 519-521.

[25]    Calvert, P. (2001). Inkjet Printing for Materials and Devices. *Chem. Mater., 13*(10), 3299-3305.

[26]    Coe, S., Woo, W.-K., Bawendi, M., & Bulovic, V. (2002). Electroluminescence from single monolayers of nanocrystals in molecular organic devices. *Nature, 420*(6917), 800-803.

[27]    Plass, R., Pelet, S., Krueger, J., Gratzel, M., & Bach, U. (2002). Quantum Dot Sensitization of Organic-Inorganic Hybrid Solar Cells. *J. Phys. Chem. B, 106*(31), 7578-7580.

[28]    Kryszewski, M., & Jeszka, J. K. (1998). Nanostructured conducting polymer composites -- superparamagnetic particles in conducting polymers. *Synthetic Metals, 94*(1), 99-104.

[29]    Kickelbick, G. (2003). Concepts for the incorporation of inorganic building blocks into organic polymers on a nanoscale. *Progress in Polymer Science, 28*(1), 83-114.

[30]    de Heer, W. A. (2004). Nanotubes and the pursuit of applications. *Mater. Res. Bull., 29*(4), 281-285.

[31]   Frank, S., Poncharal, P., Wang, Z. L., Heer, W. A., nbsp, & de. (1998). Carbon
       Nanotube Quantum Resistors. *Science, 280*(5370), 1744-1746.

[32]   Yao, Z., Kane, C. L., & Dekker, C. (2000). High-Field Electrical Transport in
       Single-Wall Carbon Nanotubes. *Physical Review Letters, 84*(13), 2941.

[33]   Javey, A., Guo, J., Wang, Q., Lundstrom, M., & Dai, H. (2003). Ballistic carbon
       nanotube field-effect transistors. *Nature, 424*(6949), 654-657.

[34]   Martel, R., Wong, H. S. P., Chan, K., & Avouris, P. (2001). *Carbon nanotube
       field effect transistors for logic applications.* Paper presented at the Electron
       Devices Meeting, 2001. IEDM Technical Digest. International.

[35]   Avouris, P., Appenzeller, J., Martel, R., & Wind, S. J. (2003). Carbon nanotube
       electronics. *Proceedings of the IEEE, 91*(11), 1772-1784.

[36]   Cao, Q., Hur, S. H., Zhu, Z. T., Sun, Y. G., Wang, C. J., Meitl, M. A., et al.
       (2006). Highly Bendable, Transparent Thin-Film Transistors That Use Carbon-
       Nanotube-Based Conductors and Semiconductors with Elastomeric Dielectrics.
       *Advanced Materials, 18*(3), 304-309.

[37]   Li, J., Hu, L., Wang, L., Zhou, Y., Gruner, G., & Marks, T. J. (2006). Organic
       Light-Emitting Diodes Having Carbon Nanotube Anodes. *Nano Lett., 6*(11),
       2472-2477.

[38]   Snow, E. S., Novak, J. P., Campbell, P. M., & Park, D. (2003). Random
       networks of carbon nanotubes as an electronic material. *Applied Physics Letters,
       82*(13), 2145-2147.

[39]   Aguirre, C. M., Auvray, S., Pigeon, S., Izquierdo, R., Desjardins, P., & Martel,
       R. (2006). Carbon nanotube sheets as electrodes in organic light-emitting diodes.
       *Applied Physics Letters, 88*(18), 183104-183103.

[40]   Pasquier, A. D., Unalan, H. E., Kanwal, A., Miller, S., & Chhowalla, M. (2005).
       Conducting and transparent single-wall carbon nanotube electrodes for polymer-
       fullerene solar cells. *Applied Physics Letters, 87*(20), 203511-203513.

[41]   Wu, Z. C., Chen, Z. H., Du, X., Logan, J. M., Sippel, J., Nikolou, M., et al.
       (2004). Transparent, conductive carbon nanotube films. *Science, 305*(5688),
       1273-1276.

[42]   Zhang, M., Fang, S., Zakhidov, A. A., Lee, S. B., Aliev, A. E., Williams, C. D.,
       et al. (2005). Strong, Transparent, Multifunctional, Carbon Nanotube Sheets.
       *Science, 309*(5738), 1215-1219.

[43]   Artukovic, E., Kaempgen, M., Hecht, D. S., Roth, S., & Gruner, G. (2005).
       Transparent and Flexible Carbon Nanotube Transistors. *Nano Lett., 5*(4), 757-
       760.

[44]   Kang, S. J., Kocabas, C., Ozel, T., Shim, M., Pimparkar, N., Alam, M. A., et al.
       (2007). High-performance electronics using dense, perfectly aligned arrays of
       single-walled carbon nanotubes. *Nature Nanotechnology, 2*, 230-236.

[45]   Takenobu, T., Takahashi, T., Kanbara, T., Tsukagoshi, K., Aoyagi, Y., & Iwasa,
       Y. (2006). High-performance transparent flexible transistors using carbon
       nanotube films. *Applied Physics Letters, 88*(3), 033511-033513.

[46]   Dresselhaus, M. S. (2001). NANOTUBES: Burn and Interrogate. *Science,
       292*(5517), 650-651.

[47]     Popov, V. N., & Lambin, P. (2006). *Carbon Nanotubes* (1st ed. Vol. 222): Springer.

[48]     Iijima, S. (1991). Helical microtubules of graphitic carbon. *Nature, 354*(6348), 56-58.

[49]     O'Connell, M. J., Bachilo, S. M., Huffman, C. B., Moore, V. C., Strano, M. S., Haroz, E. H., et al. (2002). Band gap fluorescence from individual single-walled carbon nanotubes, *Science* (Vol. 297, pp. 593-596).

[50]     Hitoshi, N. (2007). Saito Lab webpage. from http://www.surf.nuqe.nagoya-u.ac.jp

[51]     Adam, E., Aguirre, C. M., Cardin St-Antoine, B., Meunier, F., Desjardins, P., Menard, D., et al. (2007). Electroluminescence in Single-Wall Carbon Nanotube Network Transistors. *(In preparation).*

[52]     Kocabas, C., Pimparkar, N., Yesilyurt, O., Kang, S. J., Alam, M. A., & Rogers, J. A. (2007). Experimental and Theoretical Studies of Transport through Large Scale, Partially Aligned Arrays of Single-Walled Carbon Nanotubes in Thin Film Type Transistors. *Nano Lett.*

[53]     Kong, J., Cassell, A. M., & Dai, H. (1998). Chemical vapor deposition of methane for single-walled carbon nanotubes. *Chemical Physics Letters, 292*(4-6), 567-574.

[54]     Dai, H. (2002). Carbon Nanotubes: Synthesis, Integration, and Properties. *Acc. Chem. Res., 35*(12), 1035-1044.

[55]     Zhang, Y., Chang, A., Cao, J., Wang, Q., Kim, W., Li, Y., et al. (2001). Electric-field-directed growth of aligned single-walled carbon nanotubes. *Applied Physics Letters, 79*(19), 3155-3157.

[56]     Kocabas, C., Hur, S. H., Gaur, A., Meitl, M. A., Shim, M., & Rogers, J. A. (2005). Guided Growth of Large-Scale, Horizontally Aligned Arrays of Single-Walled Carbon Nanotubes and Their Use in Thin-Film Transistors. *Small, 1*(11), 1110-1116.

[57]     Breuer, O., & Sundararajm, U. (2004). Big returns from small fibers: A review of polymer/carbon nanotube composites. *Polymer Composites, 25*(6), 630-645.

[58]     Haggenmueller, R., Gommans, H. H., Rinzler, A. G., Fischer, J. E., & Winey, K. I. (2000). Aligned single-wall carbon nanotubes in composites by melt processing methods. *Chemical Physics Letters, 330*(3-4), 219-225.

[59]     Moniruzzaman, M., & Winey, K. I. (2006). Polymer Nanocomposites Containing Carbon Nanotubes. *Macromolecules, 39*(16), 5194-5205.

[60]     Velasco-Santos, C., Martinez-Hernandez, A. L., & Castano, V. M. (2005). Carbon nanotube-polymer nanocomposites: The role of interfaces. *Composite Interfaces, 11*, 567-586.

[61]     Blanchet, G. B., Fincher, C. R., & Gao, F. (2003). Polyaniline nanotube composites: A high-resolution printable conductor. *Applied Physics Letters, 82*(8), 1290-1292.

[62]     Ferrer-Anglada, N., Kaempgen, M., Skakalova, V., Dettlaf-Weglikowska, U., & Roth, S. (2004). Synthesis and characterization of carbon nanotube-conducting polymer thin films. *Diamond and Related Materials, 13*(2), 256-260.

[63] Kaempgen, M., Duesberg, G. S., & Roth, S. (2005). Transparent carbon nanotube coatings. *Applied Surface Science, 252*(2), 425-429.

[64] Kim, Y. (2003). Langmuir-Blodgett films of single-wall carbon nanotubes: Layer-by-layer deposition and in-plane orientation of tubes. *Japanese journal of applied physics. Part 1, Regular papers & short notes, 42*(12), 7629-7634.

[65] Choi, K. H., Bourgoin, J. P., Auvray, S., Esteve, D., Duesberg, G. S., Roth, S., et al. (2000). Controlled deposition of carbon nanotubes on a patterned substrate. *Surface Science, 462*(1-3), 195-202.

[66] Liu, J., Casavant, M. J., Cox, M., Walters, D. A., Boul, P., Lu, W., et al. (1999). Controlled deposition of individual single-walled carbon nanotubes on chemically functionalized templates. *Chemical Physics Letters, 303*(1-2), 125-129.

[67] Valentin, E., Auvray, S., Goethals, J., Lewenstein, J., Capes, L., Filoramo, A., et al. (2002). High-density selective placement methods for carbon nanotubes. *Microelectronic Engineering, 61-62*, 491-496.

[68] Hu, L., Hecht, D. S., & Gruner, G. (2004). Percolation in Transparent and Conducting Carbon Nanotube Networks. *Nano Lett., 4*(12), 2513-2517.

[69] Chrisey, L. A., Lee, G. U., & O'Ferrall, C. E. (1996). Covalent attachment of synthetic DNA to self-assembled monolayer films. *Nucl. Acids Res., 24*(15), 3031-3039.

[70] Schreiber, F. (2000). Structure and growth of self-assembling monolayers. *Progress in Surface Science, 65*(5-8), 151-257.

[71] Munson-McGee, S. H. (1991). Estimation of the critical concentration in an anisotropic percolation network. *Physical Review B, 43*(4), 3331.

[72] Foygel, M., Morris, R. D., Anez, D., French, S., & Sobolev, V. L. (2005). Theoretical and computational studies of carbon nanotube composites and suspensions: Electrical and thermal conductivity. *Physical Review B (Condensed Matter and Materials Physics), 71*(10), 104201-104208.

[73] Kirkpatrick, S. (1973). Percolation and Conduction. *Reviews of Modern Physics, 45*(4), 574.

[74] Jesse, S., Guillorn, M. A., Ivanov, I. N., Puretzky, A. A., Howe, J. Y., Britt, P. F., et al. (2006). In situ electric-field-induced contrast imaging of electronic transport pathways in nanotube-polymer composites. *Applied Physics Letters, 89*(1), 013114-013113.

[75] Vigolo, B., Coulon, C., Maugey, M., Zakri, C., & Poulin, P. (2005). An Experimental Approach to the Percolation of Sticky Nanotubes. *Science, 309*(5736), 920-923.

[76] Zhou, Y., Gaur, A., Hur, S. H., Kocabas, C., Meitl, M. A., Shim, M., et al. (2004). p-Channel, n-Channel Thin Film Transistors and p-n Diodes Based on Single Wall Carbon Nanotube Networks. *Nano Lett., 4*(10), 2031-2035.

[77] Bekyarova, E., Itkis, M. E., Cabrera, N., Zhao, B., Yu, A., Gao, J., et al. (2005). Electronic Properties of Single-Walled Carbon Nanotube Networks. *J. Am. Chem. Soc., 127*(16), 5990-5995.

[78] Saran, N., Parikh, K., Suh, D. S., Munoz, E., Kolla, H., & Manohar, S. K. (2004). Fabrication and Characterization of Thin Films of Single-Walled Carbon Nanotube Bundles on Flexible Plastic Substrates. *J. Am. Chem. Soc., 126*(14), 4462-4463.

[79] Zhou, Y., Hu, L., & Gruner, G. (2006). A method of printing carbon nanotube thin films. *Applied Physics Letters, 88*(12), 123109-123103.

[80] Ishii, H., Sugiyama, K., Ito, E., & Seki, K. (1999). Energy Level Alignment and Interfacial Electronic Structures at Organic/Metal and Organic/Organic Interfaces. *Advanced Materials, 11*(8), 605-625.

[81] Hill, I. G., Rajagopal, A., Kahn, A., & Hu, Y. (1998). Molecular level alignment at organic semiconductor-metal interfaces. *Applied Physics Letters, 73*(5), 662-664.

[82] Rajagopal, A., Wu, C. I., & Kahn, A. (1998). Energy level offset at organic semiconductor heterojunctions. *Journal of Applied Physics, 83*(5), 2649-2655.

[83] Kahn, A., Koch, N., & Gao, W. (2003). Electronic structure and electrical properties of interfaces between metals and ?-conjugated molecular films. *Journal of Polymer Science Part B: Polymer Physics, 41*(21), 2529-2548.

[84] Kahn, A., Zhao, W., Gao, W., Vazquez, H., & Flores, F. (2006). Doping-induced realignment of molecular levels at organic-organic heterojunctions. *Chemical Physics, 325*(1), 129-137.

[85] Vazquez, H., Flores, F., Oszwaldowski, R., Ortega, J., Perez, R., & Kahn, A. (2004). Barrier formation at metal-organic interfaces: dipole formation and the charge neutrality level. *Applied Surface Science, 234*(1-4), 107-112.

[86] Shen, Y., Hosseini, A. R., Wong, M. H., & Malliaras, G. G. (2004). How To Make Ohmic Contacts to Organic Semiconductors. *ChemPhysChem, 5*(1), 16-25.

[87] Guo, X., Small, J. P., Klare, J. E., Wang, Y., Purewal, M. S., Tam, I. W., et al. (2006). Covalently Bridging Gaps in Single-Walled Carbon Nanotubes with Conducting Molecules. *Science, 311*(5759), 356-359.

[88] Qi, P., Javey, A., Rolandi, M., Wang, Q., Yenilmez, E., & Dai, H. (2004). Miniature Organic Transistors with Carbon Nanotubes as Quasi-One-Dimensional Electrodes. *J. Am. Chem. Soc., 126*(38), 11774-11775.

[89] Tsukagoshi, K., Yagi, I., & Aoyagi, Y. (2004). Pentacene nanotransistor with carbon nanotube electrodes. *Applied Physics Letters, 85*(6), 1021-1023.

[90] Bonard, J. M., Salvetat, J. P., Stöckli, T., Forró, L., & Châtelain, A. (1999). Field emission from carbon nanotubes: perspectives for applications and clues to the emission mechanism. *Applied Physics A: Materials Science & Processing, 69*(3), 245-254.

[91] Barone, V., Peralta, J. E., Uddin, J., & Scuseria, G. E. (2006). Screened exchange hybrid density-functional study of the work function of pristine and doped single-walled carbon nanotubes. *The Journal of Chemical Physics, 124*(2), 024709-024705.

[92] Shan, B., & Cho, K. (2005). First Principles Study of Work Functions of Single Wall Carbon Nanotubes. *Physical Review Letters, 94*(23), 236602-236604.

[93] Shibuta, D. (1998). United States Patent No. 5,853,877. USPTO.

[94]    Zhang, D., Ryu, K., Liu, X., Polikarpov, E., Ly, J., Tompson, M. E., et al.
        (2006). Transparent, Conductive, and Flexible Carbon Nanotube Films and Their
        Application in Organic Light-Emitting Diodes. *Nano Lett., 6*(9), 1880-1886.

[95]    Antoniadis, H., Miller, J. N., Roitman, D. B., & Cambell, I. H. (1997). Effects of
        hole carrier injection and transport in organic light-emitting diodes. *Electron
        Devices, IEEE Transactions on, 44*(8), 1289-1294.

[96]    Scott, J. C. (2003). Metal--organic interface and charge injection in organic
        electronic devices. *Journal of Vacuum Science & Technology A: Vacuum,
        Surfaces, and Films, 21*(3), 521-531.

[97]    Kumar, S., Pimparkar, N., Murthy, J. Y., & Alam, M. A. (2006). Theory of
        transfer characteristics of nanotube network transistors. *Applied Physics Letters,
        88*(12), 123505.

[98]    Qing, C., Minggang, X., Coskun, K., Moonsub, S., John, A. R., & Slava, V. R.
        (2007). Gate capacitance coupling of singled-walled carbon nanotube thin-film
        transistors. *Applied Physics Letters, 90*(2), 023516.

[99]    Kocabas, C., Shim, M., & Rogers, J. A. (2006). Spatially Selective Guided
        Growth of High-Coverage Arrays and Random Networks of Single-Walled
        Carbon Nanotubes and Their Integration into Electronic Devices. *J. Am. Chem.
        Soc., 128*(14), 4540-4541.

[100]   Kim, W., Javey, A., Vermesh, O., Wang, O., Li, Y. M., & Dai, H. J. (2003).
        Hysteresis caused by water molecules in carbon nanotube field-effect transistors.
        *Nano Letters, 3*(2), 193-198.

[101]   Kar, S., Vijayaraghavan, A., Soldano, C., Talapatra, S., Vajtai, R., Nalamasu, O.,
        et al. (2006). Quantitative analysis of hysteresis in carbon nanotube field-effect
        devices. *Applied Physics Letters, 89*(13).

[102]   Vijayaraghavan, A., Kar, S., Soldano, C., Talapatra, S., Nalamasu, O., & Ajayan,
        P. M. (2006). Charge-injection-induced dynamic screening and origin of
        hysteresis in field-modulated transport in single-wall carbon nanotubes. *Applied
        Physics Letters, 89*(16).

[103]   Lee, J. S., Ryu, S., Yoo, K., Choi, I. S., Yun, W. S., & Kim, J. (2007). Origin of
        gate hysteresis in carbon nanotube field-effect transistors. *Journal of Physical
        Chemistry C, 111*(34), 12504-12507.

[104]   Cao, Q., Xia, M. G., Shim, M., & Rogers, J. A. (2006). Bilayer Organic-
        Inorganic Gate Dielectrics for High-Performance, Low-Voltage, Single-Walled
        Carbon Nanotube Thin-Film Transistors, Complementary Logic Gates, and p-n
        Diodes on Plastic Substrates. *Advanced Functional Materials, 16*(18), 2355-
        2362.

[105]   Yang, M. H., Teo, K. B. K., Gangloff, L., Milne, W. I., Hasko, D. G., Robert, Y.,
        et al. (2006). Advantages of top-gate, high-k dielectric carbon nanotube field-
        effect transistors. *Applied Physics Letters, 88*(11), 113507-113503.

[106]   Snow, E. S., Campbell, P. M., Ancona, M. G., & Novak, J. P. (2005). High-
        mobility carbon-nanotube thin-film transistors on a polymeric substrate. *Applied
        Physics Letters, 86*(3), 033105-033103.

[107] Arnold, M. S. (2006). Sorting carbon nanotubes by electronic structure using density differentiation. *Nature nanotechnology, 1*(1), 60-65.

[108] Meitl, M. A., Zhu, Z.-T., Kumar, V., Lee, K. J., Feng, X., Huang, Y. Y., et al. (2006). Transfer printing by kinetic control of adhesion to an elastomeric stamp. *Nat Mater, 5*(1), 33-38.

[109] Collins, P. G., Arnold, M. S., & Avouris, P. (2001). Engineering Carbon Nanotubes and Nanotube Circuits Using Electrical Breakdown. *Science, 292*(5517), 706-709.

[110] Chen, Z., Appenzeller, J., Lin, Y.-M., Sippel-Oakley, J., Rinzler, A. G., Tang, J., et al. (2006). An Integrated Logic Circuit Assembled on a Single Carbon Nanotube. *Science, 311*(5768), 1735-.

[111] Derycke, V., Martel, R., Appenzeller, J., & Avouris, P. (2001). Carbon Nanotube Inter- and Intramolecular Logic Gates. *Nano Lett., 1*(9), 453-456.

[112] Dai, H. J., Petit, P., Robert, J., Xu, C. H., Lee, Y. H., Kim, S. G., et al. (1996). Crystalline Ropes of Metallic Carbon Nanotubes. *Science, 273*(5274), 483-487.

[113] Guo, T., Nikolaev, P., Thess, A., Colbert, D. T., & Smalley, R. E. (1995). Catalytic growth of single-walled manotubes by laser vaporization. *Chemical Physics Letters, 243*(1-2), 49-54.

[114] Liu, X., Pichler, T., Knupfer, M., Golden, M. S., Fink, J., Kataura, H., et al. (2002). Detailed analysis of the mean diameter and diameter distribution of single-wall carbon nanotubes from their optical response. *Physical Review B, 66*(4), 045411.

[115] Bandow, S., Rao, A. M., Williams, K. A., Thess, A., Smalley, R. E., & Eklund, P. C. (1997). Purification of single-wall carbon nanotubes by microfiltration. *Journal of Physical Chemistry B, 101*(44), 8839-8842.

[116] Itkis, M. E., Perea, D. E., Niyogi, S., Rickard, S. M., Hamon, M. A., Zhao, B., et al. (2003). Purity evaluation of as-prepared single-walled carbon nanotube soot by use of solution-phase near-IR spectroscopy. *Nano Letters, 3*(3), 309-314.

[117] Kingston, C. T., Jakubek, Z. J., Denommee, S., & Simard, B. (2004). Efficient laser synthesis of single-walled carbon nanotubes through laser heating of the condensing vaporization plume. *Carbon, 42*(8-9), 1657-1664.

[118] Liu, J., Rinzler, A. G., Dai, H. J., Hafner, J. H., Bradley, R. K., Boul, P. J., et al. (1998). Fullerene pipes. *Science, 280*(5367), 1253-1256.

[119] Haddon, R. C., Sippel, J., Rinzler, A. G., & Papadimitrakopoulos, F. (2004). Purification and separation of carbon nanotubes, *Mrs Bulletin* (Vol. 29, pp. 252-259).

[120] Bower, C., Kleinhammes, A., Wu, Y., & Zhou, O. (1998). Intercalation and partial exfoliation of single-walled carbon nanotubes by nitric acid. *Chemical Physics Letters, 288*(2-4), 481-486.

[121] Derycke, V., Martel, R., Appenzeller, J., & Avouris, P. (2002). Controlling doping and carrier injection in carbon nanotube transistors. *Applied Physics Letters, 80*(15), 2773-2775.

[122] Chen, J., Rao, A. M., Lyuksyutov, S., Itkis, M. E., Hamon, M. A., Hu, H., et al. (2001). Dissolution of Full-Length Single-Walled Carbon Nanotubes. *J. Phys. Chem. B, 105*(13), 2525-2528.

[123] Sun, Y. P., Fu, K., Lin, Y., & Huang, W. (2002). Functionalized Carbon Nanotubes: Properties and Applications. *Acc. Chem. Res., 35*(12), 1096-1104.

[124] Nikolaev, P., Bronikowski, M. J., Bradley, R. K., Rohmund, F., Colbert, D. T., Smith, K. A., et al. (1999). Gas-phase catalytic growth of single-walled carbon nanotubes from carbon monoxide. *Chemical Physics Letters, 313*(1-2), 91-97.

[125] Alvarez, W. E., Kitiyanan, B., Borgna, A., & Resasco, D. E. (2001). Synergism of Co and Mo in the catalytic production of single-wall carbon nanotubes by decomposition of CO. *Carbon, 39*(4), 547-558.

[126] Rao, A. M., Richter, E., Bandow, S., Chase, B., Eklund, P. C., Williams, K. A., et al. (1997). Diameter-Selective Raman Scattering from Vibrational Modes in Carbon Nanotubes. *Science, 275*(5297), 187-191.

[127] Lolli, G., Zhang, L., Balzano, L., Sakulchaicharoen, N., Tan, Y., & Resasco, D. E. (2006). Tailoring (n,m) Structure of Single-Walled Carbon Nanotubes by Modifying Reaction Conditions and the Nature of the Support of CoMo Catalysts. *J. Phys. Chem. B, 110*(5), 2108-2115.

[128] Hertel, T., Hagen, A., Talalaev, V., Arnold, K., Hennrich, F., Kappes, M., et al. (2005). Spectroscopy of Single- and Double-Wall Carbon Nanotubes in Different Environments. *Nano Lett., 5*(3), 511-514.

[129] Girifalco, L. A., Hodak, M., & Lee, R. S. (2000). Carbon nanotubes, buckyballs, ropes, and a universal graphitic potential. *Physical Review B, 62*(19), 13104.

[130] Tersoff, J., & Ruoff, R. S. (1994). Structural Properties of a Carbon-Nanotube Crystal. *Physical Review Letters, 73*(5), 676.

[131] Dyke, C. A., & Tour, J. M. (2004). Covalent Functionalization of Single-Walled Carbon Nanotubes for Materials Applications. *J. Phys. Chem. A, 108*(51), 11151-11159.

[132] Wang, H., Zhou, W., Ho, D. L., Winey, K. I., Fischer, J. E., Glinka, C. J., et al. (2004). Dispersing Single-Walled Carbon Nanotubes with Surfactants: A Small Angle Neutron Scattering Study. *Nano Lett., 4*(9), 1789-1793.

[133] Okazaki, T., Saito, T., Matsuura, K., Ohshima, S., Yumura, M., & Iijima, S. (2005). Photoluminescence Mapping of "As-Grown" Single-Walled Carbon Nanotubes: A Comparison with Micelle-Encapsulated Nanotube Solutions. *Nano Lett., 5*(12), 2618-2623.

[134] W. Wenseleers, I. I. V. E. G. E. D. O. A. S. L. A. B. (2004). Efficient Isolation and Solubilization of Pristine Single-Walled Nanotubes in Bile Salt Micelles. *Advanced Functional Materials, 14*(11), 1105-1112.

[135] Ayumi Ishibashi, N. N. (2006). Individual Dissolution of Single-Walled Carbon Nanotubes in Aqueous Solutions of Steroid or Sugar Compounds and Their Raman and Near-IR Spectral Properties. *Chemistry - A European Journal, 12*(29), 7595-7602.

[136] Shelimov, K. B., Esenaliev, R. O., Rinzler, A. G., Huffman, C. B., & Smalley, R. E. (1998). Purification of single-wall carbon nanotubes by ultrasonically assisted filtration. *Chemical Physics Letters, 282*(5-6), 429-434.

[137] David, H., Liangbing, H., & George, G. (2006). Conductivity scaling with bundle length and diameter in single walled carbon nanotube networks. *Applied Physics Letters, 89*(13), 133112.

[138] Bahr, J. L., Mickelson, E. T., Bronikowski, M. J., Smalley, R. E., & Tour, J. M. (2001). Dissolution of small diameter single-wall carbon nanotubes in organic solvents? *Chemical Communications*(2), 193-194.

[139] Jost, O., Gorbunov, A. A., Pompe, W., Pichler, T., Friedlein, R., Knupfer, M., et al. (1999). Diameter grouping in bulk samples of single-walled carbon nanotubes from optical absorption spectroscopy, *Applied Physics Letters* (Vol. 75, pp. 2217-2219).

[140] Hagen, A., & Hertel, T. (2003). Quantitative analysis of optical spectra from individual single-wall carbon nanotubes, *Nano Letters* (Vol. 3, pp. 383-388).

[141] Zhao, B., Itkis, M. E., Niyogi, S., Hu, H., Zhang, J., & Haddon, R. C. (2004). Study of the Extinction Coefficients of Single-Walled Carbon Nanotubes and Related Carbon Materials. *J. Phys. Chem. B, 108*(24), 8136-8141.

[142] Fischer, J. E. (2002). Chemical doping of single-wall carbon nanotubes, *Accounts of Chemical Research* (Vol. 35, pp. 1079-1086).

[143] Brintlinger, T., Chen, Y.-F., Durkop, T., Cobas, E., Fuhrer, M. S., Barry, J. D., et al. (2002). Rapid imaging of nanotubes on insulating substrates. *Applied Physics Letters, 81*(13), 2454-2456.

[144] Homma, Y., Suzuki, S., Kobayashi, Y., Nagase, M., & Takagi, D. (2004). Mechanism of bright selective imaging of single-walled carbon nanotubes on insulators by scanning electron microscopy. *Applied Physics Letters, 84*(10), 1750-1752.

[145] Léonard, F., & Tersoff, J. (1999). Novel Length Scales in Nanotube Devices. *Physical Review Letters, 83*(24), 5174.

[146] Martel, R., Derycke, V., Lavoie, C., Appenzeller, J., Chan, K. K., Tersoff, J., et al. (2001). Ambipolar Electrical Transport in Semiconducting Single-Wall Carbon Nanotubes. *Physical Review Letters, 87*(25), 256805.

[147] Heinze, S., Tersoff, J., Martel, R., Derycke, V., Appenzeller, J., & Avouris, P. (2002). Carbon Nanotubes as Schottky Barrier Transistors. *Physical Review Letters, 89*(10), 106801.

[148] Javey, A., Guo, J., Farmer, D. B., Wang, Q., Wang, D., Gordon, R. G., et al. (2004). Carbon Nanotube Field-Effect Transistors with Integrated Ohmic Contacts and High-<img src="http://pubs.acs.org/images/gifchars/kappa.gif" border="0"> Gate Dielectrics. *Nano Lett., 4*(3), 447-450.

[149] Chen, Z., Appenzeller, J., Knoch, J., Lin, Y. M., & Avouris, P. (2005). The Role of Metal-Nanotube Contact in the Performance of Carbon Nanotube Field-Effect Transistors. *Nano Lett., 5*(7), 1497-1502.

[150] Kim, W., Javey, A., Tu, R., Cao, J., Wang, Q., & Dai, H. (2005). Electrical contacts to carbon nanotubes down to 1 nm in diameter. *Applied Physics Letters, 87*(17), 173101-173103.

[151] Leonard, F., & Talin, A. A. (2006). Size-Dependent Effects on Electrical Contacts to Nanotubes and Nanowires. *Physical Review Letters, 97*(2), 026804-026804.

[152] Behnam, A., Choi, Y., Noriega, L., Wu, Z., Kravchenko, I., Rinzler, A. G., et al. (2007). Nanolithographic patterning of transparent, conductive single-walled carbon nanotube films by inductively coupled plasma reactive ion etching. *Journal of Vacuum Science & Technology B: Microelectronics and Nanometer Structures, 25*(2), 348-354.

[153] Lee, J.-O., Park, C., Kim, J.-J., Kim, J., Park, J. W., & Yoo, K.-H. (2000). Formation of low-resistance ohmic contacts between carbon nanotube and metal electrodes by a rapid thermal annealing method. *Journal of Physics D: Applied Physics, 33*(16), 1953-1956.

[154] Leroy, W. P., Detavernier, C., Van Meirhaeghe, R. L., & Lavoie, C. (2007). Thin film solid-state reactions forming carbides as contact materials for carbon-containing semiconductors. *Journal of Applied Physics, 101*(5), 053714-053710.

[155] Tang, C. W., & VanSlyke, S. A. (1987). Organic electroluminescent diodes. *Applied Physics Letters, 51*(12), 913-915.

[156] Afzali, A., Dimitrakopoulos, C. D., & Breen, T. L. (2002). High-Performance, Solution-Processed Organic Thin Film Transistors from a Novel Pentacene Precursor. *J. Am. Chem. Soc., 124*(30), 8812-8813.

[157] Wind, S. J., Appenzeller, J., Martel, R., Derycke, V., & Ph, A. (2002). Vertical scaling of carbon nanotube field-effect transistors using top gate electrodes. *Applied Physics Letters, 80*(20), 3817-3819.

[158] Wang, Y., Maspoch, D., Zou, S., Schatz, G. C., Smalley, R. E., & Mirkin, C. A. (2006). Controlling the shape, orientation, and linkage of carbon nanotube features with nano affinity templates. *Proceedings of the National Academy of Sciences, 103*(7), 2026-2031.

[159] Rowell, M. W., Topinka, M. A., McGehee, M. D., Prall, H.-J., Dennler, G., Sariciftci, N. S., et al. (2006). Organic solar cells with carbon nanotube network electrodes. *Applied Physics Letters, 88*(23), 233506-233503.

[160] Ulbricht, R., Lee, S. B., Jiang, X., Inoue, K., Zhang, M., Fang, S., et al. (2007). Transparent carbon nanotube sheets as 3-D charge collectors in organic solar cells. *Solar Energy Materials and Solar Cells, 91*(5), 416-419.

[161] van de Lagemaat, J., Barnes, T. M., Rumbles, G., Shaheen, S. E., Coutts, T. J., Weeks, C., et al. (2006). Organic solar cells with carbon nanotubes replacing In[sub 2]O[sub 3]:Sn as the transparent electrode. *Applied Physics Letters, 88*(23), 233503-233503.

[162] Hu, L., Gruner, G., Li, D., Kaner, R. B., & Cech, J. (2007). Patternable transparent carbon nanotube films for electrochromic devices. *Journal of Applied Physics, 101*(1), 016102-016103.

[163] Martel, R., Derycke, V., Lavoie, C., Appenzeller, J., Chan, K. K., Tersoff, J., et al. (2001). Ambipolar electrical transport in semiconducting single-wall carbon nanotubes, *Physical Review Letters* (Vol. 87).

[164] Arnold, M. S., Green, A. A., Hulvat, J. F., Stupp, S. I., & Hersam, M. C. (2006). Sorting carbon nanotubes by electronic structure using density differentiation. *Nat Nano, 1*(1), 60-65.

[165] An, L., Fu, Q., Lu, C., & Liu, J. (2004). A Simple Chemical Route To Selectively Eliminate Metallic Carbon Nanotubes in Nanotube Network Devices. *J. Am. Chem. Soc., 126*(34), 10520-10521.

[166] Strano, M. S., Dyke, C. A., Usrey, M. L., Barone, P. W., Allen, M. J., Shan, H., et al. (2003). Electronic Structure Control of Single-Walled Carbon Nanotube Functionalization. *Science, 301*(5639), 1519-1522.

[167] Wang, C., Cao, Q., Ozel, T., Gaur, A., Rogers, J. A., & Shim, M. (2005). Electronically Selective Chemical Functionalization of Carbon Nanotubes: Correlation between Raman Spectral and Electrical Responses. *J. Am. Chem. Soc., 127*(32), 11460-11468.

[168] Fischer, J. E. (2002). Chemical Doping of Single-Wall Carbon Nanotubes. *Acc. Chem. Res., 35*(12), 1079-1086.

[169] Geng, H. Z., Kim, K. K., So, K. P., Lee, Y. S., Chang, Y., & Lee, Y. H. (2007). Effect of Acid Treament on Carbon Nanotube-Based Flexible Transparent Conducting Films. *J. Am. Chem. Soc., 129*(25), 7758-7759.

[170] Takenobu, T., Takano, T., Shiraishi, M., Murakami, Y., Ata, M., Kataura, H., et al. (2003). Stable and controlled amphoteric doping by encapsulation of organic molecules inside carbon nanotubes. *Nat Mater, 2*(10), 683-688.

[171] Zhao, J., Lu, J. P., Han, J., & Yang, C.-K. (2003). Noncovalent functionalization of carbon nanotubes by aromatic organic molecules. *Applied Physics Letters, 82*(21), 3746-3748.

[172] Giannozzi, P. (2004). Comment on ``Noncovalent functionalization of carbon nanotubes by aromatic organic molecules" [Appl. Phys. Lett. [bold 82], 3746 (2003)]. *Applied Physics Letters, 84*(19), 3936-3937.

[173] Brown, A. R., Deleeuw, D. M., Havinga, E. E., & Pomp, A. (1994). A Universal Relation between conductivity and field-effect mobility in doped amorphous organic semiconductors. *Synthetic Metals, 68*(1), 65-70.

[174] Coppo, P., Schroeder, R., Grell, M., & Turner, M. L. (2004). Investigation of solution processed poly(4,4-dioctylcyclopentadithiophene) thin films as transparent conductors. *Synthetic Metals, 143*(2), 203-206.

[175] Tolbert, L., Edmond, C., & Kowalik, J. (1999). Charge-transfer doping of poly(3-alkyl-2,2'-bithiophene). *Synthetic Metals, 101*(1-3), 500-501.

[176] Rao, A. M., Eklund, P. C., Bandow, S., Thess, A., & Smalley, R. E. (1997). Evidence for charge transfer in doped carbon nanotube bundles from Raman scattering. *Nature, 388*(6639), 257-259.

[177] Jackson, T. N., Yen-Yi, L., Gundlach, D. J., & Klauk, H. (1998). Organic thin-film transistors for organic light-emitting flat-panel display backplanes. *Selected Topics in Quantum Electronics, IEEE Journal of, 4*(1), 100-104.

[178] Christopher, R. N., Henning, S., James, C. B., & Robert, S. (2007). Stability of polymeric thin film transistors for x-ray imaging applications. *Applied Physics Letters, 91*(14), 142105.

[179] Tang, X.-W., Yang, Y., Kim, W., Wang, Q., Qi, P., Dai, H., et al. (2005). Measurement of ionizing radiation using carbon nanotube field effect transistor. *Physics in Medicine and Biology, 50*(3), N23-N31.

[180] Crone, B., Dodabalapur, A., Lin, Y. Y., Filas, R. W., Bao, Z., LaDuca, A., et al. (2000). Large-scale complementary integrated circuits based on organic transistors. *Nature, 403*(6769), 521-523.

[181] Limketkai, B. N., Jadhav, P., & Baldo, M. A. (2007). Electric-field-dependent percolation model of charge-carrier mobility in amorphous organic semiconductors. *Physical Review B (Condensed Matter and Materials Physics), 75*(11), 113203-113204.

[182] Pimparkar, N., Kocabas, C., Seong Jun, K., Rogers, J., & Alam, M. A. (2007). Limits of Performance Gain of Aligned CNT Over Randomized Network: Theoretical Predictions and Experimental Validation. *Electron Device Letters, IEEE, 28*(7), 593-595.

[183] Behnam, A., Guo, J., & Ural, A. (2007). Effects of nanotube alignment and measurement direction on percolation resistivity in single-walled carbon nanotube films. *Journal of Applied Physics, 102*(4), 044313-044317.

[184] Behnam, A., Noriega, L., Choi, Y., Wu, Z., Rinzler, A. G., & Ural, A. (2006). Resistivity scaling in single-walled carbon nanotube films patterned to submicron dimensions. *Applied Physics Letters, 89*(9), 093107-093103.

[185] Behnam, A., & Ural, A. (2007). Computational study of geometry-dependent resistivity scaling in single-walled carbon nanotube films. *Physical Review B (Condensed Matter and Materials Physics), 75*(12), 125432-125438.

[186] Hecht, D., Hu, L., & Gruner, G. (2006). Conductivity scaling with bundle length and diameter in single walled carbon nanotube networks. *Applied Physics Letters, 89*(13), 133112-133113.

[187] Ausman, K. D., Piner, R., Lourie, O., Ruoff, R. S., & Korobov, M. (2000). Organic Solvent Dispersions of Single-Walled Carbon Nanotubes: Toward Solutions of Pristine Nanotubes. *J. Phys. Chem. B, 104*(38), 8911-8915.

[188] Bensimon, A., Simon, A., Chiffaudel, A., Croquette, V., Heslot, F., & Bensimon, D. (1994). Alignment and sensitive detection of DNA by a moving interface. *Science, 265*(5181), 2096-2098.

[189] Bensimon, D., Simon, A. J., Croquette, V., & Bensimon, A. (1995). Stretching DNA with a Receding Meniscus: Experiments and Models. *Physical Review Letters, 74*(23), 4754.

[190] Huang, Y., Duan, X., Wei, Q., & Lieber, C. M. (2001). Directed Assembly of One-Dimensional Nanostructures into Functional Networks. *Science, 291*(5504), 630-633.

[191] Dodabalapur, A., Torsi, L., & Katz, H. E. (1995). Organic Transistors: Two-Dimensional Transport and Improved Electrical Characteristics. *Science, 268*(5208), 270-271.

[192]  Martel, R., Schmidt, T., Shea, H. R., Hertel, T., & Avouris, P. (1998). Single-and multi-wall carbon nanotube field-effect transistors. *Applied Physics Letters, 73*(17), 2447-2449.

[193]  Park, H., Park, J., Lim, A. K. L., Anderson, E. H., Alivisatos, A. P., & McEuen, P. L. (2000). Nanomechanical oscillations in a single-C60 transistor. *Nature, 407*(6800), 57-60.

[194]  Tans, S. J., Verschueren, A. R. M., & Dekker, C. (1998). Room-temperature transistor based on a single carbon nanotube. *Nature, 393*(6680), 49-52.

[195]  Zhuravlev, L. T. (2000). The surface chemistry of amorphous silica. Zhuravlev model. *Colloids and Surfaces A: Physicochemical and Engineering Aspects, 173*(1-3), 1-38.

[196]  Buch, V., Milet, A., Vacha, R., Jungwirth, P., & Devlin, J. P. (2007). Water surface is acidic. *Proceedings of the National Academy of Sciences, 104*(18), 7342-7347.

[197]  Avouris, P., Hertel, T., & Martel, R. (1997). Atomic force microscope tip-induced local oxidation of silicon: kinetics, mechanism, and nanofabrication. *Applied Physics Letters, 71*(2), 285-287.

[198]  Aziz, H., & Popovic, Z. D. (2004). Degradation Phenomena in Small-Molecule Organic Light-Emitting Devices. *Chem. Mater., 16*(23), 4522-4532.

[199]  Cui, J., Wang, A., Edleman, N. L., Ni, J., Lee, P., Armstrong, N. R., et al. (2001). Indium tin oxide alternatives - High work function transparent conducting oxides as anodes for organic light-emitting diodes. *Adv. Mater., 13*(19), 1476-+.

[200]  Melpignano, P., Baron-Toaldo, A., Biondo, V., Priante, S., Zamboni, R., Murgia, M., et al. (2005). Mechanism of dark-spot degradation of organic light-emitting devices. *Applied Physics Letters, 86*(4), 041105-041103.

[201]  Cairns, D. R., Witte II, R. P., Sparacin, D. K., Sachsman, S. M., Paine, D. C., Crawford, G. P., et al. (2000). Strain-dependent electrical resistance of tin-doped indium oxide on polymer substrates. *Applied Physics Letters, 76*(11), 1425-1427.

[202]  Han, S., Feng, X., Lu, Z. H., Johnson, D., & Wood, R. (2003). Transparent-cathode for top-emission organic light-emitting diodes. *Applied Physics Letters, 82*(16), 2715-2717.

[203]  Wu, C. C., Wu, C. I., Sturm, J. C., & Kahn, A. (1997). Surface modification of indium tin oxide by plasma treatment: An effective method to improve the efficiency, brightness, and reliability of organic light emitting devices. *Applied Physics Letters, 70*(11), 1348-1350.

[204]  Takenobu, T., Takano, T., Shiraishi, M., Murakami, Y., Ata, M., Kataura, H., et al. (2003). Stable and controlled amphoteric doping by encapsulation of organic molecules inside carbon nanotubes. *Nature Materials, 2*(10), 683-688.

[205]  Koch, N., Kahn, A., Ghijsen, J., Pireaux, J. J., Schwartz, J., Johnson, R. L., et al. (2003). Conjugated organic molecules on metal versus polymer electrodes: Demonstration of a key energy level alignment mechanism. *Applied Physics Letters, 82*(1), 70-72.

[206]   Salaneck, W. R., Seki, K., Kahn, A., & Pireaux, J. J. (2001). *Conjugated Polymer and Molecular Interfaces: Science and Technology for Photonic and Optoelectronic Applications*. New York: Marcel Dekker.

[207]   Ishii, H., & Seki, K. (1997). Energy level alignment at organic/metal interfaces studied by UV photoemission: breakdown of traditional assumption of a common vacuum level at the interface. *Electron Devices, IEEE Transactions on, 44*(8), 1295-1301.

[208]   Léonard, F., & Tersoff, J. (2000). Role of Fermi-Level Pinning in Nanotube Schottky Diodes. *Physical Review Letters, 84*(20), 4693.

[209]   Appenzeller, J., Knoch, J., Derycke, V., Martel, R., Wind, S., & Avouris, P. (2002). Field-Modulated Carrier Transport in Carbon Nanotube Transistors. *Physical Review Letters, 89*(12), 126801.

[210]   Tulevski, G. S., Nuckolls, C., Afzali, A., Graham, T. O., & Kagan, C. R. (2006). Device scaling in sub-100 nm pentacene field-effect transistors. *Applied Physics Letters, 89*(18), 183101-183103.

[211]   Lin, Y. Y., Gundlach, D. J., Nelson, S. F., & Jackson, T. N. (1997). Stacked pentacene layer organic thin-film transistors with improved characteristics. *Electron Device Letters, IEEE, 18*(12), 606-608.

[212]   Hamadani, B. H., & Natelson, D. (2004). Gated nonlinear transport in organic polymer field effect transistors. *Journal of Applied Physics, 95*(3), 1227-1232.

[213]   Appenzeller, J., Radosavljevic, M., Knoch, J., & Avouris, P. (2004). Tunneling Versus Thermionic Emission in One-Dimensional Semiconductors. *Physical Review Letters, 92*(4), 048301-048304.